



Michael Bloder, BSc

**Research on volumetric reduction of a highly saturated vacuum  
flow**

**MASTERARBEIT**

zur Erlangung des akademischen Grades  
Diplomingenieur  
Masterstudium Wirtschaftsingenieurwesen - Maschinenbau

eingereicht an der

**Technischen Universität Graz**

Betreuer/in  
Ao. Univ.-Prof. Dipl.-Ing. Dr. techn. Raimund Almbauer  
Institut für Verbrennungskraftmaschinen und Thermodynamik

Zweitbetreuer/in  
Dipl.-Ing. Stefan Posch, BSc  
Institut für Verbrennungskraftmaschinen und Thermodynamik

Graz, Februar 2018



Institut für Verbrennungskraftmaschinen und Thermodynamik  
Vorstand: Univ.-Prof. DI Dr. Helmut Eichseder



## Preamble

This master thesis was written in 2017, and 2018, for the completion of my studies' mechanical engineering and economic science at the Graz University of Technology.

Alongside the studies at the University, I also worked several years for Andritz AG in the division of Pulp & Paper. During this time, I came across several interesting topics that were befitting for a master thesis, most of them placed in the scope of thermodynamics. After some pre- studies on different topics, I choose the present topic as a master thesis. This master thesis was carried out together with the institute of internal combustion engines and thermodynamics. In this topic, I could bring in theoretical knowledge from my studies, mainly from the lectures thermodynamics and higher thermodynamics, and furthermore, I was able to apply my professional experience.

At this point my thanks goes to Univ.-Prof. Dipl.-Ing. Dr.techn. Helmut Eichseder for giving me the possibility to write this master thesis in cooperation with the institute of internal combustion engines and thermodynamics.

Special thanks goes to Professor Ao.Univ-Prof. Dipl.-Ing Dr.techn. Raimund Almbauer and Dipl.-Ing Stefan Posch, BSc who always supported me in thermodynamic matters.

I would also like to thank my colleagues from Andritz AG who supported me as well, especially to Mr. Franz Petschauer who was the main contact for me with any practical questions. I was greatly supported by Mr. Reinhard Diemat, Mr. Georg Brückler, Mr. Theussl Andre and Mr. Harrer Helmuth for the experiment I executed in the pilot plant in Graz.

Lastly, my sincerest thanks to my family and Carina Wolf, BSc, who made my studies possible and provided the necessary variety in everyday life.

# Inhaltsverzeichnis

PREAMBEL.....	III
FORMULA SYMBOLS, INDICES AND ABBREVIATIONS.....	VI
STATUTORY DECLARATION.....	VIII
ABSTRACT.....	IX
KURZFASSUNG.....	X
<b>1 INTRODUCTION.....</b>	<b>1</b>
1.1 GOAL OF THE PROJECT.....	1
<b>2 THEORETICAL BACKGROUND.....</b>	<b>3</b>
2.1 THERMODYNAMICAL FUNDAMENTALS.....	3
2.1.1 <i>Thermodynamic system</i> .....	3
2.1.2 <i>State variables</i> .....	3
2.1.3 <i>Thermodynamic process</i> .....	3
2.1.4 <i>1<sup>st</sup> law of thermodynamics</i> .....	4
2.1.5 <i>2<sup>nd</sup> law of thermodynamics</i> .....	4
2.2 PHASE TRANSITION AND AGGREGATION STATES.....	5
2.2.1 <i>Ideal gas</i> .....	5
2.2.2 <i>Real gas</i> .....	6
2.3 MIXTURE OF IDEAL GASES.....	6
2.3.1 <i>Moist air</i> .....	7
2.4 PRINCIPLES OF FLUID DYNAMICS.....	8
2.4.1 <i>Continuity equation</i> .....	8
2.4.2 <i>Momentum equation</i> .....	8
2.4.3 <i>Equation of energy</i> .....	9
2.5 HEAT TRANSFER [3], [4].....	10
2.5.1 <i>Heat conduction</i> .....	10
2.5.2 <i>Convection</i> .....	10
2.5.3 <i>Heat radiation</i> .....	11
2.6 HEAT TRANSFER BY PHASE CHANGE.....	11
2.6.1 <i>Condensation [4]</i> .....	11
2.6.2 <i>Spray condensation</i> .....	12
<b>3 THERMODYNAMIC CONSIDERATION OF THE VACUUM SYSTEM.....</b>	<b>15</b>
3.1 OVERVIEW OF THE VACUUM SYSTEM.....	15
3.1.1 <i>Location of the cooling system</i> .....	18
3.2 THERMODYNAMIC MODEL.....	18
3.2.1 <i>Process from 0 → 1: Cooling the flow until <math>\varphi=1</math></i> .....	19
3.2.2 <i>Process from 1 → 2: Condensation at the surface of the droplets</i> .....	21
3.2.3 <i>Required amount of spray water</i> .....	22
3.3 THERMODYNAMIC SAVING POTENTIAL.....	23
3.4 CONCLUSION OF THERMODYNAMIC SAVING POTENTIAL.....	25
<b>4 CFD CALCULATION.....</b>	<b>26</b>
4.1 SETUP OF THE CONDENSATION MODEL.....	26
4.1.1 <i>Lagrange vs Euler approach</i> .....	27
4.1.2 <i>Discrete phase model DPM</i> .....	28
4.1.3 <i>User Defined Function UDF</i> .....	28
4.1.4 <i>Boundary conditions</i> .....	30
4.1.5 <i>Limitations of the DPM Model</i> .....	30
4.2 EXECUTION AND RESULTS OF THE RESEARCH ON THE 2D MODEL.....	33
4.2.1 <i>Share injections on more cells</i> .....	33
4.2.2 <i>Adjusting the substance properties and condensation rate</i> .....	33
4.2.3 <i>Implementation of linear factors</i> .....	37
4.3 POSSIBLE APPROACHES TO CONTINUE WITH CFD.....	40
4.3.1 <i>Further study of the DPM model</i> .....	40
4.3.2 <i>Multiphase Model</i> .....	43

---

4.3.3	<i>Dense Discrete Phase Model (DDPM)</i> .....	43
4.4	CONCLUSION OF THE CFD CALCULATION .....	43
<b>5</b>	<b>EXPERIMENTAL INVESTIGATION</b> .....	<b>44</b>
5.1	PREPARATION OF THE TEST STAND .....	44
5.2	EXPERIMENTAL SETUP & MEASURING DEVICES .....	46
5.2.1	<i>Spray water pipe and suction box (UHLE box)</i> .....	48
5.2.2	<i>Measurement unit inlet, Debimo sensor</i> .....	48
5.2.3	<i>Spray modules</i> .....	48
5.2.4	<i>Glass cylinder</i> .....	50
5.2.5	<i>Measuring pipe</i> .....	51
5.2.6	<i>Measurement unit outlet, Debimo sensor</i> .....	53
5.2.7	<i>Water separator, vacuum pump and extraction pump</i> .....	53
5.3	EXPERIMENTAL METHODOLOGY .....	54
5.3.1	<i>Matchup of the measuring instruments</i> .....	54
5.3.2	<i>Parameters to be investigated</i> .....	56
5.3.3	<i>Execution of the experiment</i> .....	58
5.4	RESULTS AND EXPLANATION .....	59
5.4.1	<i>Reduction of used nozzles per system</i> .....	59
5.4.2	<i>Process water in the system</i> .....	59
5.4.3	<i>Redirection of the spray</i> .....	60
5.4.4	<i>Detailed results of the experimental setup</i> .....	61
5.5	CONCLUSION OF THE EXPERIMENTAL INVESTIGATION .....	69
<b>6</b>	<b>CONCLUSION</b> .....	<b>70</b>
<b>7</b>	<b>NEXT STEPS</b> .....	<b>72</b>
	<b>LITERATURE</b> .....	<b>74</b>
	<b>LIST OF FIGURES</b> .....	<b>75</b>
	<b>LIST OF TABLES</b> .....	<b>76</b>
	<b>APPENDICES</b> .....	<b>77</b>

## Formula symbols, indices and abbreviations

### Latin equation symbols

$A$	$m^2$	surface
$c_p ; c_v$	$J/(kg \cdot K)$	specific, isobar heat capacity
$c_w$	$J/(kg \cdot K)$	Specific heat capacity water
$c$	-	condensation factor
$d$	$m$	diameter
$e$	-	adjusting factor for energy equation
$e$	$J/kg$	specific energy
$e_a$	$J/kg$	specific external energy
$E_a$	$J$	external energy
$\vec{f}^B$	$m/s^2$	body forces
$f_V$	-	volume share
$h$	$J/kg$	specific enthalpy
$H$	$J$	enthalpy
$\dot{H}$	$J/s$	enthalpy flow
$h_{i(1+x)}$	$J/kg$	enthalpy per kg dry air
$h_c$	$kJ/kg$	specific condensation enthalpy
$k$	$W/(m^2 \cdot K)$	heat transfer coefficient
$l$	$m$	length
$m$	-	adjusting factor for mass equation
$m$	$kg$	mass
$m_a$	$kg$	mass of air
$m_v$	$kg$	mass of vapour
$\dot{m}$	$kg/s$	mass flow
$\dot{m}_a$	$kg/s$	mass flow air
$\dot{m}_v$	$kg/s$	mass flow vapour
$\dot{m}_w$	$kg/s$	mass flow water
$n$	-	quantity
$\vec{n}$	-	normal vector
$O$	$m^2$	surface
$p$	$bar, Pa$	pressure
$\Delta p$	$bar, Pa$	vacuum level
$p_a$	$bar, Pa$	partial pressure of air
$p_v$	$bar, Pa$	partial pressure of vapour
$p_{v'}$	$bar, Pa$	saturation pressure of vapour
$q$	$J/kg$	specific heat
$Q$	$J$	heat
$\dot{q}$	$J/(kg \cdot s)$	specific heat flow rate
$\dot{Q}$	$J/s$	heat flow rate
$R$	$J/(kg \cdot K)$	specific ideal gas constant
$R_a$	$J/(kg \cdot K)$	specific ideal gas constant air
$R_v$	$J/(kg \cdot K)$	specific ideal gas constant vapour
$RH$	-	relative humidity
$s$	$J/(kg \cdot K)$	Specific entropy
$S$	$J/K$	entropy
$t$	$s$	time
$t$	$^{\circ}C$	temperature
$T$	$K$	thermodynamic entropy

$u$	m/s	velocity
$u$	J/kg	specific inner energy
$U$	J	inner energy
$u$	m/s	velocity
$v$	m/s	velocity
$\vec{v}$	m/s	vector of velocity
$V$	$m^3$	volume
$\dot{V}$	$m^3/s$	volume flow
$w$	m	width
$w$	m/s	velocity
$W_t$	J	technical work
$x$	m	coordinate
$x = m_v/m_a$	–	degree of humidity
$y$	m	coordinate
$y_{D,G}$	-	inert gas share
$z$	m	coordinate

### Greek symbols

$\eta$	–	utilization factor
$\mu_i$	–	mass share of component i
$\nu_i$	–	mole share of component i
$\lambda$	W/(m·K)	thermal conductivity
$\rho$	kg/m <sup>3</sup>	density
$\Upsilon$	-	psychrometer constant
$\vec{\tau}$	N/mm <sup>2</sup>	stress vector
$\bar{\theta}$	–	heating factor
$\varphi = p_v/p_v'$	–	relative humidity
$\varphi_i$	–	volume share of component i

### Operators

$\nabla$	Nabla operator
$\sum$	Sum

### Further Indices

2D	two- dimensional
3D	three- dimensional
CFD	Computational Fluid Dynamics
max	maximal
min	minimal
UDF	User Defined Function

## **Statutory declaration**

I declare that I have authored this thesis independently, that I have not used other than the declared sources/resources, and that I have explicitly indicated all material which has been quoted either literally or by content from the sources used. The text document uploaded to TUGRAZonline is identical to the present master's thesis.

Michael Bloder

Graz, date



## Abstract

This master thesis deals with the volumetric flow reduction of the vacuum system of pulp drying machines, without reducing the vacuum height and the flow at the position where vacuum is applied. An important characteristic is that the air in the system is highly saturated.

Vacuum is applied in many sections of a pulp drying machine and is very energy consuming. Approximately 1/3 of all the energy used during the operation of a drying machine can be assigned to the vacuum system. Not only operating costs are high, also investment costs are remarkable. Therefore, this master thesis focuses its' research on reducing the costs for the vacuum system.

The thermodynamic fundamentals of first and second law of thermodynamics and the basics of ideal gases and mixtures related to them are provided. Deeper consideration is given on the mixture of vapour and (dry) air that form the moist air. The principles of fluid dynamics and the mass and heat transfer by phase changes are presented as well and finally, some consideration about surface condensation is provided.

The investigated vacuum system is introduced as well, by describing its schematic and the main components. Additionally, the thermodynamic cooling and condensation model is provided and based on this the potential of volumetric flow reduction is presented in the end.

Next, a CFD calculation is introduced. Hence, ANSYS FLUENT 15.0 and the discrete phase model (DPM) was used. To simulate the condensation from the highly saturated moist air (continuous phase) to the droplets injected (discrete phase) an UDF is provided. Results and a conclusion of the CFD calculation are presented at the end of this section.

Additionally, an experimental setup is described. The documentation consists of the planning, assembling and the methodical implementation of the experiment carried out at the pilot plant in Graz. The results and findings of the investigation are described in this chapter as well.

Finally, a conclusion of the results, and a forecast of the continuation, and the next steps based on the results from the experimental investigation and the CFD calculation are specified.

In the chapters 3, 4 and 5 a short conclusion of researches carried out in the current chapter is prepared, that is linking to the overall research goals of the thesis.

## Kurzfassung

In dieser Masterarbeit wird die mögliche volumetrische Vakuumstromreduktion des Vakuumsystems einer Zellstoffentwässerungsmaschine untersucht, wobei die Entwässerungseigenschaft, dass das Vakuum ausübt nicht beeinträchtigt werden darf. Der Vakuumstrom kann als gesättigter, feuchter Luftstrom angenommen werden.

Vakuum findet in vielen Bereichen der Zellstoffentwässerung seine Anwendung. Es wird sowohl zum entwässern des Zellstoffes selbst als auch zur Entladung der Pressfilze eingesetzt. Daher ist die Energieaufnahme mit rund 1/3 des gesamten Energiebedarfs der zum Betrieb benötigt wird beachtlich. Neben den Betriebskosten sind auch die Investitionskosten nicht außer Acht zu lassen. Daher ist das Ziel in dieser Masterarbeit, die Kosten die für das Vakuumsystem anfallen durch eine Volumenstrom- Reduktion zur verringern.

Die thermodynamischen Grundlagen rund um den ersten und zweiten Hauptsatz sowie die Eigenschaften von idealen Gasen und deren Mischungen werden im Zuge einer Literaturrecherche vorgestellt. Dabei wird besonders auf die Mischung der beiden idealen Gase „trockene Luft“ und „Dampf“ eingegangen, die zusammen die Mischung „feuchte Luft“ ergeben. Des Weiteren wird auf die Strömungsgrundlagen eingegangen und der Wärme- und Stofftransport infolge Kondensation erklärt. Schlussendlich wird auf die sogenannte Oberflächenkondensation genauer eingegangen.

Im darauffolgenden Kapitel wird auf das Vakuumsystem von Zellstoffentwässerungsmaschinen genauer eingegangen und dessen Eigenschaften erläutert. Des Weiteren wird das thermodynamische Kondensationsmodell erklärt und darauf aufbauend, das volumetrische Reduktionspotential des Vakuumstroms an jeder Vakuumbeaufschlagten Position einer Zellstoffentwässerungsmaschine präsentiert.

Im darauffolgenden Teil wird eine CFD Berechnung, durchgeführt mit der Software ANSYS FLUENT 15.0, vorgestellt. Um die Kondensation zu simulieren wurde das „Discrete Phase Model“ (DPM) verwendet und zusätzlich noch mit einer „User Defined Function“ (UDF) erweitert. Die Resultate werden in Bezug auf die Aufgabenstellung am Ende des Kapitels erklärt.

Ergänzend zur CFD Berechnung wird ein Versuchsaufbau präsentiert. Der Versuchsaufbau, das verwendete Equipment sowie die verwendeten Messgeräte werden in diesem Kapitel präsentiert. Die Methodik der Versuchsdurchführung und die Ergebnisse des Versuchs werden am Ende präsentiert.

Schlussendlich werden die gesamten Ergebnisse der Arbeit zusammengefasst und die nachfolgenden Schritte für dieses Projekt werden erläutert.

Zusätzlich zur gesamten Zusammenfassung ist für die Kapitel 3, 4 und 5 jeweils eine separate Zusammenfassung der einzelnen durchgeführten Schritte aus dem jeweiligen Kapitel angefügt, die den Bezug zur Aufgabenstellung nochmals herstellen.

# 1 Introduction

Andritz Pulp&Paper is one of the leading suppliers for pulp mills and pulp drying systems. In the following master thesis, the focus is put on the pulp dewatering machine. It is the part of the pulp mill that forms the chemically treated pulp from a suspension with approximately 2% pulp content (98% water) to a sheet with pulp content (dryness) of >50%.

Vacuum is used in many sections of the machine during the process of pulp dewatering. On the one hand it is used directly for pulp dewatering and on the other hand vacuum is used to dewater felts and other equipment to enhance dewatering properties at the different presses. In the sketch below, all vacuum applied positions of a standard machine (Twin Wire Former) are marked.

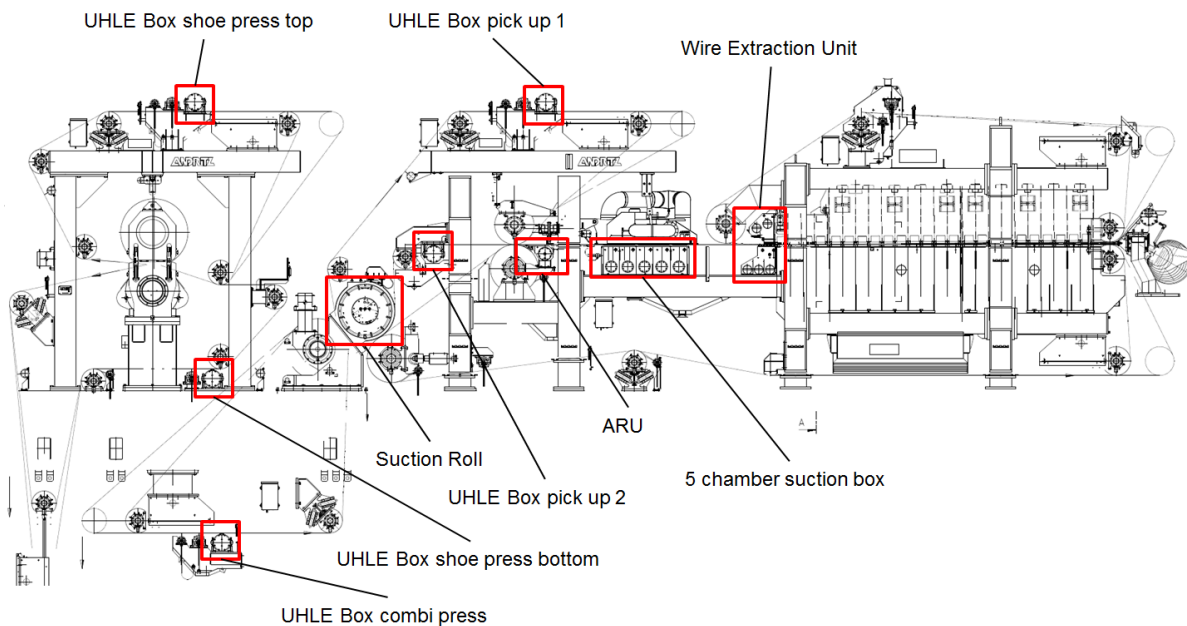


Figure 1-1: Vacuum applied positions of a standard Twin Wire Former [17]

To improve dewatering properties the process temperatures have a tendency to get higher. Due to the higher process temperatures, the specific volume of the moist air flow increases and the partial pressure of the vapour rise with a higher temperature, which results in a higher vapour content in the moist air flow. Both, the higher spec. volume and the higher vapour component lead to increased volumetric flow and therefore, the vacuum pumps (or radial blowers) and all the equipment needs to be sized enlarged and therefore, higher investment costs arise. Furthermore, energy costs for generating the vacuum increase significantly and lead to higher operating costs. Nowadays, roughly 1/3 of the whole energy consumption of a modern dewatering machine is used for generating the vacuum.

## 1.1 Goal of the project

To reduce costs of investment for the equipment and operation, a thermodynamic system should be developed to reduce the volumetric flow from the suction boxes to the vacuum pumps. The vacuum level and the flow must not be reduced at the vacuum boxes in order not to change the dewatering properties. Therefore, the flow should be cooled down after the vacuum applied positions to increase the density of the dry air and to reduce the content of vapour in the highly saturated moist air flow.

The cooling effect should be achieved by using cold water that is injected by a spray into the vacuum pipes. The ground is that the water can be reused in other parts of the process. The contained process water can be assumed to be minimal and therefore, be ignored.

By injecting the cooling spray, the thermodynamic saving potential and the volumetric flow reduction of such a system should be shown. Additionally, parameters that have an influence on the volumetric flow reduction should be defined and their effect on it should be investigated.

## 2 Theoretical background

In this chapter, the used methods of thermodynamical fundamentals and coherences, which are important to understand, are described and explained. Besides the basics, such as the 1<sup>st</sup> law of thermodynamics and the principles of fluid dynamics, the focus is mainly put on condensation of vapour in the moist air. Other basics are briefly presented.

### 2.1 Thermodynamical fundamentals

Thermodynamics is built on the laws of physics and chemistry. It is dealing with the transformation of different forms of energy, such as mechanical, chemical and heat energy whereby, mechanical and heat energy are the most important for technical thermodynamics. In most cases it is not sufficient to observe the macroscopical phenomena and not the microscopical. Therefore, macroscopical properties for the most important substances are available in tables, charts or diagrams [1], [2].

#### 2.1.1 Thermodynamic system

For most of the thermodynamic problems, it is necessary to define a system with its borders. Depending on how the borders are chosen and depending on the kind of process, the system can either be closed or opened, homogenous or heterogeneous, steady state or transient, adiabatic or non-adiabatic [1].

#### 2.1.2 State variables

The following section is directly taken from [1]. Once a system is homogeneously balanced, its thermodynamic condition can be described independent from its location with a small number of physical variables, such as temperature  $T$ , pressure  $p$ , volume  $V$  and mass  $m$ . These physical variables are called state variables and can be divided as follows:

- **Intensive** state variables are independent from the size of the system, such as temperature  $T$  and pressure  $p$ .
- **Extensive** state variables depend on the size of the system, such as mass  $m$ , volume  $V$  or inner energy  $U$ .
- **Specific** or **molar** state variables are variables that are based to the mass  $m$  (specific) or on the amount of a substance  $n$  (molar). They are also independent from the size of the system.
- **Thermic** state variables are pressure  $p$ , temperature  $T$  and specific volume and are coupled by the thermodynamic state equations.

$$F(p, T, v) = 0 \quad (2-1)$$

- **Caloric** state variables are specific inner energy  $u$  and specific enthalpy  $h$ . They are defined by the caloric state equations

$$f(u, T, v) = 0 \quad f(h, T, v) = 0 \quad (2-2)$$

- Specific entropy  $s$  is an independent state variable and is defined by an entropy state equation.

$$F(s, T, v) = 0 \quad (2-3)$$

#### 2.1.3 Thermodynamic process

If the thermodynamic balance becomes disrupted, e.g. by adding energy, the state of the thermodynamic system will change. This change is called a “process” and is accompanied with a transport of heat, work or mass over the borders of the system.

### 2.1.4 1<sup>st</sup> law of thermodynamics

The first law of thermodynamics reflects the conservation of energy. It states that energy of a system can neither be generated nor destroyed but only changes if energy is transported over the borders of the thermodynamic system. In the case of a closed system, energy can be transferred as heat  $Q$  and work  $W$ . In the case of an open system, energy can also be transported by mass transfer.

In its general form the 1<sup>st</sup> law of thermodynamics for a transient and open system is defined as follows:

$$\delta W_t + \delta Q_a + \sum_i dm_i(h_i + e_{ai}) = dU + dE_a \quad (2-4)$$

The left side of the equation describes the energy transferred over the borders of the system, such as technical work  $W$ , heat  $Q_a$  and the energies of the transferred mass flows  $m_i$ . On the right side of the equation the inner energies of the system are shown, such as the inner energy  $U$  and the external energy  $E_a$ . The external energy consists of potential and kinetic energy.

### 2.1.5 2<sup>nd</sup> law of thermodynamics

The 2<sup>nd</sup> law of thermodynamics states that natural processes such as heat transfer, mixing processes and friction processes are irreversible. This explicitly means that heat can only be transported from a body with a higher temperature to a lower one. To define the direction of energy transport it is necessary to introduce the state variable entropy. Entropy is a measure for the irreversibility of a process. Therefore, the 2<sup>nd</sup> law of thermodynamics can be defined as follows:

**In all natural systems irreversible entropy is generated:  $dS_{irr} \geq 0$**

## 2.2 Phase transition and aggregation states

All of the following equations, definitions and considerations are taken from [1] and [2].

For pure substances aggregation states and phase transitions are similar and therefore, they can be treated generally. By the help of the specific heat capacity, coherences between thermic and caloric state variables are defined. For solids and liquids it can be assumed that  $c_v \approx c_p \approx c$  as the change of density can be disregarded. For gases this assumption is not valid and therefore,  $c_v \neq c_p$ .

The change of aggregation states from solid to liquid and liquid to gaseous for a pure substance is shown in the T-s diagram in Figure 2-1 and takes place at constant pressure  $p$  and temperature  $T$ . For a change of aggregation, the heat of evaporation or condensation emerges.

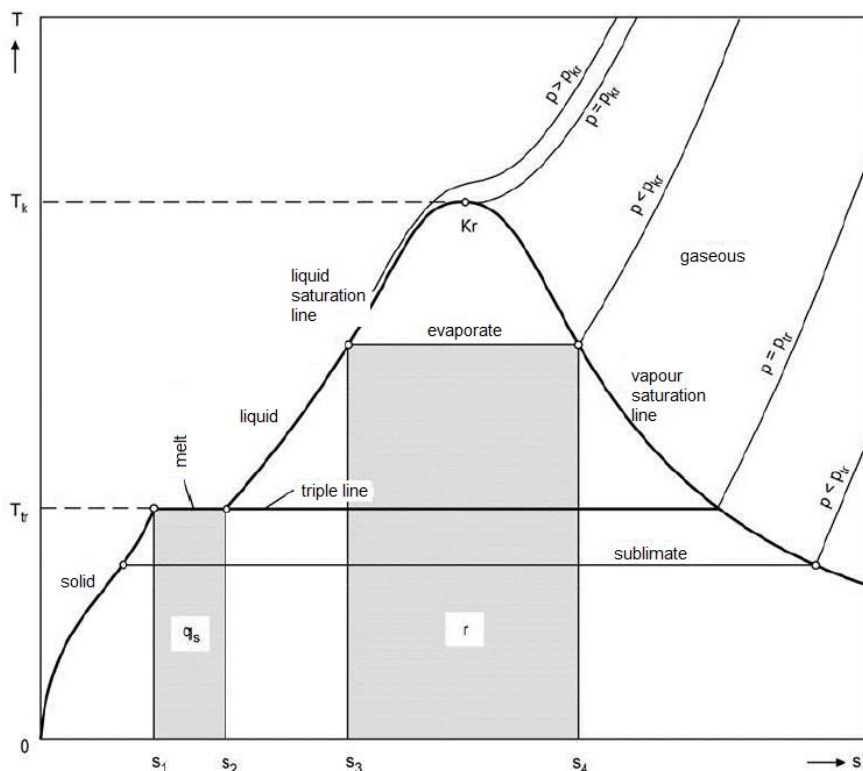


Figure 2-1: T-s – diagram of a pure substance [1]

### 2.2.1 Ideal gas

The assumption of ideal gas is per definition an idealisation but is valid for a wide range of gases, such as pure air and moist air. Moist air is actually a mixture between pure air and vapour. In the gas theory, the interaction of forces between the atoms is disregarded, apart from an exchange of momentum when the molecules collide with each other. The thermal state equation for ideal gases is defined as follows:

$$p * v = R * T \quad (2-5)$$

This ideal gas equation includes both, the laws from Boyle- Mariotte and Gay-Lussac.

The ideal gas equation points out that specific inner energy and specific enthalpy only depend on the temperature and therefore both specific heat capacities  $c_v$  and  $c_p$  can only vary with temperature but are independent of pressure. This leads to the following definitions:

$$u(T) = \int_{T_0}^T c_v(T) dT + u_0 \quad (2-6)$$

$$h(T) = \int_T^T c_p(T) dT \quad (2-7)$$

For further basic theory of ideal gases please refer to technical literature, such as [1]. Mixture of ideal gases; and particularly moist air; are described in the upcoming chapters.

### 2.2.2 Real gas

Real gases do not play a role in this master thesis but for the sake of completeness they are briefly described. Real gas calculations need to be carried out if temperatures and pressure levels are in regions where the enthalpy depends on temperature and pressure, e.g. two- phase area, and the assumption of ideal gas would lead to inaccurate results. Real gas behaviours can be calculated applying extensive equations and are described by approximations with mathematical approaches.

## 2.3 Mixture of ideal gases

All of the following equations, definitions and considerations are taken from [1] and [2].

As already described in the chapter of ideal gases forces, except for the momentum exchange between molecules and particles, can be neglected. This is also valid for a mixture of two or more ideal gases. It is assumed that each of the components occupy the same volume  $V$  and have the same temperature  $T$ . As all components satisfy to the law of ideal gases they have different specific volumes  $v_i$  and different (partial-) pressures  $p_i$ .

In Dalton's law it is defined as follows, the sum of all partial pressures  $p_i$  results in the total pressure  $p$ .

$$p = \sum_{i=1}^k p_i \quad (2-8)$$

The composition of a mixture of  $k$  ideal gases can be defined in three different ways:

1. Definition of mass- shares

$$\mu_i = \frac{m_i}{m} ; \quad \sum_{i=1}^k \mu_i = 1 \quad (2-9)$$

2. Definition of mole- shares

$$v_i = \frac{n_i}{n} ; \quad \sum_{i=1}^k v_i = 1 \quad (2-10)$$

3. Definition of volume- shares

$$\varphi_i = \frac{V_i}{V} ; \quad \sum_{i=1}^k \varphi_i = 1 \quad (2-11)$$

For ideal gases, the volume- share equals the mole-share. Therefore, the specific caloric state variables can be defined as follows:

$$u = \sum_{i=1}^k \mu_i * u_i \quad (2-12)$$



$$h = \sum_{i=1}^k \mu_i * h_i \quad (2-13)$$

$$c_v = \sum_{i=1}^k \mu_i * c_{vi} \quad (2-14)$$

$$c_p = \sum_{i=1}^k \mu_i * c_{pi} \quad (2-15)$$

### 2.3.1 Moist air

Moist air is a mixture of dry air (pure air) and vapour at moderate pressures and temperatures and it is one of the most important compositions of ideal gases. Dalton's law is valid.

$$p = p_a + p_v \quad (2-16)$$

An important property of moist air is that in a closed system and a given composition the amount of dry air does not change, while the vapour content can change due to condensation or evaporation. Therefore, it is appropriate to refer specific values of the mixture on 1kg of dry air instead on 1kg mixture. The degree of humidity  $x$  can therefore, be defined as follows:

$$x = \frac{m_v}{m_a} \quad (2-17)$$

For dry air the law for ideal gases is valid.

$$p_a * V = m_a * R_a * T \quad (2-18)$$

In working ranges of temperatures  $t < 100^\circ\text{C}$  and until the vapour saturation line the vapour can be assumed as ideal gas as well.

$$p_v * V = m_v * R_v * T \quad (2-19)$$

The properties of saturated air can be looked up in tables or charts. For all temperatures, a partial pressure of saturation  $p_v'(t)$  is assigned at which condensation starts or evaporation takes places. A mixture of air and vapour is designated as saturated if its' relative humidity  $\varphi = 1$  if the actual vapour pressure  $p_v$  equals  $p_v'(t)$ . Relative humidity is defined as the quotient of the actual partial pressure of vapour and the saturated vapour pressure.

$$\varphi = \frac{p_v}{p_v'(t)} \quad (2-20)$$

The partial pressure of saturation cannot be exceeded. Excess vapour is condensed and takes place along the vapour saturation line of the T-s diagram, as shown in Figure 2-1.

## 2.4 Principles of fluid dynamics

In the following chapter the principles of fluid dynamics are briefly presented to understand the coherences between thermodynamic and fluid dynamics. For deeper reflection and mathematical derivation, a reference is made to the relevant literature. All of the following assumptions and formulas are based on [3].

In most technical problems, it is not sufficient to work with just the 1<sup>st</sup> and 2<sup>nd</sup> law of thermodynamics. Most processes working with fluids can only be appropriately described by the mechanics of fluids, e.g. heat transfer. To describe physical quantities in time and place it is necessary to define the conservation equations for mass, momentum and energy.

The following definitions are based on a fixed control volume with timewise constant volume  $dV$  and timewise constant surface  $dO$ .

### 2.4.1 Continuity equation

Based on the axiom that mass can neither be generated nor demolished, the continuity equation integral form is defined as follows:

$$\int_V \frac{\partial \rho}{\partial t} dV = - \int_O (\rho \vec{v} \cdot \vec{n}) dO \quad (2-21)$$

In differential form the equation of continuity can be defined as:

$$\frac{\partial \rho}{\partial t} + (\vec{\nabla} \cdot \rho \vec{v}) = 0 \quad (2-22)$$

In words the equation of continuity can be defined as follows:

$$\left( \begin{array}{c} \text{timewise change of mass within} \\ \text{the control volume} \end{array} \right) + (\text{mass influx}) - (\text{mass outflux}) = 0$$

### 2.4.2 Momentum equation

The timewise change of momentum is attributable to the forces acting on the surface and volume forces on the control volume. The momentum is a vectorial quantity and therefore, an equation can be defined for each direction x, y and z.

In integral form the equation of momentum is defined as follows:

$$\begin{aligned} \int_V \frac{\partial}{\partial t} (\rho \vec{v}) dV + \int_O \rho \vec{v} (\vec{v} \cdot \vec{n}) dO \\ = \int_O -p \vec{n} dO + \int_O \vec{\tau}_x \vec{n}_x dO + \int_O \vec{\tau}_y \vec{n}_y dO + \int_O \vec{\tau}_z \vec{n}_z dO \\ + \int_V \rho \vec{f}^B dV \end{aligned} \quad (2-23)$$

In differential form for all three coordinate directions:

$$\frac{\partial \rho u}{\partial t} + (\vec{\nabla} \cdot \rho u \vec{v}) = -\frac{\partial p}{\partial x} + \frac{\partial \tau_{xx}}{\partial x} + \frac{\partial \tau_{yx}}{\partial y} + \frac{\partial \tau_{zx}}{\partial z} + \rho f_x^B \quad (2-24)$$

$$\frac{\partial \rho v}{\partial t} + (\vec{\nabla} \cdot \rho v \vec{v}) = -\frac{\partial p}{\partial y} + \frac{\partial \tau_{xy}}{\partial x} + \frac{\partial \tau_{yy}}{\partial y} + \frac{\partial \tau_{zy}}{\partial z} + \rho f_y^B \quad (2-25)$$

$$\frac{\partial \rho w}{\partial t} + (\vec{\nabla} \cdot \rho w \vec{v}) = -\frac{\partial p}{\partial z} + \frac{\partial \tau_{xz}}{\partial x} + \frac{\partial \tau_{yz}}{\partial y} + \frac{\partial \tau_{zz}}{\partial z} + \rho f_z^B \quad (2-26)$$

In words the equation of momentum can be written as:

$$\begin{aligned} & \left( \begin{array}{l} \text{timewise change of impulse} \\ \text{within the control volume} \end{array} \right) + (\text{outgoing impulse}) - (\text{incoming impulse}) \\ & \text{equals all forces acting on the surfaces and in the volume} \end{aligned}$$

Applying Stokes' law for Newtonian fluids:

$$\rho \left[ \frac{\partial u}{\partial t} + (\vec{v} \cdot \vec{\nabla})u \right] = -\frac{\partial p}{\partial x} + \mu \left( \frac{\partial^2 u}{\partial x^2} + \frac{\partial^2 u}{\partial y^2} + \frac{\partial^2 u}{\partial z^2} \right) + \rho f_x^B \quad (2-27)$$

$$\rho \left[ \frac{\partial v}{\partial t} + (\vec{v} \cdot \vec{\nabla})v \right] = -\frac{\partial p}{\partial y} + \mu \left( \frac{\partial^2 v}{\partial x^2} + \frac{\partial^2 v}{\partial y^2} + \frac{\partial^2 v}{\partial z^2} \right) + \rho f_y^B \quad (2-28)$$

$$\rho \left[ \frac{\partial w}{\partial t} + (\vec{v} \cdot \vec{\nabla})w \right] = -\frac{\partial p}{\partial z} + \mu \left( \frac{\partial^2 w}{\partial x^2} + \frac{\partial^2 w}{\partial y^2} + \frac{\partial^2 w}{\partial z^2} \right) + \rho f_z^B \quad (2-29)$$

These are named the ‘‘Navier- Stokes’’ equations.

### 2.4.3 Equation of energy

Timewise change of the total energy (kinetic, potential and inner energy) of a control volume equals the sum of the work of the external forces, the heat transfer and the energy gained by inner heat sources.

The integral form of the equation of energy can therefore, be defined as follows:

$$\begin{aligned} & \int_V \frac{\partial}{\partial t} \left[ \rho \left( e + \frac{\vec{v}^2}{2} \right) \right] dV + \int_O \rho \left( e + \frac{\vec{v}^2}{2} \right) (\vec{v} \cdot \vec{n}) dO \\ & = \int_V (\rho \vec{v} \cdot \vec{f}^B) dV - \int_O (p \vec{v} \cdot \vec{n}) dO + \int_O (\vec{v} \cdot \vec{\tau}_x) n_x dO \\ & + \int_O (\vec{v} \cdot \vec{\tau}_y) n_y dO + \int_O (\vec{v} \cdot \vec{\tau}_z) n_z dO - \int_O (\vec{q} \cdot \vec{n}) dO + \int \dot{q}_Q dV \end{aligned} \quad (2-30)$$

In differential form:

$$\begin{aligned}
& \frac{\partial}{\partial t} \left[ \rho \left( e + \frac{\vec{v}^2}{2} \right) \right] + \left( \vec{\nabla} \cdot \rho \vec{v} \left( e + \frac{\vec{v}^2}{2} \right) \right) \\
& = \rho (\vec{v} \cdot \vec{f}^B) - (\vec{\nabla} \cdot \rho \vec{v}) + \frac{\partial}{\partial x} (u\tau_{xx} + v\tau_{xy} + w\tau_{xz}) \\
& + \frac{\partial}{\partial y} (u\tau_{yx} + v\tau_{yy} + w\tau_{yz}) + \frac{\partial}{\partial z} (u\tau_{zx} + v\tau_{zy} + w\tau_{zz}) - (\vec{\nabla} \cdot \vec{q}) + \dot{q}_Q
\end{aligned} \tag{2-31}$$

In words the equation of energy can be described as

$$\begin{aligned}
& \left( \begin{array}{c} \text{timewise change of energy} \\ \text{within the control volume} \end{array} \right) + \left( \begin{array}{c} \text{outgoing} \\ \text{energy flux} \end{array} \right) - \left( \begin{array}{c} \text{incoming} \\ \text{energy flux} \end{array} \right) = \\
& = \left( \begin{array}{c} \text{power of the} \\ \text{outer forces} \end{array} \right) + \left( \begin{array}{c} \text{heat transfer through} \\ \text{conduction} \end{array} \right) + \left( \begin{array}{c} \text{inner} \\ \text{heat sources} \end{array} \right)
\end{aligned}$$

## 2.5 Heat transfer [3], [4]

Energy can be transferred by interaction from a system to its environment. From the 2<sup>nd</sup> law of thermodynamics it is known that heat can be transferred only from objects with higher temperatures to those with lower ones. This means that heat transfer is a result of a temperature gradient. There are three different possibilities to describe the heat transfer:

- Heat conduction
- Convection
- Heat radiation

In the following sections these three possibilities are described in a basic way. For deeper understanding please refer to the relevant literature.

### 2.5.1 Heat conduction

Considerable heat conduction occurs in fluids or solids. The reasons for this can be explained through microscopical consideration. Heat conduction arises due to impact of particles with different kinetic energies, which is equivalent to different temperature. Energy is transferred from particles with higher kinetic energy to particles with lower kinetic energy. In solids and fluids, the distances between particles are small and therefore, the impacts take place statistically more often than in the gaseous phase, where the distance between the particles is larger.

For solids and fluids the heat conduction can be described by the following simplified energy equation:

$$\frac{\partial T}{\partial t} = \frac{\lambda}{\rho c} \left( \frac{\partial^2 T}{\partial x^2} + \frac{\partial^2 T}{\partial y^2} + \frac{\partial^2 T}{\partial z^2} \right) + \frac{\dot{q}_q}{\rho c} \tag{2-32}$$

### 2.5.2 Convection

Energy is not only transported by heat conduction but also by the use of a flow in a fluid or gas. This is called convection and consists of two components, firstly the molecular motion and secondly the macroscopical fluid motion. The fluid motion moves the molecules and with it the temperature difference and therefore, the heat transfer is increased.

### 2.5.3 Heat radiation

All bodies that have a temperature  $T > 0\text{K}$  emit heat radiation in the form of electromagnetic radiation. With increasing temperature the amount of emitted heat increases by the power of four. Therefore, a heat flux from bodies with a higher temperature to bodies with lower temperature arises. As described, this effect takes place for all bodies but only of importance when working with high temperatures, respectively temperature differences.

## 2.6 Heat transfer by phase change

Another way of transferring heat between two systems (elements, molecules, ...) is by phase change. For this project only condensation (from gaseous to fluid phase) is relevant, ergo, only this method is described in greater detail. For the sake of completeness, it is noted that phase change also occurs by sublimation/re-sublimation (from gaseous to solid and reverse), melting/congelation (from solid to fluid and reverse) or evaporation (from liquid to gaseous).

### 2.6.1 Condensation [4]

Condensation of a pure substance takes place without temperature change, as in all other phase changes as well. The energy transfer is confined with the latent heat that gets free and is submitted over the border of the system to its surroundings. The heat transfer is dominated by convection due to the movement in the fluids and in the gaseous phase. Condensation has a wide range of applications in energy and process engineering. There are three possibilities of condensation that are of technical importance:

- Surface condensation

Condensation appears at a wall with a temperature lower than the saturation temperature:  $T_w < T_{sat}$

- Homogeneous condensation

Condensation appears through a decrease of pressure  $p$ , which leads to a decrease of saturation temperature  $T_{sat}$

- Spray condensation (direct contact condensation)

Cooling of gaseous phase appears by direct contact with fluid phase as shown in Figure 2-2.

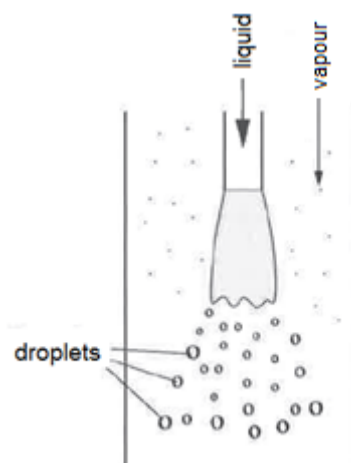


Figure 2-2: Spray condensation [4]

For this master thesis only spray condensation is of relevance, ergo, only this method is described in further detail. For the other two methods of condensation please be referred to technical relevant literature, such as [4].

## 2.6.2 Spray condensation

Spray condensation describes the transition of the gaseous phase by direct contact with the fluid phase. If the gaseous phase comes in contact with a droplet of a temperature that is below saturation temperature, then condensation can take place. Therefore, the fluid is sprayed, in most applications in small droplets, into the gaseous phase and condensation takes place at the surface of the atomized droplets. The gaseous phase can either be present as pure vapour or can be mixed with an inert gas, e.g. moist air which is the sum of dry air and vapour. [5]

The smaller the sprayed droplets are, the bigger the ratio gets of the droplet surface to the droplet mass. With a higher surface area, the condensation takes place faster and more effectively. [8]

All of the following text passages are from [7]. Spray condensation is used in a wide range of technical applications. There are many advantages compared to the condensation on a solid surface, such as low investment costs, resilience against surface contamination and high heat transfer due to high surface to volume ratio. As a disadvantage, it must be mentioned that spray condensation is invalid in applications where it is not allowed to mix the spray with the gaseous phase.

Disregarding the heat transfer to the surroundings (adiabatic system), the energy equation for spray condensation can be written as follows:

$$\frac{dU}{dt} = (\dot{H}_{l,in} + \dot{H}_{g,in}) - (\dot{H}_{l,out} + \dot{H}_{g,out}) \quad (2-33)$$

In this equation  $\dot{H}_{l,in}$  and  $\dot{H}_{l,out}$  are the enthalpy flows of the cooling liquid, and  $\dot{H}_{g,in}$  and  $\dot{H}_{g,out}$  are the enthalpy flows of the gaseous phase, respectively the mixture of vapour and inert gas. The change of inner energy in time  $dU/dt$  of the spray condensation needs to be only observed at transient calculations.

Under the assumption of constant substance values, and in the case of a steady state process, the heat transferred to the cooling spray is defined as:

$$\dot{Q} = \dot{m} * c_p * (T_{out} - T_{in}) \quad (2-34)$$

The maximum transferable heat is defined as:

$$\dot{Q}_m = \dot{m} * c_p * (T_S - T_{in}) \quad (2-35)$$

With equation (2-34) and (2-35) the dimensionless end temperature of the condensate-spray mixture can be defined. This quotient is also known as heating figure:

$$\bar{\theta} = \frac{(T_{out} - T_{in})}{(T_S - T_{in})} \quad (2-36)$$

### 2.6.2.1 Heat transfer on a single droplet [7]

As the surface of the cooling spray is large the highest possible heat transfer can be reached if the condensation takes place at a single droplet. The most important application for this is the condensation of vapour (gaseous water) at the surface of liquid droplets. Most of the calculations and estimated methods are based on the assumption that the diameter can be assumed to stay constant and the heat transfer resistance is negligible. Another common simplification is that droplets do not affect each other. With increased relative velocity between the liquid droplets and the vapour, the heat transfer increases as well. The increased

heat transfer can be explained by the oscillation of the droplets and the flow in the droplet. On the other hand, high condensation rates can lead to decreased heat transfer.

In [7] an example clarifies important coherences that are shown in Figure 2-3 and Figure 2-4. In this example the speed of the steam flow is 2m/s, droplets are sprayed normal to the flow with a velocity of 6m/s, saturation temperature is assumed to be 40°C. None of the parameters are changed during the process.

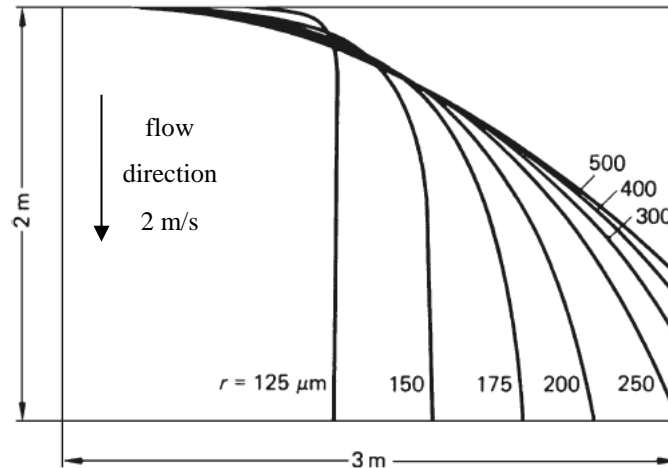


Figure 2-3: Trajectory of droplets in dependence of the radius [7]

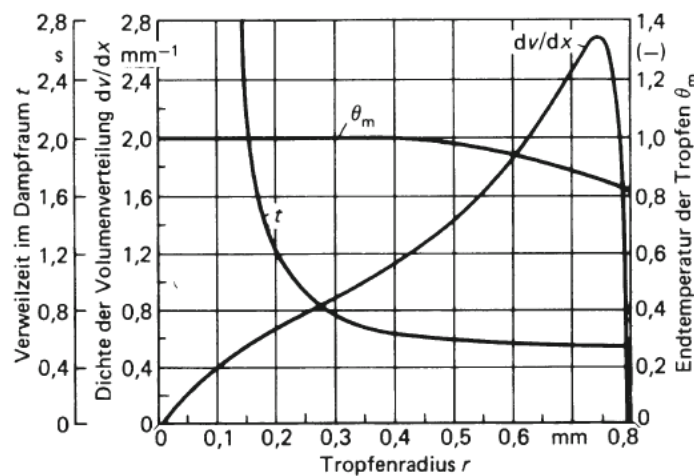


Figure 2-4: End temperature  $\theta_m$ , dwell time  $t$  and volume share  $dv/dx$  of the droplets [7]

Figure 2-3 shows that droplets with larger radii are less redirected from the flow.

One important finding shown in Figure 2-4 is that  $\theta_m$ , which is comparable with  $\bar{\theta}$  from equation (2-36), is 1 over a wide range of radius and decreases with larger radii. This means for a radius smaller than 0,4mm the heat transferred from the vapour flow to the droplets is at a maximum. With higher droplet diameters the heat transfer decreases below its maximum possible value. Dwell time decreases with increased radii of the droplets.

### 2.6.2.2 Condensation in the presence of an inert gas

In Figure 2-5 the influence of the inert gas share  $y_{D,G}$  on the heat transfer  $k'$  is shown. It shows that even the presence of small amounts of inert gas, e.g. pure air, leads to a remarkable decline of the heat transfer compared to the case of pure vapour. Furthermore, it is obvious

that a higher flow speed increases the heat transfer. [6]

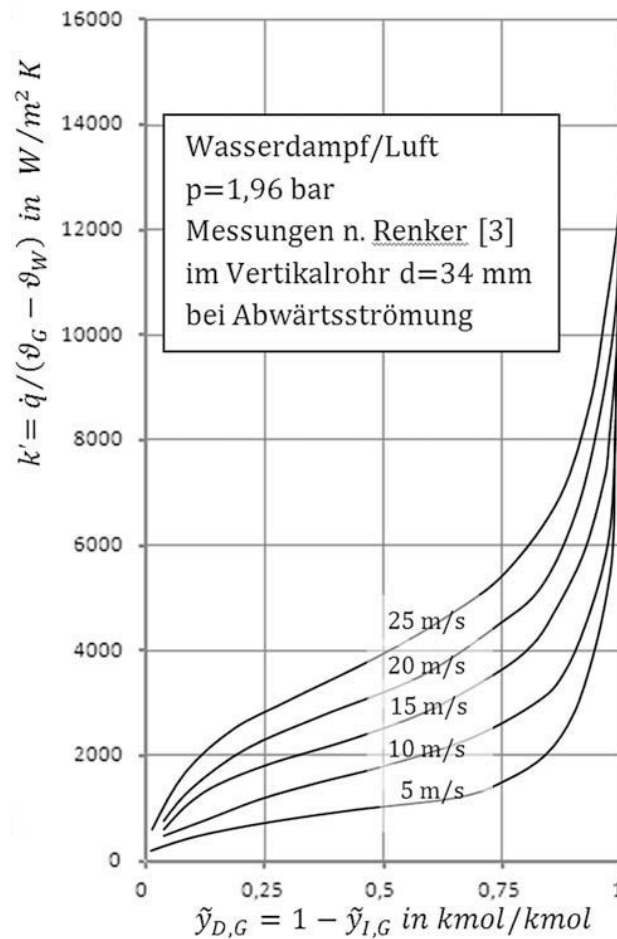


Figure 2-5: Influence of the inert gas share on the heat transfer [6]

Figure 2-6 shows the influence of the presence of the inert gas air to the condensation rate. At the x-axis the mass content of air is plotted. On the y-axis a temperature ratio is plotted, where  $T_D$  is the saturation temperature of the steam in the flow,  $T_{Ph}$  is the saturation temperature at the phase boundary and  $T_{Ein}$  is the incoming temperature of the sprayed droplets.

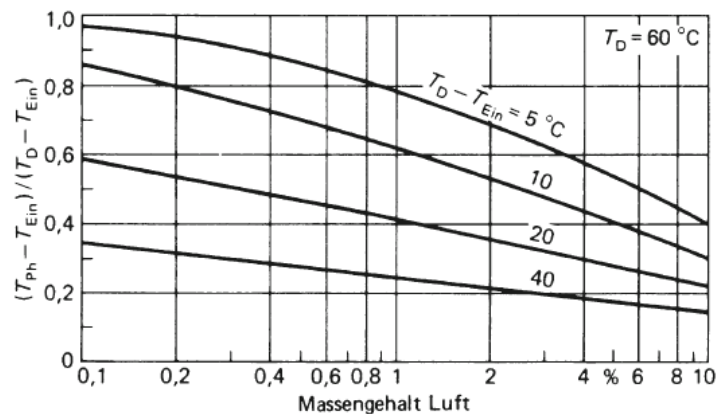


Figure 2-6: Influence of air on the condensation of vapour (gaseous water) [6]

Likewise, in this chart it is obvious, that condensation speed dramatically decreases with the presence of even small mass shares of air in the vapour.



### 3 Thermodynamic consideration of the vacuum system

As already defined in the introduction from Andritz, and after a literature review, no alternatives to the sprayed water droplets to cool a large air flow of up to several 100 m<sup>3</sup>/min on a technical and economical reasonable way was identified.

A heat exchanger is mentioned at this point as a dissatisfactory example for a technical and economical solution. To reach a high heat transfer, the heat exchanger needs to be in direct contact with the hot vacuum flow and therefore, it needs to be implemented directly into the piping. As the flow can contain fibres and other small dirt contaminants, the heat exchanger would be covered with a layer after a few hours of operation time and the heat transfer coefficient between the moist air flow, and as a result, the heat exchange would decrease dramatically. As most of the machines run for weeks or even months on end until they are shut down again for maintenance work, from a technical point of view a heat exchanger is a poor solution. Furthermore, high effort would be necessary for cleaning the heat exchanger, which results in higher customer operational and maintenance costs.

Due to the above mentioned arguments, an economically and technically reasonable solution is to cool the air flow with injected droplets. The sprayed water is heated up due to latent and sensible heat transfer from the hot moist air flow. The heated droplets can be reused in the further process and therefore, the transferred heat does not get lost. An investigation of possible usage of the heated spray water in the further process was not part of this master thesis. All of the following considerations are based on the assumption that the cooling system is realized with droplets that are sprayed directly into the moist air flow.

For a better understanding, the vacuum system of a standard dewatering machine is introduced in the following chapter. Built up on that, the thermodynamic process is mathematically described and the theoretical background is presented.

#### 3.1 Overview of the vacuum system

For a better understanding of the vacuum system Figure 3-1 shows the schematic of a vacuum flow system.

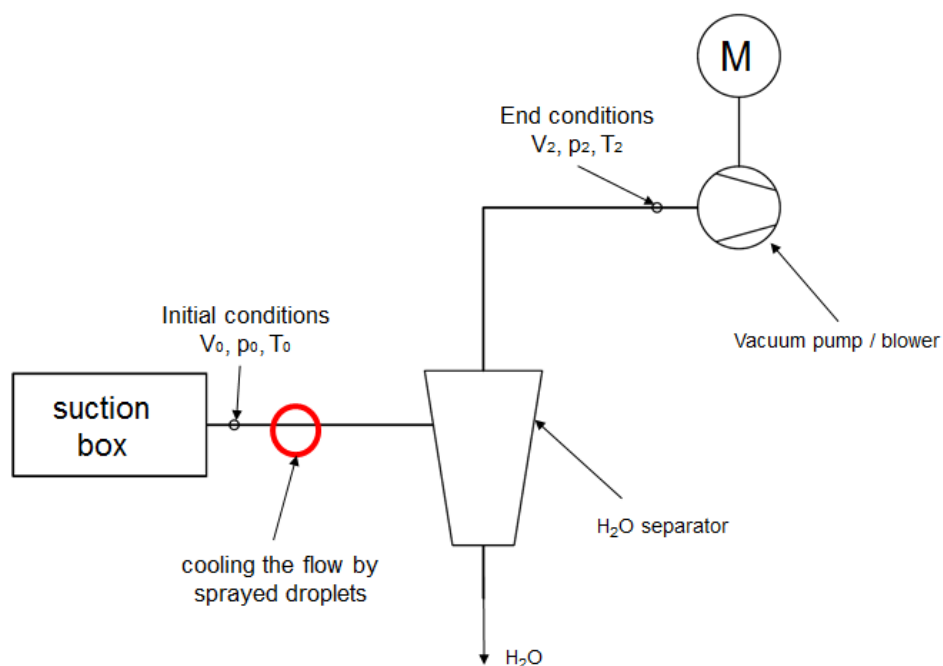


Figure 3-1: Schematic overview of the process for cooling the moist air flow

As already described in the introduction, vacuum is used in many sections of the dewatering machine. The schematic structure and the process are similar for all vacuum applied positions. The main components are the vacuum box (Figure 3-2), the water separator (Figure 3-3) and the vacuum pump (Figure 3-4), or the blower together with the drive. They are connected to each other by a piping system.

### Suction Box

The aim of the suction box is to dewater the pulp sheet or to dewater/unload the felts. Therefore, different vacuum levels and air flows are used. Process water, moist air and eventually vapour, additional to the vapour in the moist air, are drawn into the suction box. At this point the initial conditions  $V_0, p_0$  and  $T_0$  can be measured. For the cooling system, the process water and the additional vapour should not be considered, according to Andritz, and therefore, it can be assumed that only highly saturated moist air is present for thermodynamic considerations.

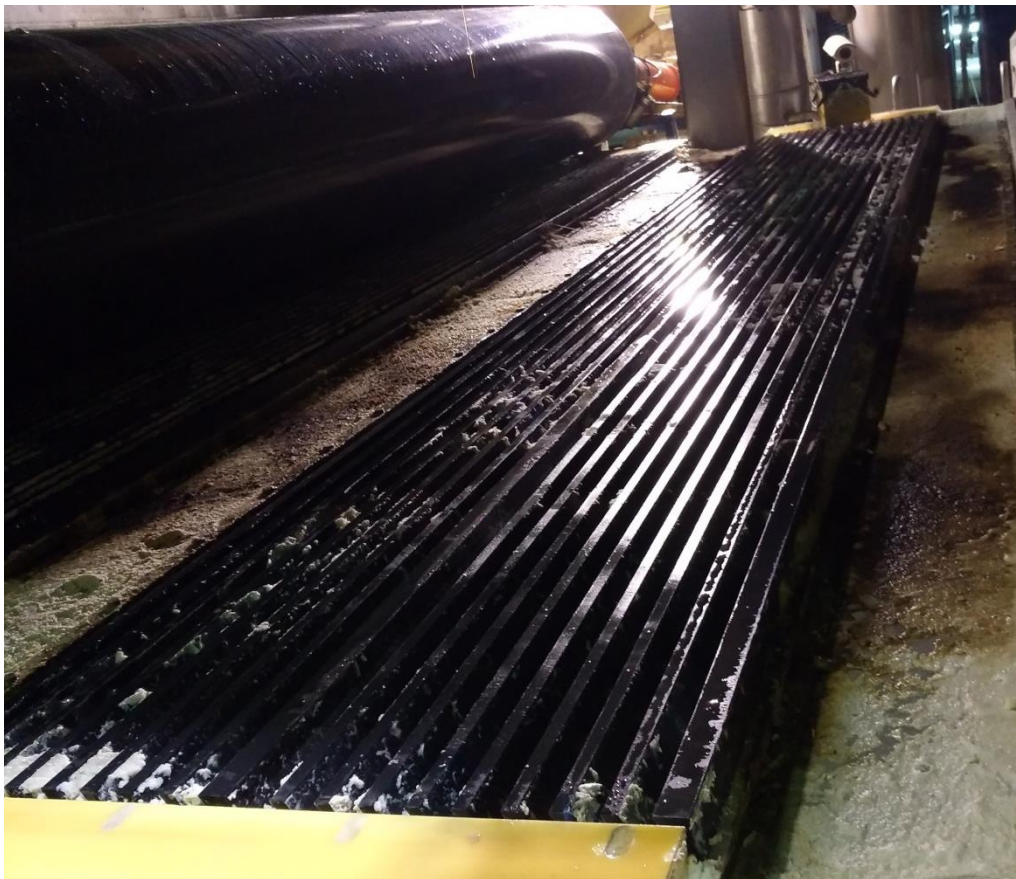


Figure 3-2: Typical linings of the suction box of a dewatering machine [17]

### Water separator

The aim of the water separator is to separate the liquid process water, that comes from the dewatering process. The water in the case of the installation of the cooling spray also needs to be separated by the separators. The separated water is accumulated in the so called “white water tank” and is reused in the dewatering process. The (moist) air is sucked through the separator and heads forward to the vacuum pump or blower.



Figure 3-3: Typical water separators of a dewatering machine [17]

### **Vacuum pump/blower**

Depending on the application, vacuum pumps or blowers are used for vacuum generation. Vacuum pumps are not sensitive to droplets in the sucked air flow, while blowers on the other hand, are much more sensitive to droplets in the vacuum flow. The trend shows that blowers are used for more applications as they are cheaper to install. So, it is important that the droplets transported to the vacuum generators are reduced to a minimum and all the process water, and the sprayed droplets, are led away as much as possible in the water separator.

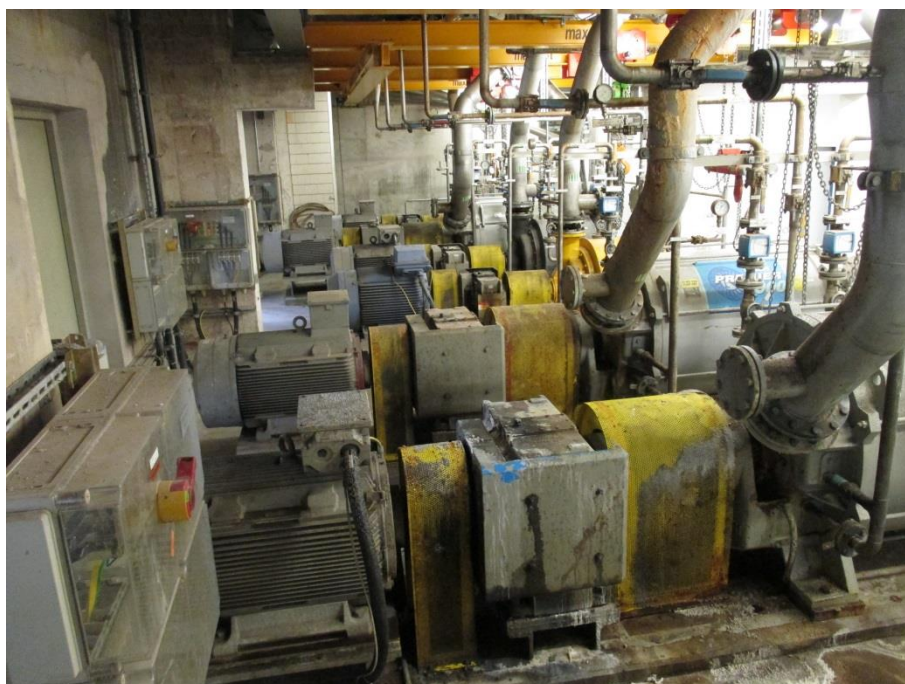


Figure 3-4: Typical vacuum pumps (incl. drive) for a standard dewatering machine [17]

### 3.1.1 Location of the cooling system

As shown in Figure 3-1, the cooling system of the vacuum flow is assumed to be installed in the pipe between the suction box and the water separator. The reason for this is that cooling already in the suction box might result in negative effects on the dewatering properties of the suction box and is therefore, not allowed. The first possible position for injecting the cooling spray is at the beginning of the pipe after the suction box. As there is a high amount of cooling spray water necessary to cool the vacuum flow, the process needs to be completed at the water separator due to the requirement that there exists only a minimum of water droplets in the flow to the vacuum pumps/blowers, resulting that the time available for condensation is limited. It is defined by the velocity of the flow and the length of the pipe between the vacuum box and the water separator.

### 3.2 Thermodynamic model

Before getting into details about how to cool a moist air flow in the vacuum pipes, the thermodynamic and economic saving potential of a cooling system is provided in the following chapter. For this purpose the mathematic model is presented. All of the following formulas and the thermodynamic procedure are taken from [1] and [9]. Not all steps are explained in detail. For this purpose, reference is either made to chapters 2.2 and 2.3 or to relevant literature such as [1] and [9]. The thermodynamic model is shown in Figure 3-5.



Figure 3-5: Model and boundaries of the thermodynamic system

The system is considered to be adiabatic to the environment, only the heat transfer from the vacuum flow to the sprayed droplets is present. Furthermore, the system is open, heterogeneous and can be assumed to be in a steady state.

The flow that should be cooled is moist air, a mixture of dry air and vapour, with a relative humidity  $\varphi$  of almost, or even, 1. Hereinafter the “dry air” is declared as “air”. As described in the theory part, the moist air can be considered as a mixture of two separate ideal gases. Once only the process of the vapour (gaseous water) is considered, the thermodynamic change of state can be divided in two separate steps as shown in Figure 3-6.

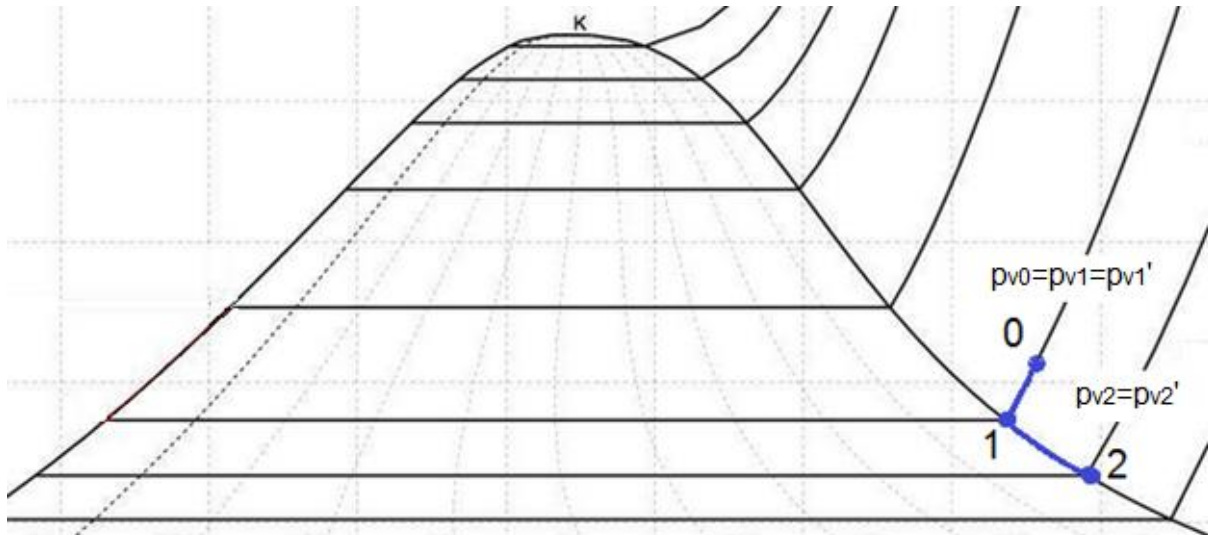


Figure 3-6: Ts diagram for water

- 0 → 1: Cooling along an isobar flow until  $\varphi=1$  (saturated vapour)
- 1 → 2: Condensation on the surface of the sprayed droplets along the vapour saturation line

The reduction of volumetric flow can be divided in two shares as well. The first share is the decrease of the specific volume, due to the lower temperature that only represents a small share of the volumetric reduction. It takes place along the whole process from 0 to 2. The main share is the condensation of the vapour in the moist air, which only occurs in the second step from 1 to 2.

The initial conditions at the state 0, the temperature  $T_0$ , the relative humidity  $\varphi_0$ , the overall pressure  $p_0$  and the volumetric flow  $\dot{V}_0$  can be assumed as given. Additionally, the ideal gas constants for air  $R_a$  and for vapour  $R_v$  are available from [9].

The overall pressure  $p_0 = p_1 = p_2 = p$  is assumed to be constant along the whole process.

### 3.2.1 Process from 0 → 1: Cooling the flow until $\varphi=1$

This step occurs only if  $\varphi < 1$ . The moist air flow is cooled down on an isobar without condensation as long as  $\varphi < 1$ . That means that no mass transfer takes place in the process from 0 → 1. With the given initial conditions, this process is mathematically and thermodynamically described as follows:

The partial pressure at saturation  $p'_{v0}$  can be reviewed in [9].

$$p_{v0} = p'_{v0} * \varphi_0 \quad (3-1)$$

$$p_{a0} = p - p_{v0} \quad (3-2)$$

$$\dot{m}_{a0} = \frac{p_{a0} * \dot{V}_0}{R_a * T_0} \quad (3-3)$$

$$\dot{m}_{v0} = \frac{p_{v0} * \dot{V}_0}{R_v * T_0} \quad (3-4)$$

$$\dot{m}_0 = \dot{m}_{a0} + \dot{m}_{v0} \quad (3-5)$$

With the masses the degree of humidity can be defined.

$$x_0 = \frac{m_{v0}}{m_{a0}} \quad (3-6)$$

If no condensation takes place, the partial pressure  $p_v$  of the vapour and the mass of the steam in the flow are constant. The mass flow of air  $\dot{m}_{a0}$  is regardless constant along the whole process. As a result of that the degree of humidity stays constant as well, as long as no condensation takes places.

$$p_{v0} = p_{v1} = p'_{v1} \quad (3-7)$$

$$p_{a1} = p - p_{v1} \quad (3-8)$$

$$\dot{m}_{v0} = \dot{m}_{v1} \quad (3-9)$$

$$\dot{m}_{a0} = \dot{m}_{a1} = \dot{m}_{a2} = \dot{m}_a \quad (3-10)$$

$$\dot{m}_1 = \dot{m}_{a1} + \dot{m}_{v1} \quad (3-11)$$

$$x_0 = x_1 \quad (3-12)$$

With the partial pressure of saturation  $p'_{v1}$  from equation (3-7) the temperature  $T_1$  can be reviewed in [9] and the thermodynamic state at 1 can be defined.

$$\dot{V}_1 = \frac{R_a * \dot{m}_a * T_1}{p_{a1}} = \frac{R_v * \dot{m}_{v1} * T_1}{p_{v1}} \quad (3-13)$$

### Heat transfer from 0 → 1

As long as no condensation takes place, only sensible heat is transferred from the moist air to the injected droplets. The thermodynamic substance values  $c_w$ ,  $c_{pv}$  and  $c_{pa}$  are assumed to be constant, due to the low temperature differences along the whole process, and can also be reviewed in [9].

By simplification of the first law of thermodynamics from equation (2-4) the transferred heat can be written as:

$$\delta Q_a = dH \rightarrow \dot{Q}_{0 \rightarrow 1} = \dot{H}_1 - \dot{H}_2 \quad (3-14)$$

Integration and rearrangement of equation (3-14) result in a new form that is based on 1 kg of air mass flow  $\dot{m}_a$  in the system. The reference per kg of  $\dot{m}_a$  is useful as the mass of air is constant along the process. To redefine equation (3-14) the specific enthalpy based on 1 kg of air flow must be introduced whereby the derivation is omitted.

$$h_{i(1+x)} = c_{pa} * T_i + x_i * (\Delta h_c + c_{pv} * T_i) \quad (3-15)$$

In this case no condensation enthalpy occurs. Using equation (3-15) the transferred heat can be written as follows.

$$\dot{Q}_{0 \rightarrow 1} = (h_{1(1+x)} - h_{0(1+x)}) * \dot{m}_a \quad (3-16)$$

Seen from the moist air, the heat  $\dot{Q}_{0 \rightarrow 1}$  is negative as it is transferred away from the moist air. This means that the heat is submitted from the air flow to the sprayed droplets. In this stage only sensible heat is transferred, but no mass transfer takes places.

### 3.2.2 Process from 1 → 2: Condensation at the surface of the droplets

The next step of cooling and reduction of volumetric air flow continues with relative humidity of  $\varphi=1$ , that leads to condensation of vapour. For this project, it is assumed that there exists no further vapour apart from the vapour in the moist air. The condensation of the vapour in the moist air takes place along the vapour saturation line shown in the Ts diagram in Figure 2-1 and therefore,  $\varphi_2$  is defined as follows:

$$\varphi_1 = \varphi_2 = 1 \quad (3-17)$$

After the condensation process a certain temperature  $T_2$  will occur, which needs to be assumed for this step. With this temperature and the partial pressure of saturation  $p'_{v2}$  given in [9], together with equation (3-17), the partial pressure is defined as follows:

$$p_{v2} = p'_{v2} * \varphi_2 \rightarrow p_{v2} = p'_{v2} \quad (3-18)$$

With the constant overall pressure  $p$  the partial pressure of the air  $p_{a2}$  increases:

$$p_{a2} = p - p_{v2} \quad (3-19)$$

Applying equation (3-19) the volumetric flow  $\dot{V}_2$  and the condensed mass flow  $\Delta\dot{m}_{H_2O}$  is defined.

$$\dot{V}_2 = \frac{R_a * \dot{m}_a * T_2}{p_{a2}} \quad (3-20)$$

$$\dot{m}_{v2} = \frac{\dot{V}_2 * p_{v2}}{R_v * T_2} \quad (3-21)$$

$$\dot{m}_2 = \dot{m}_{v2} + \dot{m}_{a2} \quad (3-22)$$

$$x_2 = \frac{\dot{m}_{v2}}{\dot{m}_{a2}} \quad (3-23)$$

$$\Delta\dot{m}_w = (x_1 - x_2) * \dot{m}_a \quad (3-24)$$

The volumetric flow reduction due to the injection of the droplets can therefore, be defined as follows:

$$\Delta\dot{V} = \dot{V}_0 - \dot{V}_2 \quad (3-25)$$

### Heat transfer from 1 → 2

Additional to the sensible heat, the latent heat that results from the condensation is transferred from the moist air to the droplets. In addition to the above described substance properties, the enthalpy of condensation  $h_c$  is calculated assuming that the enthalpy of the vapour depends only on the temperature.

From the 1<sup>st</sup> law of thermodynamics the heat transfer can be calculated applying equation (3-16). For the calculation of the enthalpies  $h_{i(1+x)}$  it is referred to equation (3-15).

$$\dot{Q}_{1 \rightarrow 2} = (h_{2(1+x)} - h_{1(1+x)}) * \dot{m}_a \quad (3-26)$$

In the step 1 → 2 the main share of the transferred heat can be repatriated on the sensible heat transfer.

The overall heat transfer for the entire process is the sum of both heat transfers.

$$\dot{Q}_{0 \rightarrow 2} = \dot{Q}_{0 \rightarrow 1} + \dot{Q}_{1 \rightarrow 2} \quad (3-27)$$

### 3.2.3 Required amount of spray water

Until now only the process of the air flow was considered. The condensation heat for cooling the air flow is transferred to the sprayed droplets.

$$\dot{Q}_w = -\dot{Q}_{0 \rightarrow 2} \quad (3-28)$$

The process of heat transfer is comparable with a heat exchanger where both, the cooled and the cooling medium, have the same flow direction. The principle of an equal direction heat exchanger is shown in Figure 3-7 below:

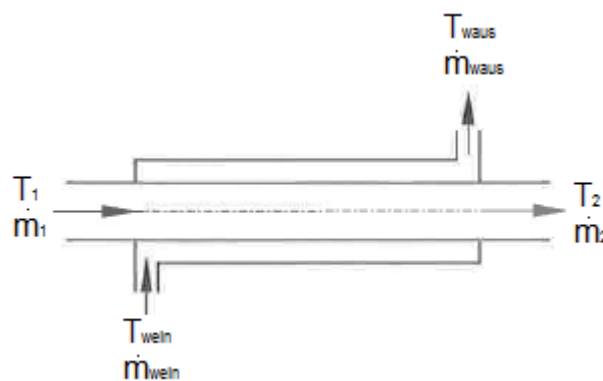


Figure 3-7: Equal direction heat exchanger [4]

Theoretically, the process takes place as long as no difference in temperature exists between cooled and cooling flow. Once both media have got the same temperature the process is finished, but thermodynamically this takes infinite time. Therefore, a difference in temperature will result at the end of the process as shown in Figure 3-8:

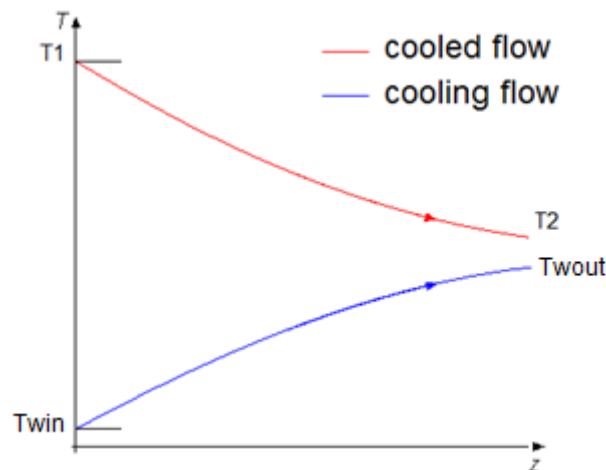


Figure 3-8: Temperature development of an equal direction heat exchanger [10]

The smaller the temperature difference between the cooled and the cooling flow (here: moist air flow and sprayed droplets) gets, the slower the heat transfer takes place.

The temperature of the droplets at the beginning of the process  $T_{win}$  is given by the temperature of the available cooling water. The temperature of the droplets at the end of the process  $T_{wout}$  results from the process, depending on the process parameters such as available



time, air flow temperatures, vacuum heights and more. Additionally, the heat conductance at the surface of the droplets is an important factor. As long as no calculation or measurements of the heat transfer are available the temperature at the end of the process  $T_{wout}$  needs to be estimated.

The amount of water necessary for the process can therefore, be defined as follows:

$$\dot{m}_w = \frac{\dot{Q}_w}{c_w * (T_{wout} - T_{win})} \quad (3-29)$$

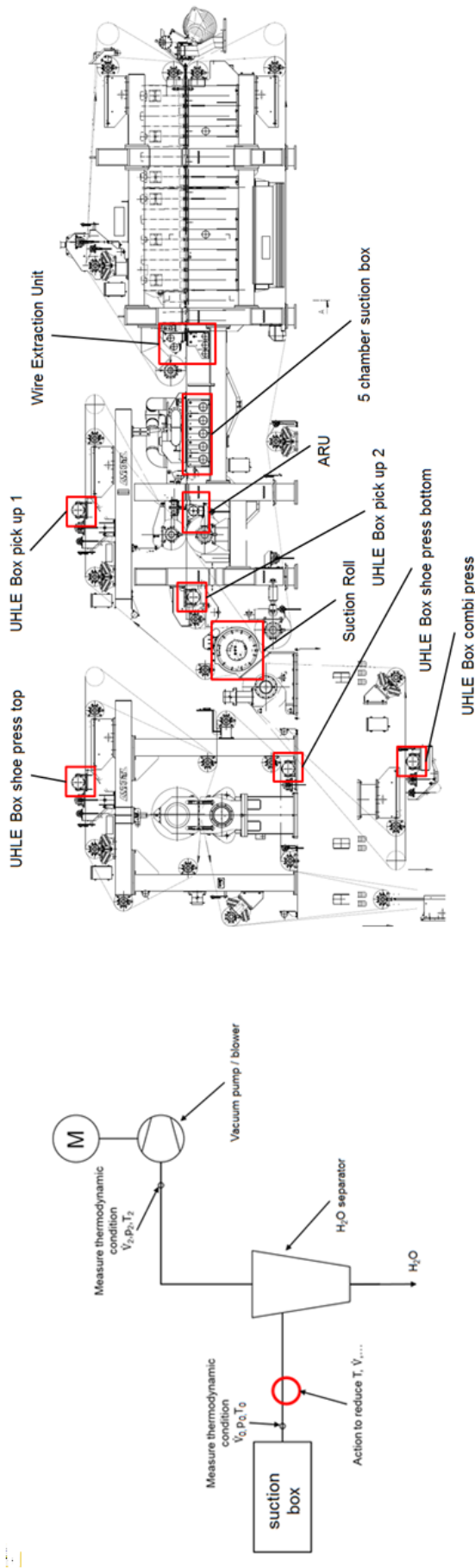
### 3.3 Thermodynamic saving potential

Based on the above described derivation of the cooling process the thermodynamic saving potential can be calculated for each point of a standard dewatering machine, which is shown in Figure 3-9.

As there are no actual measurements of the initial conditions available, the temperature and relative humidity for each vacuum applied position are estimated, based on measurements carried out approximately 10 years ago. The vacuum levels are based on measurements on machines carried out within the last few years.

The achieved temperatures at the end of the process are assumed exemplary, and a temperature difference between  $T_{wout}$  and  $T_2$  of 2°C is assumed. Furthermore, the cooling water inlet temperature is assumed with 15°C, they depend on the location of the mill.

Of course, the estimated end temperatures  $T_2$  and  $T_{wout}$  might be optimistic but at the very least, they show that there is a significant saving potential of up to 40%, depending on the vacuum applied position, for such a cooling technology. Even lower cooling effects and volumetric flow reductions may lead to lower investment costs but most certainly will result in decreasing operating costs, and therefore, can be profitable.



Input												
Start conditions	Top WEU	Bottom WEU	FSB 1	FSB 2	FSB 3	FSB 4	FSB 5	ARU/WSR	Suction Roll C1	Suction Roll C2	Uhle Box (5x)	
$V_0$	m3/min	13	25	27	28	39	45	56	265	257	515	
$t_0$	°C	60	60	65	65	65	65	65	55	55	50	
$\phi_0$	-	0.8	0.8	1	1	1	1	1	0.9	0.9	0.7	
$\Delta p_0$	bar	0.3	0.3	0.3	0.3	0.35	0.4	0.45	0.3	0.25	0.45	
$p_u$	bar	1	1	1	1	1	1	1	1	1	1	
End conditions												
$t_2$	°C	40	40	40	40	40	40	40	40	40	40	
$\Delta p_2$	bar	0.3	0.3	0.3	0.3	0.35	0.4	0.45	0.3	0.25	0.45	
Cooling water												
$t_{min}$	°C	15	15	15	15	15	15	15	15	15	15	
$t_{out}$	°C	38	38	38	38	38	38	38	38	38	38	
Results												
$m_{H_2O}$	kg/s	0.123	0.236	0.209	0.216	0.268	0.270	0.288	0.781	2.619	2.767	4.292
$m_{H_2O}$	kg/s	0.024	0.046	0.077	0.080	0.112	0.129	0.160	0.179	0.443	0.430	0.533
$X_0$	kg <sub>v</sub> /kg <sub>a</sub>	0.197	0.197	0.371	0.371	0.417	0.477	0.557	0.230	0.169	0.155	0.124
$\Delta V_{b-1}$	%	1.44%	1.44%	0.00%	0.00%	0.00%	0.00%	0.00%	0.72%	0.73%	0.73%	2.23%
$\Delta m_{H_2O-2}$	kg/s	0.014	0.028	0.061	0.063	0.089	0.104	0.131	0.118	0.238	0.229	0.090
$\Delta V_{0-2}$	%	18.87%	18.87%	33.51%	33.51%	35.78%	38.47%	41.74%	21.87%	14.94%	14.17%	5.66%
$\Delta Q_{0-2}$	kW	38.79	74.59	157.80	163.64	229.07	266.05	333.96	311.31	635.22	615.04	273.91
$m_{H_2O\_cool}$	kg/s	0.40	0.78	1.64	1.70	2.38	2.76	3.47	3.24	6.60	6.39	2.85

Figure 3-9: Thermodynamic saving potential at vacuum system for a standard TWF

### **3.4 Conclusion of thermodynamic saving potential**

After introducing the schematic of a vacuum system of a dewatering machine the thermodynamic model is presented and described mathematically. In this description, the process of volumetric flow reduction is divided in two steps. The first step only consists of sensible heat transfer but no mass transfer. In the second step, beside the sensible heat, also the latent heat transfer and the mass transfer occur due to condensation of the vapour in the moist air.

Based on the thermodynamic model presented, the possible volumetric flow reduction for each vacuum applied point for a dewatering machine is shown. Assuming the end temperature of the moist air flow after the cooling process for each vacuum applied position for a dewatering machine, a volumetric flow reduction of up to 40% can be reached. It is shown that the thermodynamic saving potential is significant.

## 4 CFD calculation

So far no considerations about how the cooling and condensation process takes place were provided, only the theoretical background and the theoretical saving potential were shown, based on the estimated temperatures. As there are many parameters that affect the volumetric flow reduction it was decided to build a CFD model to simulate the cooling and condensation process for the moist air flow system. For the CFD calculation the software ANSYS FLUENT 15.0 was used. As a User Defined Function (UDF) was necessary, the used operating system was Linux, as the compilation of UDFs works more stable than on other operating systems.

The advantage of a CFD simulation is that once a model is built up and verified, many simulations and therefore, the influence of many parameters, can be investigated on their effect in a short time. Compared to a large experimental investigation, a CFD calculation is not only less time consuming, but also much cheaper. The following parameters should be investigated with the CFD model:

1. Flow parameters
  - Vacuum level
  - Volumetric flow & flow velocity
  - Temperature of the moist air
  - Humidity of the moist air
2. Geometry parameters
  - Length of the pipe
  - Shape of the pipe
3. Spray parameters
  - Spray directions
  - Size of the droplets
  - Pressure, volume flow and velocity of the sprayed droplets
  - Temperature of the cooling water

### 4.1 Setup of the condensation model

The setup of the condensation model is carried out referring to [14]. They presented a CFD calculation that is comparable to the case in this master thesis. In [14] the condensation of moist air in the presence of sprayed droplets was analysed with the software ANSYS FLUENT. Droplets were sprayed into the channel against the direction of the moist air flow and condensation was enforced. The schematic of the model is shown below in Figure 4-1:

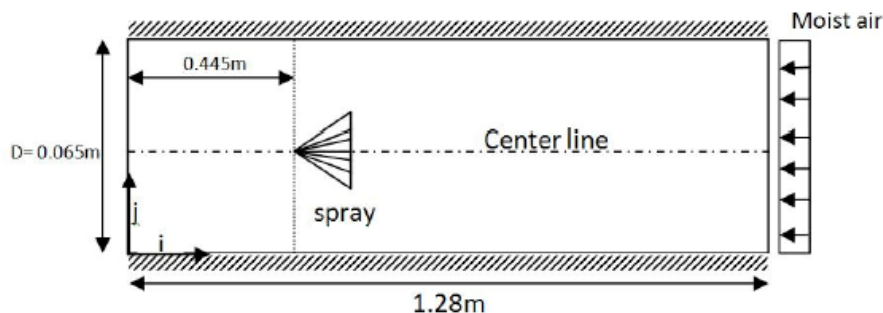


Figure 4-1: Schematic for the spray dryer [14]

They did a variation of droplet diameter, adjusted the amount of sprayed water and compared the effect on the volumetric flow. The main difference between their model and the task given in this master thesis, was the size of the system. While [14] were working with spray rates between 0,003 kg/s and 0,006 g/s in this master thesis the required spray rates are in a range between 0,4 kg/s, and up to, 7 kg/s.

For solving this complex issue in this master thesis the energy equation was enabled in ANSYS FLUENT. The k- $\epsilon$  turbulence model was applied, as this is used for fully developed flows with high Reynolds numbers. The k- $\epsilon$  model was used in [14] as well. In order to implement the water droplets the discrete phase model was used.

#### 4.1.1 Lagrange vs Euler approach

For solving this kind of problem, it is necessary to distinguish between the Lagrangian and the Eulerian approach. The following section is taken from [4].

The Lagrangian approach works with mass fixed coordinates and the particles or elements are tracked on their way through the control volume (CV). Individually tracking each particle through the CV costs a lot of computational power.

$$\mathbf{X} = \begin{pmatrix} X \\ Y \\ Z \end{pmatrix} \quad (4-1)$$

On the other hand the Eulerian approach works with space fixed coordinates. Only the influx and outflux are detected but not their way through the CV.

$$\mathbf{x} = \begin{pmatrix} x \\ y \\ z \end{pmatrix} \quad (4-2)$$

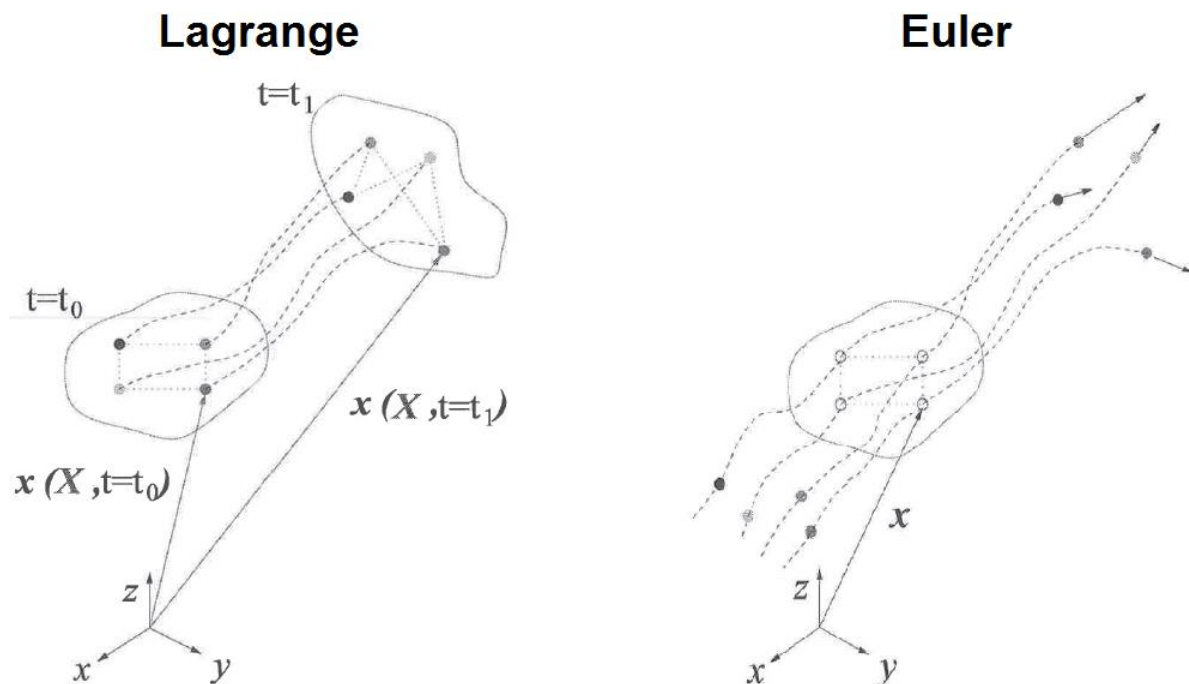


Figure 4-2: Lagrangian vs. Eulerian approach

The Eulerian approach can be construed as an actual position of the Lagrangian coordinates.

Since the volume of water droplets sprayed into the vacuum flow is quite low compared to the moist air flow, it is expedient to use a Lagrangian instead of an Eulerian model for tracking the droplets on their way through the CV.

To solve the Lagrangian movement of droplets ANSYS Fluent has imbedded the Discrete Phase Model. The continuous phase is still treated with the Eulerian model. Therefore, working with DPM is named the Eulerian- Lagrangian approach.

#### **4.1.2 Discrete phase model DPM**

All the following passages and assumptions are based on [14] and [15], for further information please be referred to literature. The DPM model distinguishes between the continuous phase (Eulerian approach) and the discrete phase (Lagrangian approach).

In this case, the continuous phase is already a mixture of two materials, the dry air and the vapour, which together add up in moist air. The discrete phase consists of spherical injected water droplets. ANSYS FLUENT calculates the trajectories of these discrete phase entities. Furthermore, heat (in general energy) and mass transfer between the discrete and the continuous phase are simulated. ANSYS FLUENT provides several features for the discrete phase models, such as [14]:

- calculation of the discrete phase trajectory using a Lagrangian formulation that includes the discrete phase inertia, hydrodynamic drag and gravity
- heating and cooling of the discrete phase
- vaporization and boiling of the liquid droplets
- consideration of particle collision
- ...

One model that would have been necessary in this thesis is not implemented into ANSYS FLUENT, this is the condensation model. To simulate and compute condensation between the continuous and discrete phase, heat and mass transfer between both phases, it was necessary to implement a user defined function (UDF) into ANSYS FLUENT. The UDF is described in chapter 4.1.3.

For the DPM model the initial position, velocity, size and temperature of the individual particles within the domain must be defined. Using these initial conditions, together with the physical properties, e.g. material and phase, of the discrete phase the trajectory, the heat and mass transfer between the continuous and the discrete phase are calculated. The interaction between the continuous and the discrete phase must be permitted separately to allow mass and heat transfer between both phases. By entering the number of continuous phase iterations per DPM iteration the frequency of the update of the DPM source can be adjusted. Generally increasing this number leads to increased stability but requires much more time for converging. [14]

#### **4.1.3 User Defined Function UDF**

Using a UDF allows customizing all available functions in ANSYS FLUENT to enhance its capacity. UDF's are written in the language "C" and are compiled to ANSYS FLUENT. [16]

ANSYS FLUENT provides a wide range of predefined UDF's. Many approved UDF's are shown in [16]. If no suitable UDF is available in [16], they can be written by oneself and can be compiled to ANSYS FLUENT. One of these predefined functions, which is a combination of several separate UDF's, is dealing with the simulation of condensation together with the usage of the DPM model. This UDF fitted well for the task from this master thesis. Just small adjustments were necessary to get the UDF run for this application. In the next paragraphs the

most important functions and tasks of this UDF are described.

Although ANSYS FLUENT calculates the relative humidity automatically, the relative humidity is additionally calculated locally within the UDF for every cell in the domain. To calculate the relative humidity the saturation pressure is calculated locally for each cell as well. If the relative humidity exceeds 100% for a local cell, a mass transfer (condensation) from continuous to discrete phase takes place with the speed defined by the condensation rate. The condensation rate  $c$  is a value that has to be aligned by empirical attempts to reflect the reality and can be understood as dimensionless velocity of mass transfer. With the condensation rate the mass transfer shown in equations (4-3) and (4-4), and the heat transfer shown in equation (4-5) from the continuous to the discrete phase, is.

$$m_{P\_cond} = c * \sqrt{A} * (RH - 1) * P\_DT_{(p)} \quad (4-3)$$

$$m_p = m_{p0} + m_{P\_cond} \quad (4-4)$$

$$H_{latent} = m_{P\_cond} * h_{cond} \quad (4-5)$$

$P\_DT_{(p)}$  from equation (4-3) is a time step defined by ANSYS FLUENT. For more information about  $P\_DT_{(p)}$  please refer to [16].

With the new droplet mass after condensation  $m_p$  calculated in (4-4) the new droplet diameter can be calculated as shown in (4-6):

$$d_p = \sqrt[3]{\frac{6 * m_p}{\rho_p * \pi}} \quad (4-6)$$

As the used UDF consists of several separate functions they also intervene in several areas of ANSYS FLUENT. These areas and functions are shortly described in the following section:

- The DPM\_SWITCH is implemented in the DPM model as a custom law. Using this function, ANSYS FLUENT switches from the implemented sensible heat transfer to the latent heat transfer defined in the UDF, once the local relative humidity in a cell exceeds 100%. Transferring latent heat also means that mass transfer takes place.
- If the relative humidity for a local cell exceeds 100% the DPM\_LAW is applied for this cell. This law is also implemented in the DPM model in the custom laws. In this law, the mass of condensation is defined according to equation (4-3) and the new diameter is defined in applying equation (4-6). Additionally, it is assumed that after the condensation process a thermal equilibrium between the particle and the continuous phase exists.
- With the DPM\_SOURCE function the sources are added from the continuous to the discrete phase. These sources are the condensed mass transferred from the continuous phase to the DPM droplet according to equation (4-4), and the energy source added to the droplet (the latent heat) due to the condensation according to equation (4-5). Of course this procedure refers to the law defined in the UDF.

As these operations are carried out individually for each cell in the domain, usually both laws, the law implemented in ANSYS FLUENT and the user defined law, are applied at the same time in the domain.

#### 4.1.4 Boundary conditions

Considering the above described requirements, a model was built for starting and carrying out initial trials. For test purposes the first model used was a 2D model which is shown in Figure 4-4. The advantage of a 2D CFD compared to a 3D CFD calculation is that convergence is reached faster as the internal memory usage is less and the stability of the calculation is usually higher. After the initial (successful) tests, it was expected to change from 2D to 3D CFD model.

The boundary conditions of the continuous phase are shown in Figure 4-3:

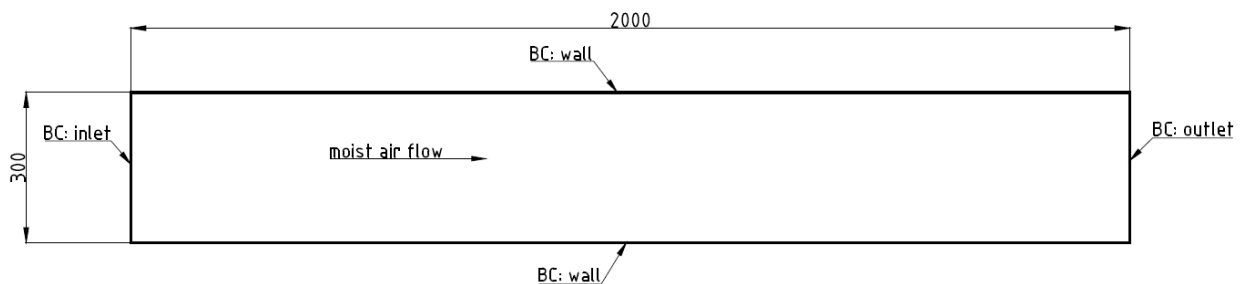


Figure 4-3: Boundary conditions of the 2D model

- BC at inlet: temperature and velocity
  - The gas at the inlet consists of dry air and vapour that end up in moist air. To define the relative humidity in ANSYS FLUENT the mass ratio between the dry air and the vapour has to be entered. The ratio is a function of the vacuum level and the temperature.
- BC at outlet: pressureless outlet
- BC at wall: no slip wall, adiabatic

#### 4.1.5 Limitations of the DPM Model

In [15] the limitations of the particle volume fraction are described. Accordingly, it is necessary that the discrete phase is sufficiently diluted to ensure that the particle- to- particle interactions, and the effects of the particle volume on the gas phase, are negligible. This means that the discrete phase must be present in a fairly low volume fraction, generally not higher than 10-12%. The mass fraction may greatly exceed this limit [15]. There are also several other limitations, but as they are not directly related to this master thesis topic, please refer to [15] for further literature.

The limitation of the volume fraction has a great effect on this master thesis. This is described based on a 2D model in the following description. Similar considerations are valid for the 3D model as well. For the 2D calculation, ANSYS FLUENT uses the same approach as for the 3D simulation. The missing third dimension is generated by multiplying the 2D profile with a certain unit depth. In this example the unit depth of the third dimension is assumed to be 10mm, same as the sight length of the used cells in the model.

The origin of the spray in the discrete phase model, the so called “injection”, is defined by its’ x- and y- coordinates for a 2D model. At the cell of the injection the highest volume loads of the discrete phase occur and therefore, this and its’ neighbour cells are the most critical ones for exceeding the limit of volume fraction share. This problem is explained for a spray- origin cell with the properties shown in Table 4-1 and Figure 4-4. Since the actual considered model is two dimensional, all cells have the same size and are quadratic shaped.



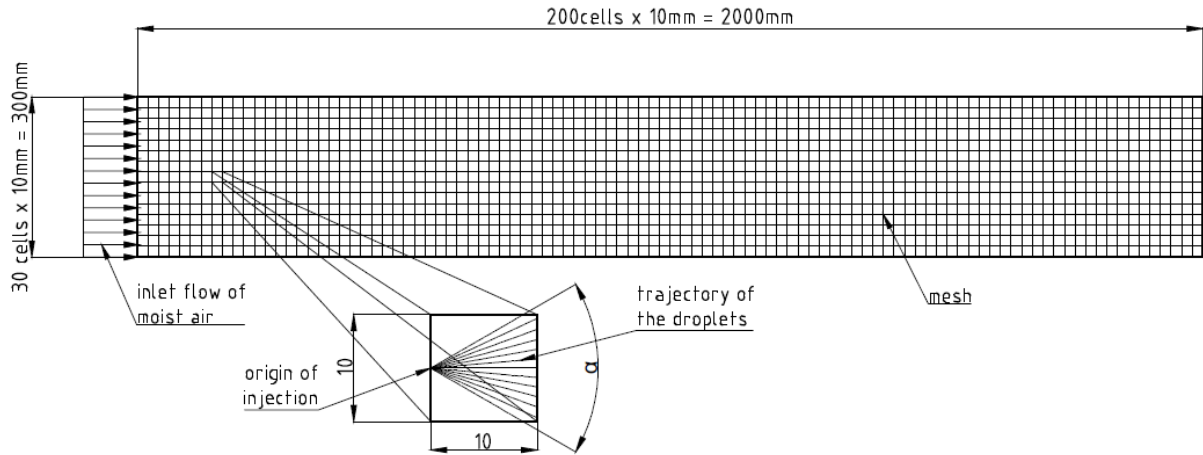


Figure 4-4: Origin cell of the DPM spray

<b>Properties of 2D model</b>			
Number of cells in the simulation	$n$	6000	-
Length of the model	$l$	300	mm
Width of the model	$w$	2000	mm
Side length of a cell	$a$	10	mm
<b>DPM spray properties</b>			
Spray velocity at outlet	$v_{spray}$	6	m/s
Mass flow of the spray	$m_{spray}$	0,15	kg/s
Density of the sprayed water	$\rho$	998,2	kg/m <sup>3</sup>
<b>Volume fraction in cell</b>			
	$f_V$	25,05	%

Table 4-1: Properties of the discrete phase and the used model

$$f_V = \frac{\dot{m}_{spray}}{\rho * v_{spray} * a^2} \quad (4-7)$$

All values presented for the DPM injection in Table 4-1 are realistic values that may be used for industrial sized machines. The dimensions of the vacuum pipe are typical for many machines. The velocity of the spray volume flow  $v_{spray}$  is defined by the company "Lechler" for nozzles with a spray of 9 l/min (0,15 kg/s). The acceleration of the droplets due to the higher velocity of the moist air flow is neglected, as the influence is small considering only one cell. On the other hand, the spray angle is not considered which would increase the volume fraction even more as it extends the dwell time of a spray droplet in a cell. The effect for the spray angle outweighs the effect of the acceleration and therefore, the volume fraction of a cell  $f_V$  would even increase due to these two effects. For this calculation, the spray is considered to be at the beginning of the cell, seen in flow direction. This represents the worst-case scenario, as the dwell time gets maximized as a result.

It is apparent that even with a small number of cells, and therefore large cells, in the domain a high volume fraction in the cell can be expected. It is clear that the volume fraction in the origin cell of the DPM spray exceeds the limits. That means that it is necessary to decrease the number of cells in the domain even more to pass the <10-12% volume fraction limit. A

further decrease of cells means that mesh independency is probably not achieved. Once the limit of volume fraction exceeds even just one cell, ANSYS FLUENT diverges after a few iterations.

The same problem will occur changing from 2D to 3D simulations. Even an increase of volume fraction is likely to occur. In the 2D model shown in Figure 4-4, the size of the cells is equally distributed. In a 3D domain for a round pipe it is truly impossible to build a mesh with equally sized cells and therefore, smaller and bigger cells exist. Especially at the wall of the pipe a boundary layer with smaller cells is advised to achieve a high resolution of the results. Therefore, small cells exist and the risk of exceeding the maximum volume fraction gets even greater.

## 4.2 Execution and results of the research on the 2D model

From the introduction above it becomes clear, that it is necessary to make some adjustments to get the simulation running in a satisfying way. These adjustments and manipulations are described in the next chapter.

### 4.2.1 Share injections on more cells

To get rid of this problem an attempt to share the injection of the DPM spray on two or more cells by defining more injection positions simulating only one single nozzle was tried. This procedure was limited as several nozzles must be used to reach the high amount of cooling water necessary and therefore, a single nozzle cannot be divided on too many cells. This becomes clear in Figure 4-4, as there are only 30 cells in cross direction, which limits the splitting of single nozzles on more cells.

Another issue arises as the injections are sprayed into the domain with a cone angle of approximately  $60^{\circ}$ - $90^{\circ}$ . Some of these trajectories may overlap and the limit of volume fraction might be exceeded to a high extent as well.

### 4.2.2 Adjusting the substance properties and condensation rate

Another possible solution to prevent exceeding the maximum volume fraction is to adjust the substance properties of the DPM spray or the continuous phase. Adjusting the substance properties, such as increasing specific heat capacity of the DPM spray or decreasing condensation enthalpy of the continuous phase, allows reducing the amount of spray water injected while keeping the transferred heat constant. Increasing the specific heat capacity of the injected spray by the factor  $z$  allows decreasing the mass rate of injected water by the same factor  $z$ , while the possible maximum heat transfer remains unchanged. The mass reduction was realised by keeping the number of droplets injected per time constant but decreasing the diameter. The reason for this was that the surface to volume ratio did not change as much as when the diameter of the droplets would have been left constant but the number of droplets would have been reduced instead.

From formula (4-7) it is obvious that the volume fraction in a local cell decreases due to the reduced mass injected. The goal of the manipulation of the specific heat capacity was to reduce the amount of water injected while the results concerning condensation rate, temperature reduction and volumetric reduction, remained unchanged.

Despite the adjustment of these factors that have been carried out, it was not possible to reach the same results after adjusting the substance properties. An example explaining the results of the adjustment of the substance properties is shown in this section. The results were evaluated for temperature and mass share of gaseous vapour in the moist air with a distance of 1,0m downstream to the inlet and, normal to the flow direction, as shown in Figure 4-5. This procedure was repeated with stepwise increased specific heat capacities, and therefore, decreased amount of water. Additionally, the condensation rate was increased by the factor of the reduced surface of droplets. All other settings and properties of the model were kept constant. As a basis, a rather low mass flow was chosen to pass the <10-12% volume fraction limit, also with non- changed substance properties. The settings are shown in Table 4-2.

			basis	1 ( $c_{H_2O} * 5$ )	2 ( $c_{H_2O} * 5$ )	3 ( $c_{H_2O} * 10$ )	4 ( $c_{H_2O} * 10$ )	5 ( $c_{H_2O} * 15$ )	7 ( $c_{H_2O} * 20$ )	8 ( $c_{H_2O} * 20$ )
Mass flow of the spray	$m_{spray}$	kg/s	0,1000	0,0200	0,0040	0,0100	0,0020	0,0067	0,0050	0,0010
Specific heat capacity of spray water	$c_{H_2O}$	J/(kg*K)	4182	20910	104550	41820	209100	62730	83640	418200
Number of droplets	$n_{droplet}$	1/s	23916	23916	23916	23916	23916	23916	23916	23916
Diameter of droplets	$d_{droplet}$	mm	1	0,585	0,585	0,464	0,464	0,405	0,368	0,368
No of cells in the model	$n_{cells}$	-	24.000	24.000	24.000	24.000	24.000	24.000	24.000	24.000
Condensation factor	$c$	-	0,0008	0,0008	0,002339	0,0008	0,003713	0,0008	0,0008	0,005894

Table 4-2: Settings and properties of the simulation

The DPM properties are listed below and the location of the spray is shown in Figure 4-5.

- Pure liquid water H<sub>2</sub>O droplets
- Temperature of the spray: 70°C
- Velocity of the spray: 6m/s
- Location of the spray: 100mm downstream from the inlet in the centre of the canal
- Shape of the spray: 100mm virtual line\*

\* To allow a higher mass injected into the system it was decided to inject the spray along a virtual 100mm long line in the centre of the duct, instead of injecting the whole water from one position. This allows higher mass loads and therefore, the cooling and condensation effects are improved. The flow was sprayed straight in the direction of the inlet flow.

The moist air at the inlet was set with the following flow properties:

- Mixture of air and vapour
- Relative humidity: 100% → mass share of vapour: 40%; mass share of dry air: 60%
- Temperature: 343K
- Inlet velocity: 14 m/s
- Absolute pressure in the system: 0,6 bar → vacuum level  $\Delta p$  0,4bar

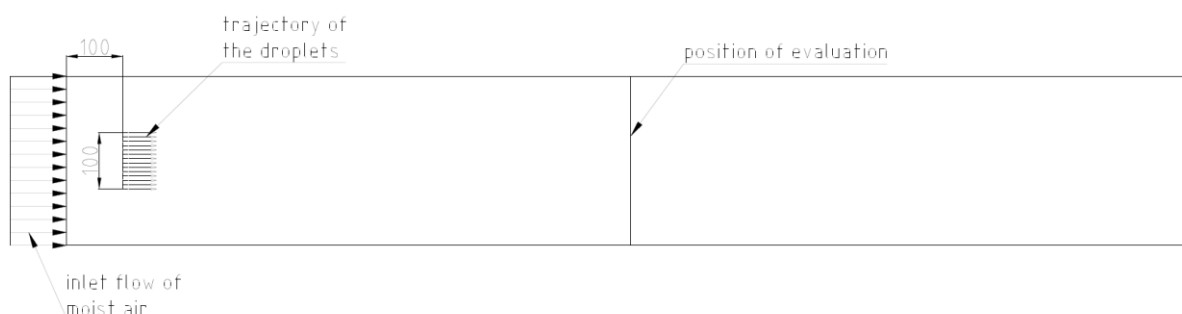


Figure 4-5: Position and 2D- geometry of the spray

The evaluation of the results are shown in the charts below. They are applied on the mass share of vapour in the air in a cross profile of the continuous phase shown in Figure 4-6 and the cross profile of the temperature of the moist air shown in Figure 4-7. The position for evaluation of the cross profile is shown in Figure 4-5. As a basis, the original values (not adjusted substance properties, black solid trend) are shown in the charts. Solid trends represent results after adjusting the substance properties only. The dashed trends represent results of adjusted substance properties and increased condensation rate. Additionally, each one of the CFD graphics show the mass fraction of vapour in the moist air and the temperature of the moist air for the “basis settings” is presented below the charts.

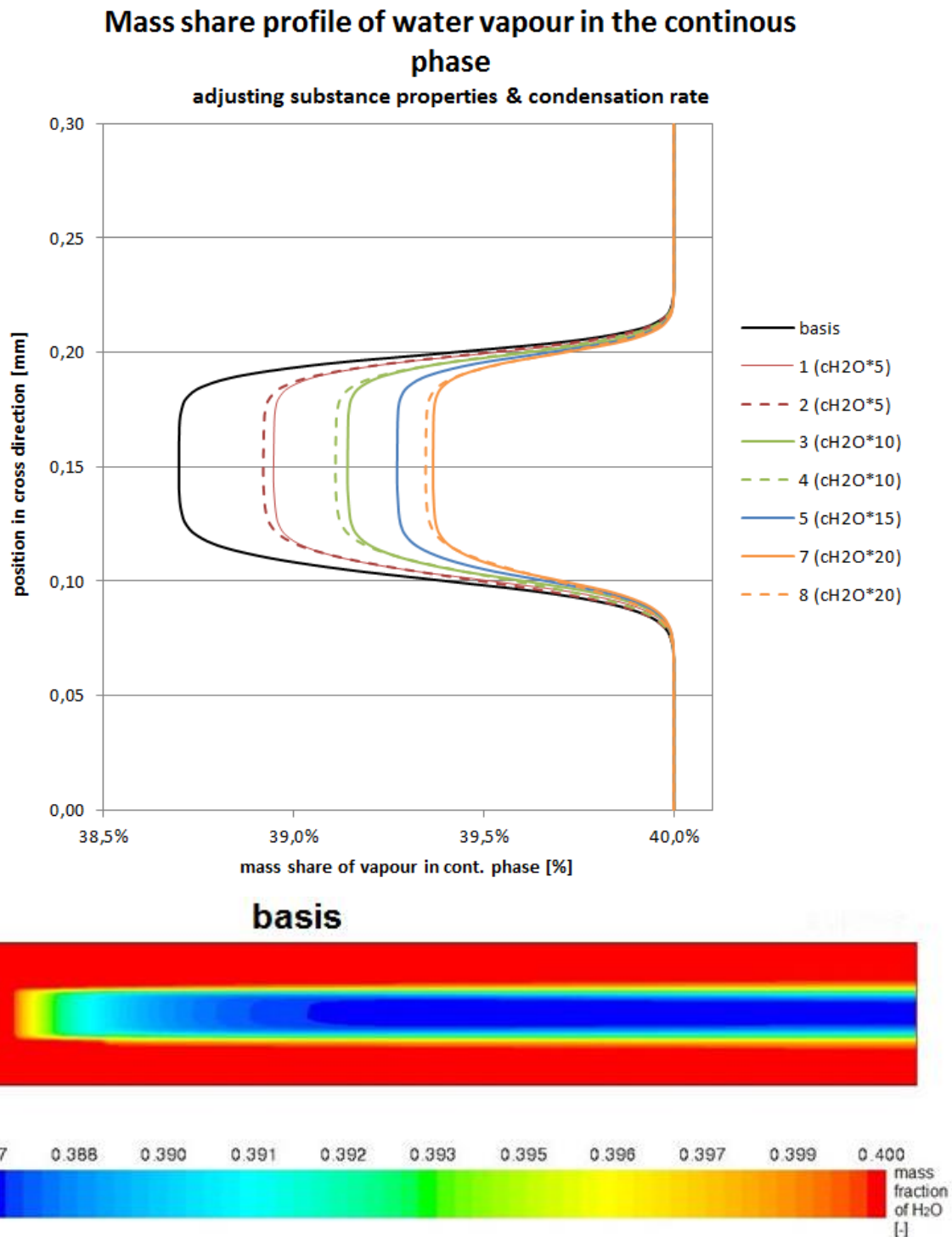


Figure 4-6: Mass fraction profile of vapour in the moist air

It is clear from Figure 4-6 that the adjustment of the specific heat only (solid trends) did not represent the same result as the basis. There were significant differences in the results after adjusting the substance properties. Evidently an increase of the specific heat capacity of the liquid water  $c_w$  decreases the amount of condensed vapour. This means that condensation proceeded slower with increased  $c_w$  and decreased mass transfer to the DPM.

Based on this result the condensation rate  $c$  was increased by the factor of the surface reduction in order to compensate lower mass transfer (dashed trends). Understandably mass transfer increased slightly by increasing the condensation rate. Based on this finding the condensation rate was further increased stepwise. This worked adequately, but only if the

condensation rate did not exceed a certain value. Exceeding this value resulted in convergence problems as the transfer rate seemed to get too high and ANSYS FLUENT was not able to handle higher mass and heat transfer between the continuous and discrete phase anymore.

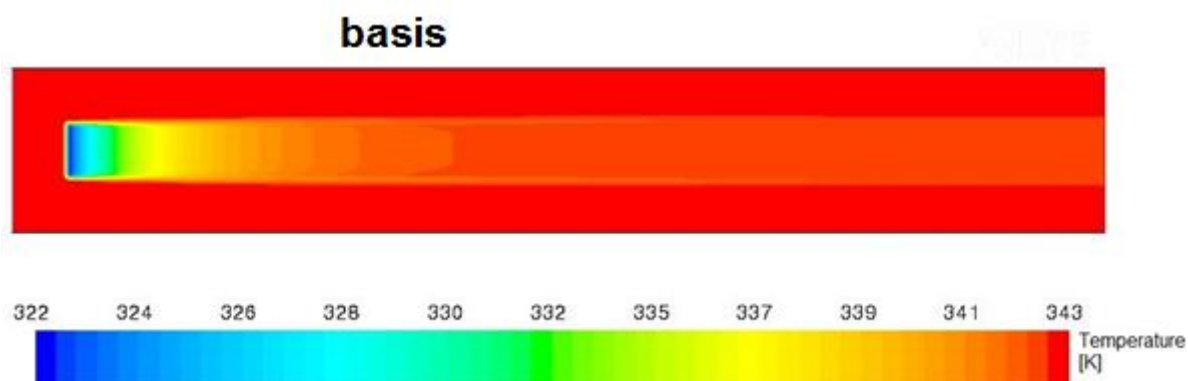
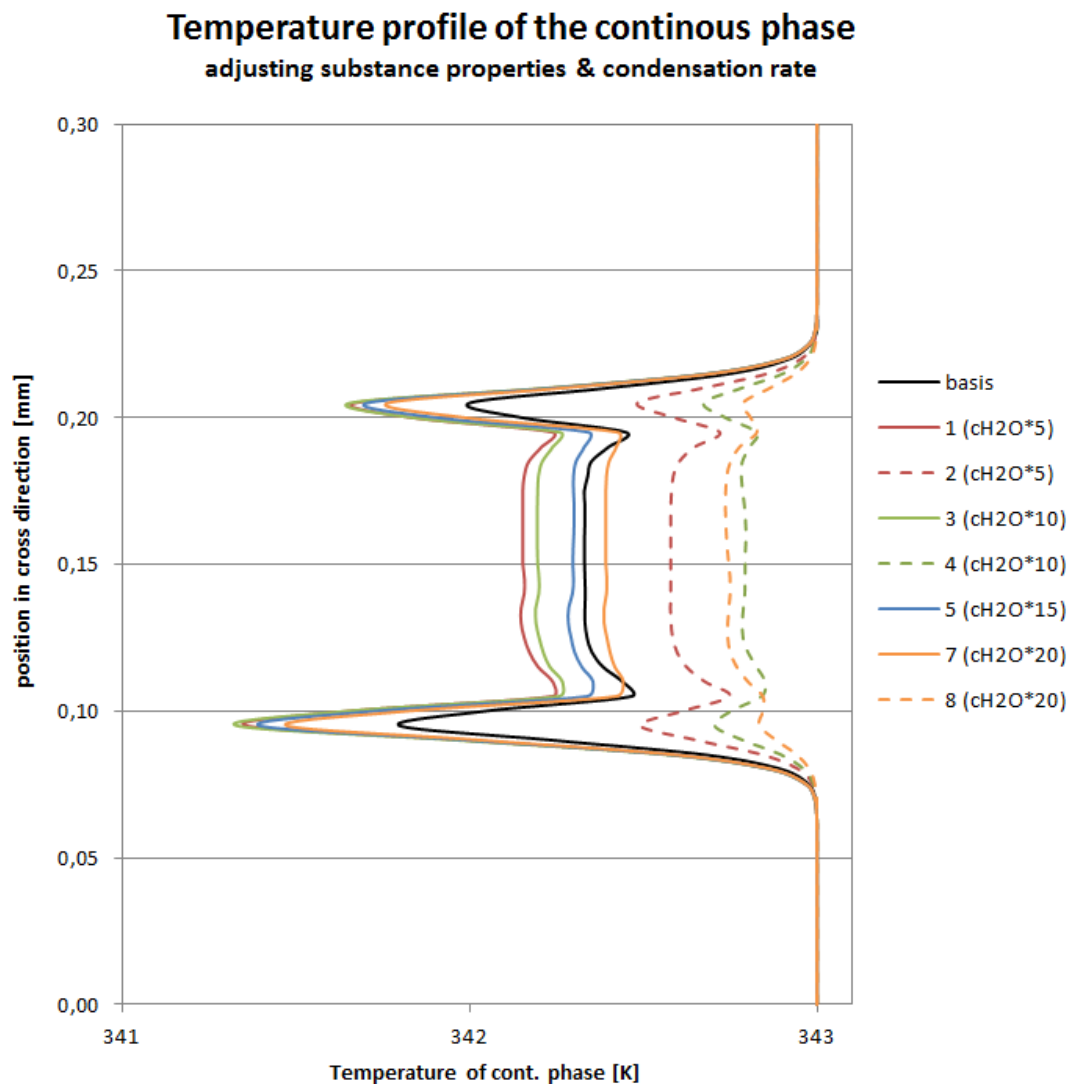


Figure 4-7: Temperature profile of the moist air

Compared to the mass share profile the temperature profile does not show a coherence between increased specific heat capacity and change in temperature. Multiplying the heat capacity by five led to decreased temperature. Increasing the heat capacity further led to a minor temperature alteration. Adjusting the condensation rate led to small temperature

changes. There are no obvious direct coherences between the temperature profile and adjusting the heat capacity or condensation rate.

It can be concluded that adjusting the substance properties and the condensation rate did not lead to the desired results. Therefore, linear factors were introduced into the UDF to adjust the energy and mass transfer from the continuous phase to the DPM spray. This procedure is described in the next chapters.

### 4.2.3 Implementation of linear factors

For both the energy and the mass transfer, a linear factor was introduced to adjust the transfers from the continuous phase to the discrete phase. They were empirically adjusted to match the profiles after manipulating the substance properties back to the basis profile. Condensation rates were kept constant at this time. As transferred mass and energy depend on each other, both factors of course influenced each other as well. Therefore, it was necessary to adjust the empirical factors iterative several times. With these two factors it was possible to adjust both, the profile of vapour share in the continuous phase and the temperature profile of the continuous phase in a way that the profiles of the initial, original substance properties were reached again (basis). This is shown in Figure 4-8 and Figure 4-9. The position of the profile in flow direction was the same as shown before. The linear factors for adjusting the mass and energy equation are shown in Figure 4-3. All other factors were kept constant.

			basis	3 (c <sub>H2O</sub> *10)	3.1 (c <sub>H2O</sub> *10)	3.2 (c <sub>H2O</sub> *10)
Mass flow of the spray	m <sub>spray</sub>	kg/s	0,1000	0,0100	0,0100	0,0100
Specific heat capacity of spray water	c <sub>H2O</sub>	J/(kg*K)	4182	41820	41820	41820
Number of droplets	n <sub>droplet</sub>	1/s	23916	23916	23916	23916
Diameter of droplets	d <sub>droplet</sub>	mm	1	0,464	0,464	0,464
No of cells in the model	n <sub>cells</sub>	-	24.000	24.000	24.000	24.000
Condensation factor	c	-	0,0008	0,0008	0,0008	0,0008
Factor adjusting the mass eqn	m	-	-	-	1,35	1,80
Factor adjusting the energy eqn	e	-	-	-	1,33	1,80

Table 4-3: Factors to adjust the mass and energy equation

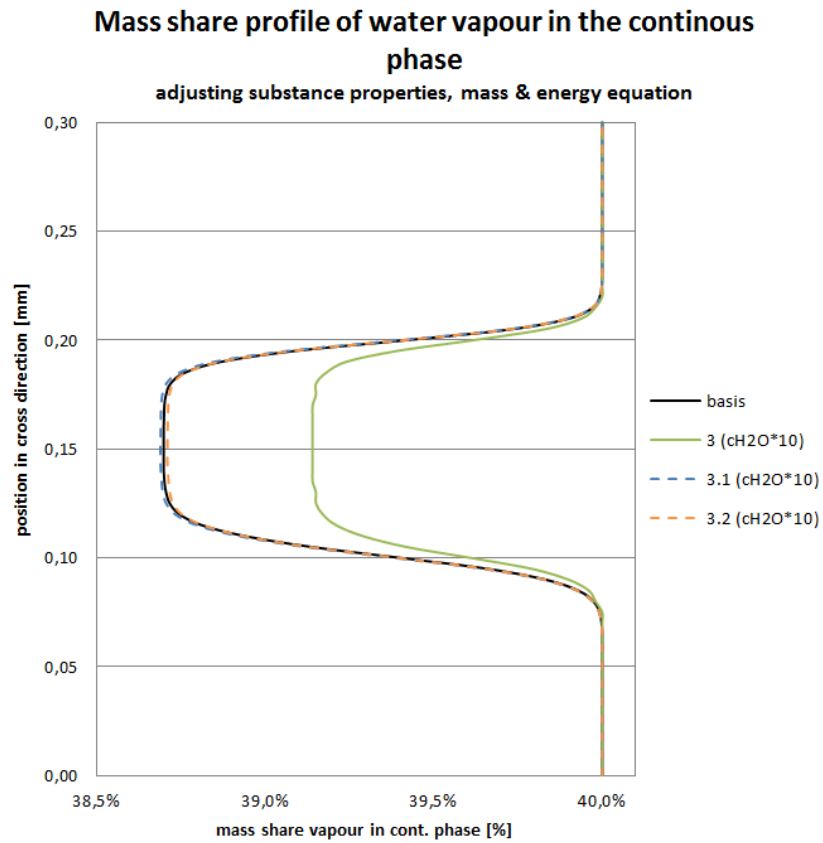


Figure 4-8: Mass fraction of vapour in the moist air after manipulating the mass & energy equation

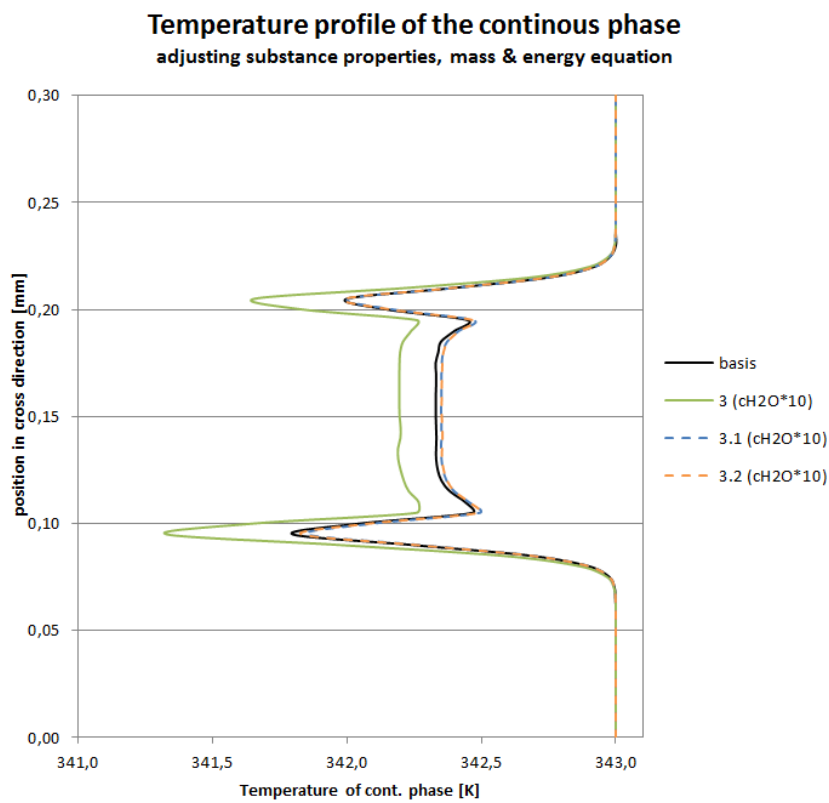


Figure 4-9: Temperature of the moist air after manipulating the mass & energy equation



Unfortunately, this only worked satisfactory for a specific position in the domain and unchanged boundary conditions. Changing the position of the measurement downstream or upstream or varying any boundary conditions led to the result that the profiles did not fit anymore to the “basis” anymore.

From the results shown it can be assumed that the described procedure does not yield satisfactory results, although different manipulations were tried.

Another issue shown in Figure 4-10 is that ANSYS FLUENT did not correctly show the physical relative humidity.

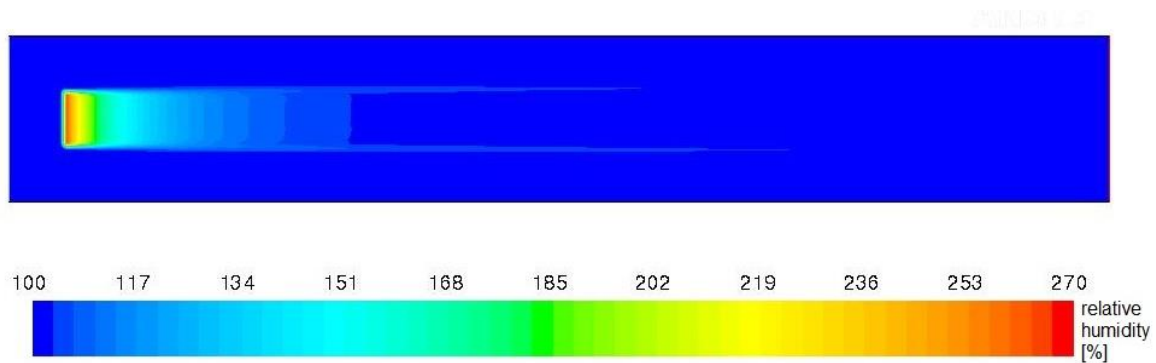


Figure 4-10: Relative humidity, basis (non- manipulated)

It is obvious that the relative humidity by far exceeds 100%, especially directly at the position of the injection and further downstream. This shows that the model with the actual settings does not reproduce correct physical results. It took further downstream the domain until the physical results were shown correctly again.

Finally, it was decided that this procedure does not lead to suitable results with an acceptable time effort. Therefore, it was decided to conduct an experimental investigation instead of continuing to work with CFD.

### 4.3 Possible approaches to continue with CFD

Before describing the experimental investigation in the next chapter, a few possible approaches and solutions for the problem faced are briefly explained.

#### 4.3.1 Further study of the DPM model

Not considered so far was the change of the ratio between the initial mass of the sprayed DPM droplet, before and after condensation. As shown in this chapter, the mass ratios change due to the condensation. This approach, and the solution, are described in the next section by showing a comparison of the condensation on an individual droplet between manipulated (marked with inverted comma `) and non-manipulated substance properties. To give a replicable explanation, the condensation process is divided into two steps:

- a)  $0 \rightarrow 1$ : The latent heat is transferred from the continuous phase to the discrete phase. No mass transfer is considered in this step.
- b)  $1 \rightarrow 2$ : Sensible heat transfer, because of the different temperatures of the condensed molecule, and the droplet and mass transfer from continuous to discrete phase, are considered.

#### $0 \rightarrow 1$ latent heat transfer

This step starts at the beginning of the condensation (state 0) and ends once the condensation is finished at state 1. Latent heat is transferred from the condensing particle of the continuous phase to the discrete phase droplet. The mass of the condensing molecule is not added to the droplet in state 1.

The boundary conditions for the condensation process are described in the equation below. Before the first condensation, temperatures of the condensing molecule from the continuous phase and temperatures of the DPM droplet are the same for both, the manipulated and non-manipulated substance properties. At this state, mass ratios and specific heat ratios between the manipulated and non-manipulated system is inversely proportional to each other.

$$\frac{m_0}{m'_0} = \frac{c'_w}{c_w} = z; m_c = m'_c; T_c = T'_c; T_0 = T'_0 \quad (4-8)$$

Enthalpy at state 0 of an individual droplet is defined as follows:

$$H_0 = m_0 * c_w * T_0 \quad H'_0 = m'_0 * c'_w * T'_0 \quad (4-9)$$

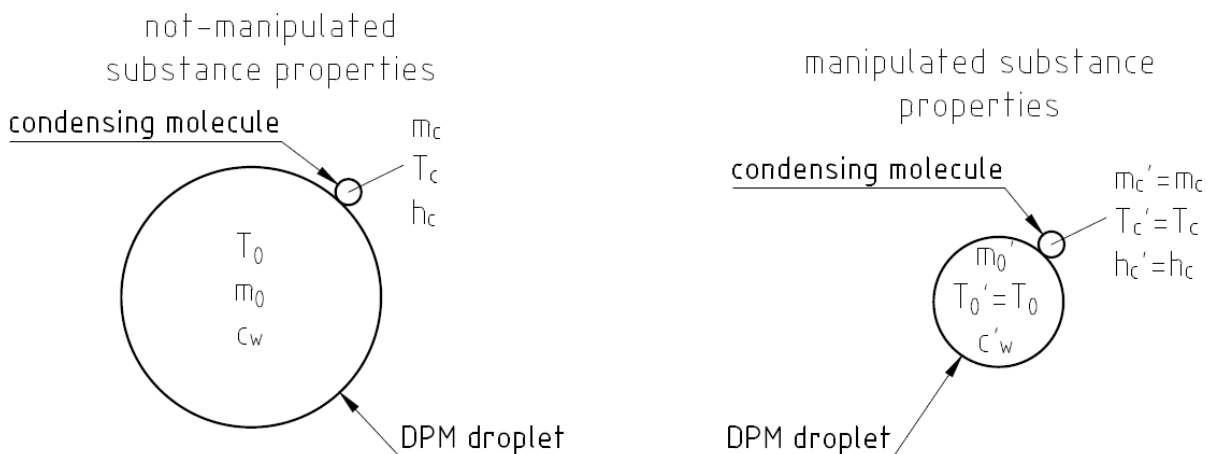


Figure 4-11: Properties of the sprayed droplet and the condensing particle at state 0

From equations (4-8) and (4-9) it is clear that  $H'_0 = H_0$ .

Once the molecule condensates the enthalpy of condensation,  $H_C$  is transferred from the particle to the droplet. As mentioned above, mass transfer is not considered from 1→2. The enthalpy, and mass at state 1, can be defined as follows:

$$H_1 = m_0 * c * T_0 + h_c * m_c \quad H'_1 = m'_0 * c' * T'_0 + h_c * m_c \quad (4-10)$$

$$m_1 = m_0 \quad m'_1 = m'_0 \quad (4-11)$$

With the mass definition in state 1 from (4-11), enthalpy in state 1 can also be written as follows:

$$H_1 = m_1 * c * T_1 = m_0 * c * T_1 \quad H'_1 = m'_1 * c' * T'_1 = m'_0 * c' * T'_1 \quad (4-12)$$

Finally, both the manipulated and the non- manipulated situation end up with the same results,  $H'_1 = H_1$  and  $T'_1 = T_1$  at state 1.

### 1 → 2 sensible heat transfer

In the 2<sup>nd</sup> step the mass transfer and the sensible heat transfer from the condensed particle to the droplet are treated.

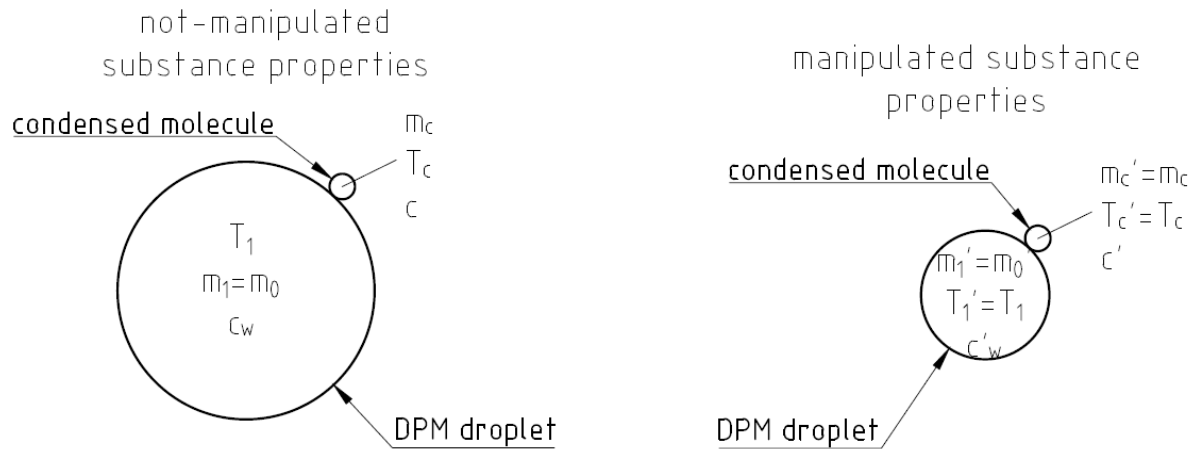


Figure 4-12: Properties of the droplet and the condensed particle at state 1, is as follows:

$$H_2 = m_1 * c_w * T_1 + m_c * T_c * c_w \quad H'_2 = m'_1 * c'_w * T'_1 + m_c * T_c * c'_w \quad (4-13)$$

$$= T_2 * m_2 * c_w \quad = T'_2 * m'_2 * c'_w$$

With the definition of the masses at state 2, it is as follows:

$$m_2 = m_1 + m_c \quad m'_2 = m'_1 + m_c \quad (4-14)$$

From (4-14) it is clear that mass ratios between the manipulated and non- manipulated system change after the mass of the condensed molecule is added to the DPM droplet and therefore, the enthalpies change as well:

$$\frac{m_2}{m'_2} < \frac{m_1}{m'_1} \rightarrow H'_2 > H_2 \quad (4-15)$$

With the change of mass ratios, and the resulting difference of the enthalpies, it is necessary to reduce the enthalpy  $H'_2$  to  $H'_{2adj}$  as follows:

$$\Delta H_2 = H'_2 - H_2 = m_c * T_c * (c_w' - c_w) \quad (4-16)$$

$$H'_{2adj} = H'_2 - \Delta H_2 \quad (4-17)$$

Although enthalpies are adjusted accordingly, the mass ratios between the manipulated and non-manipulated system are not the same anymore before and after condensation. This would result in differences for the next step of condensation if no further actions would be taken. As a direct result of that, it is necessary to accordingly adjust the manipulated specific heat capacity for the next step as well.

$$c'_{w0\_new} = \frac{m_2 * m'_0}{m'_2 * m_0} * c'_0 \quad (4-18)$$

That means that  $c'_w$  is reduced along the condensation process. Figure 4-13 shows the properties of the DPM droplet after completing the condensation and before the next step starts.

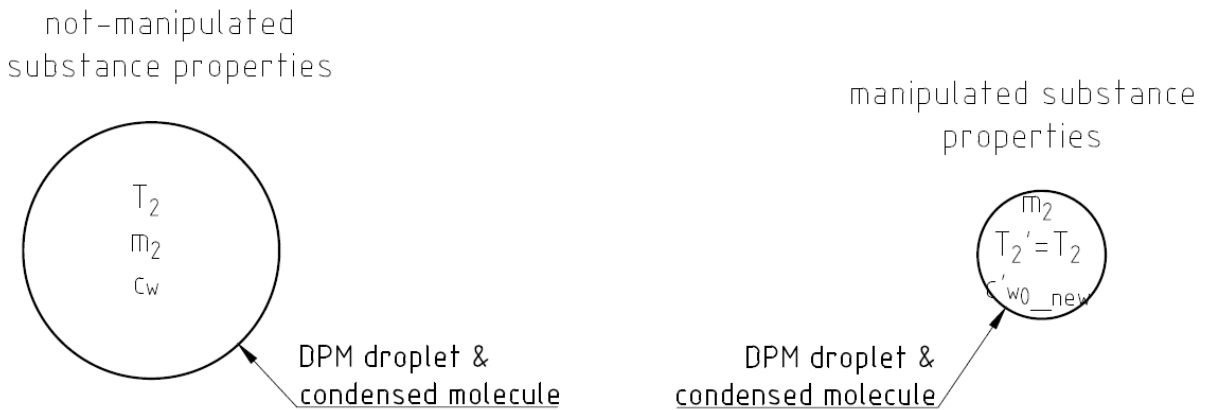


Figure 4-13: Properties of the droplet and the particle at state 2

This step most likely improves the result but does not explain the big differences that occur due to changing the substance properties.

Of course other research and investigation using the DPM model could be obtained. For example, further research about the adjustment of the condensation factor and the implemented linear factors after manipulating the specific heat capacity could be carried out.

Apart from working with the used model, it might be beneficial to use other models and settings in ANSYS FLUENT that are briefly described in the next step. For further information on the following models please refer to [15] and [18].

### **4.3.2 Multiphase Model**

With a multiphase model two or more phases or materials can interact in a domain with each other. The multiphase model is a pure Eulerian model. The presence of more phases is defined by a ratio of their volume fractions. Mass and energy transportation from one to the other phase is enabled. A disadvantage compared to the DPM is that the injection of the sprayed droplets cannot be defined in a satisfactory way and therefore, continuation with multiphase was not carried out.

### **4.3.3 Dense Discrete Phase Model (DDPM)**

The DDPM model is based on the multiphase model using the Eulerian approach and is a hybrid Euler-Euler and an Euler- Lagrange approach. Compared to the DPM, the DDPM allows the volume fraction to far exceed 12% [18]. Compared to the DPM, the DDPM is less used and therefore fewer literature can be found. Due to this, it was decided not to continue with the DDPM.

These possibilities would be rather time consuming and would far exceed the scope of the thesis. Furthermore, an experiment seems to reflect the reality better than a CFD calculation. Therefore, an experiment was decided as the best approach in place of investing more effort in a CFD calculation.

## **4.4 Conclusion of the CFD calculation**

In this chapter a CFD calculation is introduced in order to simulate condensation of a moist air flow and evaluate the volumetric flow reduction process. With the model the influence of different parameters on the volumetric flow should be investigated. With the used model it was not possible to give answers to these questions as ANSYS FLUENT was not capable to simulate the injection of high amounts of cooling droplets. All approaches to solve this issue did not lead to satisfactory results. Therefore, it was decided to continue the investigation with an experimental setup instead of continuing working with CFD.

At the end of this chapter, some possible further steps that might solve the issues are described.

## 5 Experimental investigation

Due to the issues that arose while working on the CFD calculation, it was decided to stop with it and concentrate on an experimental study instead. The goals of the experiment were defined the same as they were for the CFD calculation, to investigate the influence of different parameters on the volumetric flow reduction of the moist air.

The experiments were carried out in the pilot plant at Andritz AG. The costs for the experimental setup were then covered by Andritz AG.

### 5.1 Preparation of the test stand

For this master thesis, not only the experiment itself and the evaluation of the results were carried out, but also many other tasks had to be organized and executed before experiment commencement. Beside the target to get results about the influence of different parameters on the condensation of the vapour of the moist air, it was also important to reuse available facilities to keep costs and time effort for rebuilding the existing vacuum system as low as possible. Furthermore, daily business at the pilot plant must not be disrupted at any time.

As for the dewatering machine in the pilot plant many vacuum systems were available, it was decided to use one of these systems and adapt it for the experiments. The system used was the so called “shoe press” module because it was foreseeable that this module would not be needed for any other experiments during the experimental investigation. The existing, initial vacuum system was sized for small working width, which meant lower volumetric flow. Therefore, all the piping, vacuum pumps and all other equipment was much smaller compared to industrial sized machines.

For industrial sized machines vacuum pipe diameters of approximately 300mm and more, depending on the working width of the machine and the position of the vacuum box, are standard. The velocity of the vacuum flow in the pipes for industrial size machines is approximately 10-20 m/s.

Therefore, the existing vacuum system needed to be adapted to realistically replicate it as precise as possible. Unfortunately, the adaption of the vacuum system to industrial sized systems was only possible until a certain point as it was limited by the available vacuum pumps. Therefore, a compromise had to be taken. As most of the equipment of the vacuum system was not allowed to be changed the rebuild mainly depended on the size of the piping. Three important parameters describing the volumetric flow reduction that needed to be considered defining the diameter are described in the following:

- Dwell time of the sprayed droplets in the vacuum flow which is a function of the velocity of the moist air flow.
- Vacuum height which is a thermodynamic parameter. The degree of humidity  $x$  of the vapour in the moist air depends on the vacuum height. With increased degree of humidity  $x$  the volumetric flow reduction due to condensation increases as well.
- Using a too narrow pipe diameter causes the injected droplets to splash against the wall of the pipe instead of being redirected, as shown in
- Figure 5-1. The injected droplets would flow down on the wall of the pipe and the condensation rate will decrease, as the available surface for the condensation decreases dramatically.

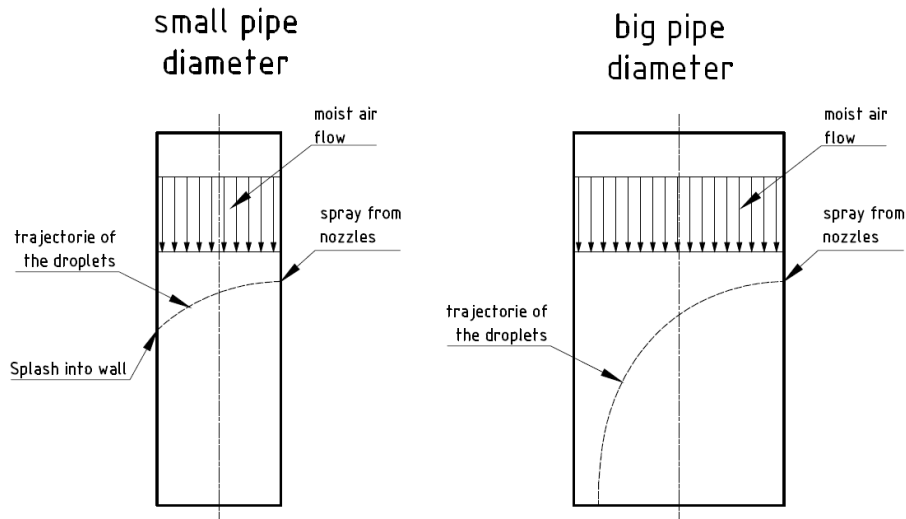


Figure 5-1: Problem with too narrow pipe diameters

These three parameters were working against each other. A bigger diameter leads to lower flow velocity and less volumetric flow (=higher dwell time of sprayed droplets) and vacuum height in the pipe. On the other hand, a smaller diameter leads to a splash of the injected droplets against the wall directly after injecting into the system.

Finally, as a compromise the diameter for the section of the measurement was defined with 200mm. Another reason for setting the diameter at this size was that raw pipe material was available in sufficient amount in this size and therefore, extra costs were kept low.

After defining the diameter of the section of measurements the test stand was constructed (see chapter 5.2) and all necessary equipment was purchased. Afterwards assembly was organized and carried out.

## 5.2 Experimental setup & measuring devices

The schematic of the experimental setup and a photo are shown in Figure 5-2 and Figure 5-3. It consisted of several elements and measuring instruments that are described in the following chapter.

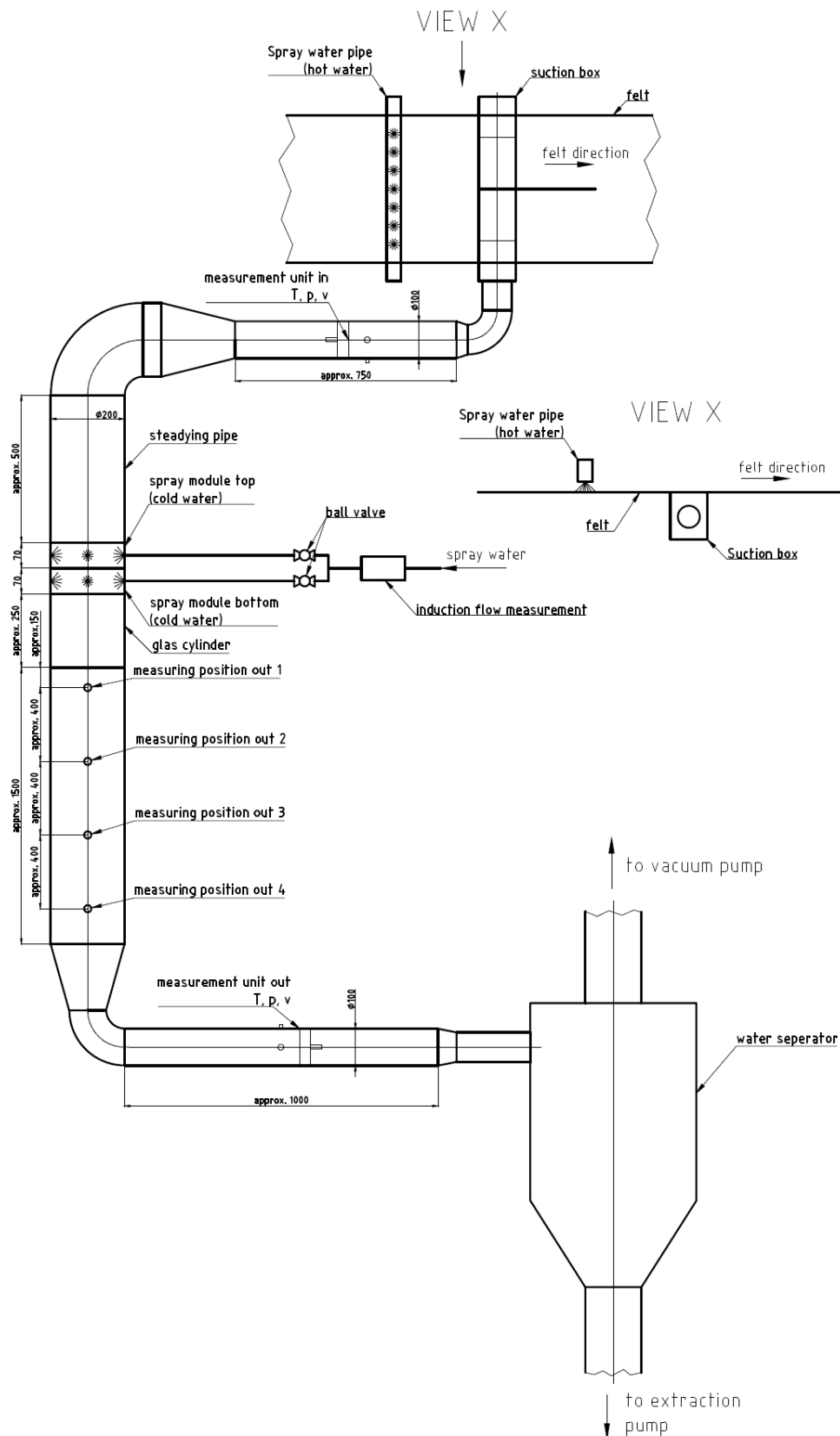


Figure 5-2: Schematic of the experimental setup





Figure 5-3: Photo of the experimental setup

### 5.2.1 Spray water pipe and suction box (UHLE box)

To generate high temperatures and a high relative humidity, target was a relative humidity of 100%, in the system to carry out the experiment, hot water was applied on the running felt in front of the vacuum box with a spray pipe. The temperatures of the water applied were between 60 and 80°C. Directly after the spray the vacuum box – in this case the so called UHLE box of the top felt of the shoe press – sucked the water out of the felt and together with the process water the moist air flow was sucked through the felt into the vacuum piping system. Depending on the temperature of the water applied a certain temperature of the air flow was set.

### 5.2.2 Measurement unit inlet, Debimo sensor

The pipe out of the suction box had a diameter of 80mm. Afterwards the diameter was increased to 100mm. In this section temperature, volumetric air flow, absolute pressure, vacuum level and velocity were measured with a differential pressure sensor of Debimo, which is shown in Figure 5-4 below:

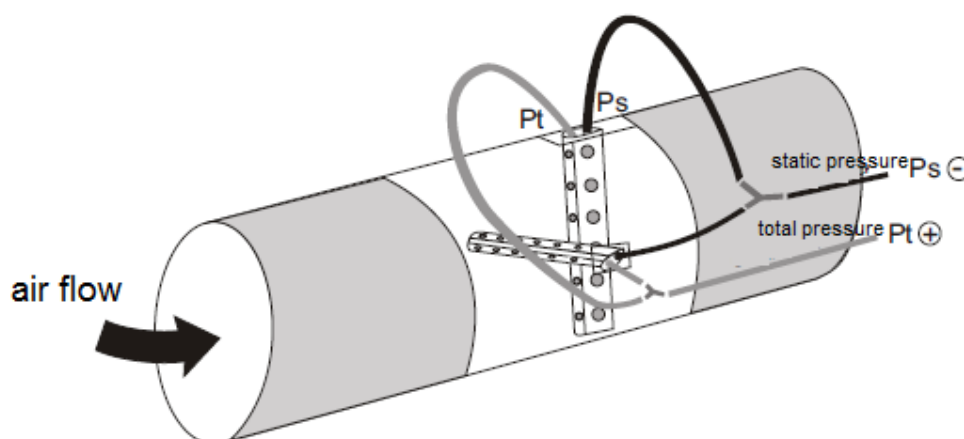


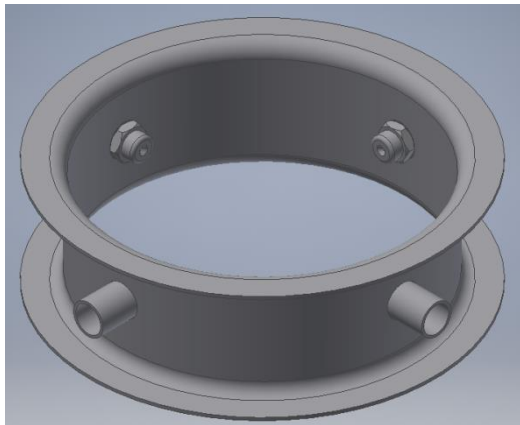
Figure 5-4: Debimo air flow measurement [11]

The principle of the Debimo measuring device is comparable with the Prandtl tube that measures the absolute and the static pressure. The flow velocity, which is a function of the dynamic pressure, was calculated accordingly. For further information about the Debimo differential pressure sensor please refer to [11]. The results of the measurements were shown in real time on the online system of the operator panel.

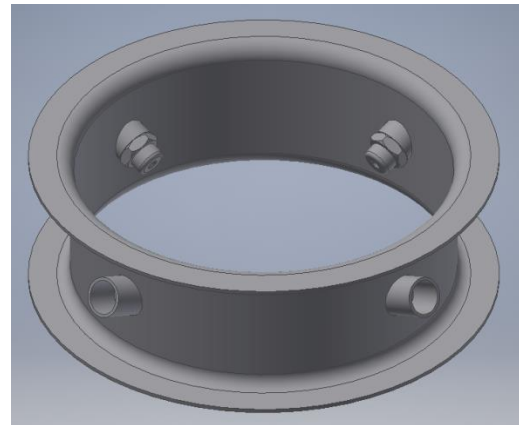
### 5.2.3 Spray modules

After determining the initial conditions the pipe diameter was increased to a final diameter of 200mm. Until this position, the pipe direction was horizontal but with an elbow the flow was redirected to a vertical direction top- down. After an approximately 500mm long pipe, two installation positions for spray modules were available that could be changed individually. With these spray modules the droplets were injected into the system by the use of nozzles. The modular system allowed a quick change of the individual spray modules, without being very time consuming which was an important property as the modules needed to be changed several times.

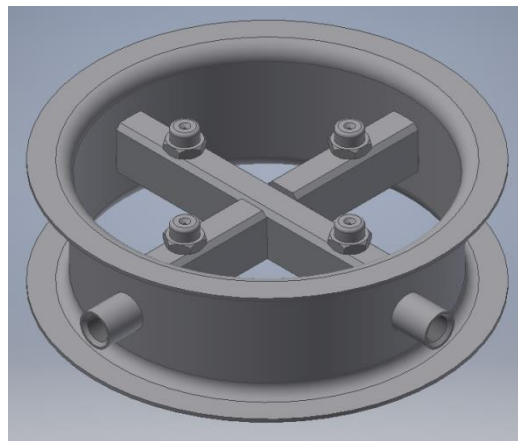
Altogether three different spray modules were designed and manufactured to evaluate the effect of the spray direction on the efficiency of the volumetric flow reduction. In the first module, the spray direction was normal to the air flow direction. In the second module, the spray direction was approximately 25° in or against the spray direction, depending on the mounting direction. The third module, allowed a spray in or against the moist air flow direction, depending on the direction of the installation. Each module was constructed to install up to four spray nozzles, shown in Figure 5-5.



normal to moist air flow



skewed to moist air flow



in or against moist air flow

Figure 5-5: Used spray modules in experiment

In addition to the different spray directions, it was important to investigate the influence of the diameter of the sprayed droplets on the volumetric flow reduction of the moist air. Therefore, spray nozzles in three different sizes from the company “Lechler” were used. All nozzles used were full cone nozzles and had a spray angle of 90°. The properties of the used nozzles are presented in Table 5-1. Figure 5-6 shows a 3D model of the nozzle.

Type	Q @ 2bar l/min	D30* @ 2 bar µm	Spray-angle °	nominal Q at differnt pressure p						
				0,5 bar	1,0 bar	2,0 bar	3,0 bar	5,0 bar	7,0 bar	10,0 bar
				l/min						
490.686	5,00	160,6	90	2,87	3,79	5,00	5,99	7,21	8,25	9,52
490.766	8,00	238,6	90	4,59	6,06	8,00	9,41	11,54	13,20	15,22
490.846	12,50	237,4**	90	7,18	9,47	12,50	14,70	18,03	20,63	23,80

Table 5-1: Used spray nozzle sizes [12]

\*: Definition of D30 and a detailed droplet analysis can be found in the appendices

\*\* : For type 490.846 a droplet diameter D30 is given at 3 bar and a spray angle of 120°

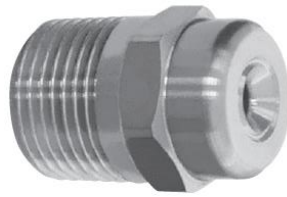


Figure 5-6: Full cone nozzle from “Lechler” [12]

According to the supplier of the nozzles, increasing the pressure decreases the diameter of the droplets, therefore, the atomization gets finer. According to the data sheets, the mean velocity of the nozzle in vertical directions was given between 5 and 6 m/s at nominal flow and pressure conditions. Naturally, increasing pressure increases the speed as well. Unfortunately, no quantitative statements were available from the supplier, neither to the development of the speed nor to the diameter of the droplets in relation to changing the pressure. Datasheets of the used nozzles can be found in the appendices.

All nozzles were applicable for all spray modules and therefore, a large range of influencing parameters on the volumetric flow reduction of the moist air was coverable.

The amount of water sprayed into the vacuum system was adjusted with a ball valve and measured with an inductive flowmeter model “Optiflux 4300” from KROHNE. Both simultaneous installed modules were individually suppliable with cooling water by adjusting the hand valves.

#### 5.2.4 Glass cylinder

To make the spray visible a glass cylinder with a diameter of 200mm was installed directly after the spray modules. The glass cylinder was manufactured by the company “Ruprecht” and a photo is shown in Figure 5-7. To make the atomisation and redirection of the spray visible a laboratory screw joint was prepared at the side to insert the spray nozzle directly into the glass cylinder.

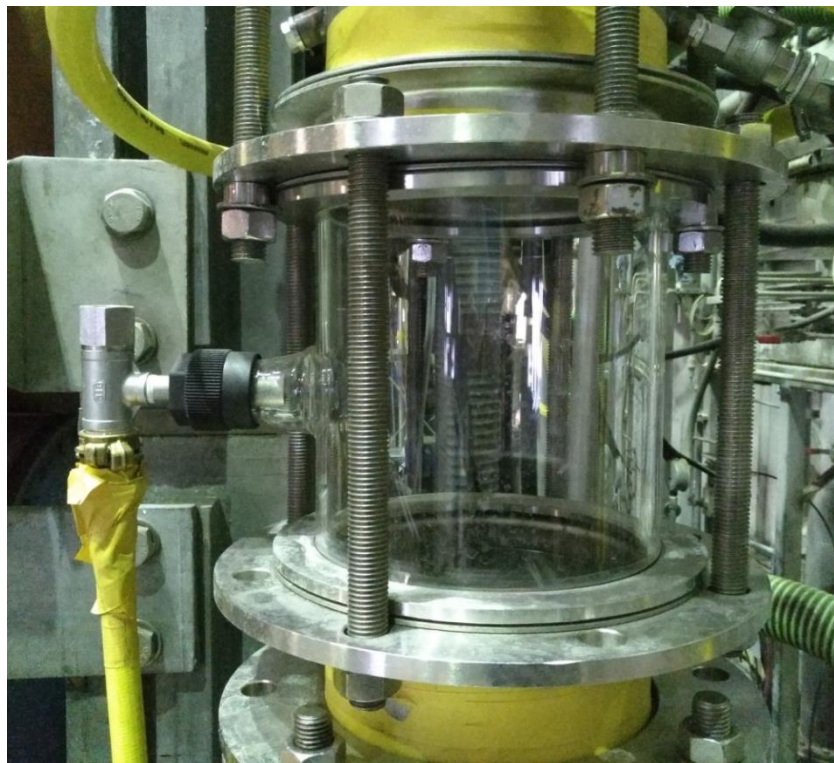


Figure 5-7: Glass cylinder with laboratory screw joint installed in the experimental setup

### 5.2.5 Measuring pipe

An approximately 1500mm long pipe was installed and connected to the glass cylinder. In this pipe four nipples were welded for measuring the relative humidity after different distances from the spray injection, to evaluate the development of the temperature and the relative humidity as a function of the dwell time of the droplets in the moist air flow. With the temperature the volumetric flow reduction was ascertainable. The four nipples were placed at a distance approximately 400mm to each other.

The measurement of the temperature and the relative humidity was planned to be performed with a testo measuring device, which was already available at Andritz AG. It provided an easy and comfortable way of measuring the temperature and relative humidity in one step, without carrying out any further calculation. Additionally, this device was proven in many other applications and provided satisfactory results. Unfortunately, it turned out that high relative humidity, close to 100%, and the attendance of droplets greatly distorted the results and made them useless.

Therefore, it was decided instead to use a psychrometer. All the following thermodynamic formulations are taken from [1]. With a psychrometer the degree of humidity  $x$  and the relative humidity  $\varphi$  of moist air flows, can be evaluated. Therefore, two thermometers are necessary. The first measures the temperature of the dry air  $t_{dry}$ . The second thermometer is coated with a moist piece of absorbent cotton and measures the saturated temperature  $t_{moist}$ . The principle is shown in Figure 5-8 below:

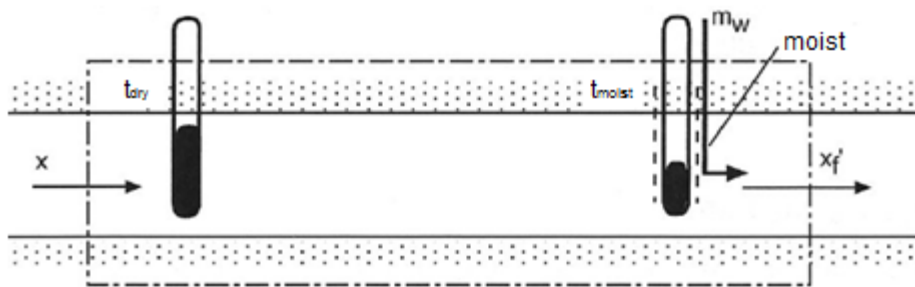


Figure 5-8: Principle of a psychrometer [1]

The calculation of the relative humidity was carried out with the measured temperatures using the equations from [13]. For detailed information please refer to [13].

$$\varphi = \frac{e}{E_{dry}} \quad (5-1)$$

$$E_{dry} = 6,112 * e^{\left(\frac{17,62*t_{dry}}{243,12+t_{dry}}\right)} \quad (5-2)$$

$$E_{moist} = 6,112 * e^{\left(\frac{17,62*t_{moist}}{243,12+t_{moist}}\right)} \quad (5-3)$$

$$e = E_{moist} - Y * (t_{dry} - t_{moist}) \quad (5-4)$$

Commonly, the psychrometer- constant is assumed to be  $Y = 0,67$ .

The chart from Figure 5-9 was used to estimate the relative humidity directly at the test stand.

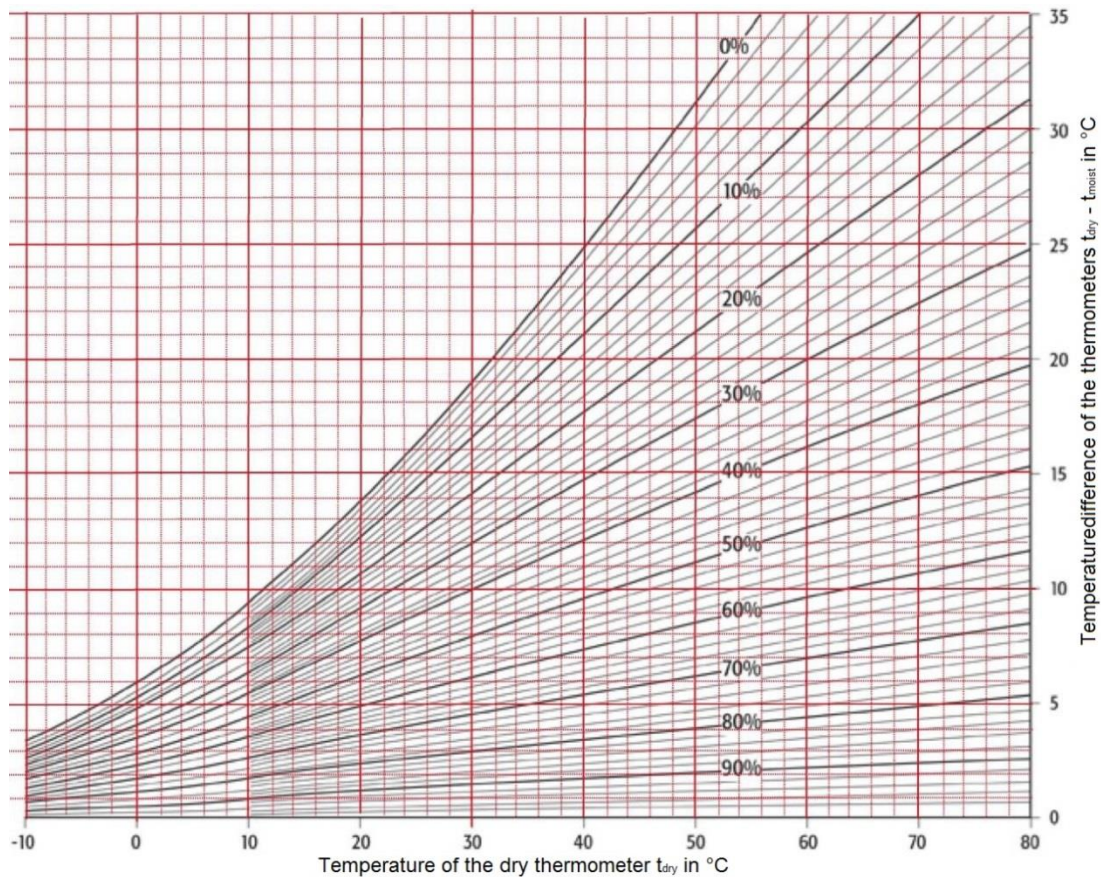


Figure 5-9: Relative humidity as a function of measured temperatures  $t_{dry}$  and  $t_{moist}$  [13]

The two plugin thermometers used were from the company TFA Wertheim, model 30.1040. The measurement was carried out at one of the four nipples in the measuring pipe at one time. To prevent air sucking into the vacuum a sealing plate was used between the nipple and plugin thermometer.

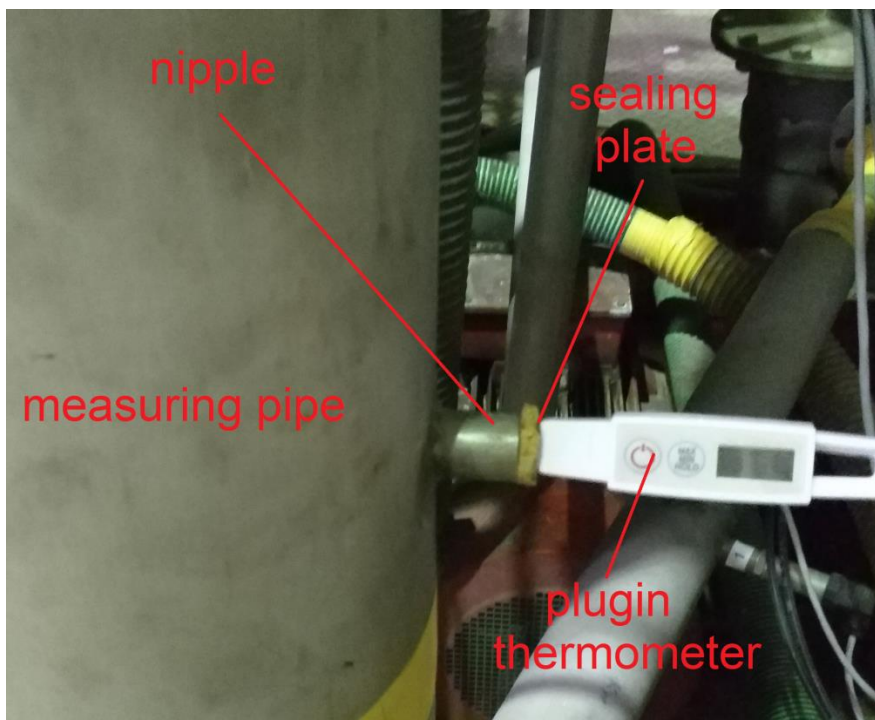


Figure 5-10: Measurement of the temperature and relative humidity

### **5.2.6 Measurement unit outlet, Debimo sensor**

After the 4<sup>th</sup> measuring point, the pipe diameter was reduced to 100mm, and with an elbow, the flow was redirected in a horizontal direction again. At this position another Debimo differential pressure sensor was installed to measure the temperature, volumetric air flow, absolute pressure, vacuum level and velocity at the end of the test section. It was intended that a difference between the inlet and outlet measurement was computable. As a direct result of the high amount of water that accumulated at the bottom of the system the differential pressure sensor at the outlet did not provide applicable results.

### **5.2.7 Water separator, vacuum pump and extraction pump**

Afterwards the pipe diameter was then reduced to 80mm. The flows of moist air and water were forwarded tangential into the existing water separator. The aim of the water separator was to separate the moist air flow from the water in the flow. The water was separated to the bottom and was sucked out of the separator by use of an extraction pump. The extraction pump was necessary due to the large air and water flow in the vacuum system, to improve the separation of the moist air flow, and lastly, to prevent too much water being sucked to the vacuum pumps.

### 5.3 Experimental methodology

In the following chapter the methodology and the execution of the experimental are described.

#### 5.3.1 Matchup of the measuring instruments

The measuring instruments used were already introduced in chapters 5.2.1 to 5.2.7. Before starting the experiment, they were calibrated and compared to each other to ensure that the measured results were as realistic as possible.

#### Verifying Debimo differential pressure sensor

The temperature, volumetric air flow, absolute pressure, vacuum level and velocity of the top inlet Debimo differential sensor, fit to the results of the other measurement devices. The flow speed was verified with a vane anemometer from testo, model 0635 9540. Its latest calibrated in 09.2016 by testo Kalibrierdienst and can therefore, be assumed to be accurate. The temperature of the Debimo differential pressure sensor was verified with a plugin thermometer from TFA Wertheim, model 30.1040. The vacuum height was measured with an analogue vacuum manometer from WIKA, model number 111.10.100-1BAR G1/2B.

In order to verify the Debimo sensor a vacuum was enabled but no water was applied on the felt. Therefore, the temperature and the humidity of the air were lower than in the experiment afterwards. The reason for this was that a high relative humidity of the moist air, or the presence of water droplets in the flow, most likely damages the vane anemometer that was used for verification.

The verification showed that the measured values of the top Debimo differential pressure sensor are accurate as observable in Table 5-2. Bottom Debimo differential pressure sensor was not calibrated as it was already known that the high attendance of water in the system that accumulates around the sensor (lowest position of the system) would lead to dissatisfactory results.

Measuring device	Temperature	$\Delta p$	v
	°C	bar	m/s
Top Debimo differential pressure	25,6	-0,14	12,9
Plugin thermometer	25,6	-	-
Barometer	-	-0,15	-
Vane anemometer	-	-	13,1

Table 5-2: Verification of the top Debimo differential pressure sensor

#### Verifying the moist air measurements

As already described above, the relative humidity was measured according to the psychrometric principle. The verification was carried out with a humidity measuring device from testo, model 0420 0023, which was calibrated for the last time in 09/2016 by testo Kalibrierdienst. Results from this device can therefore, be considered as accurate.

As the testo humidity measurement device can only handle relative humidity <100% and dry air flow without droplets or higher amounts of water, the comparative measurement was carried out without adding hot water on the felt. The measurements were carried out twice. Firstly, without vacuum (felt was not running and lifted away from the suction box) and secondly, with a vacuum reading of approximately -0,15bar relative pressure. Both times, the position of the measurement was at the 4<sup>th</sup> nipple in the measurement section. The results are shown as follows in Table 5-3:



Measuring device	T <sub>dry</sub>	T <sub>moist</sub>	RH	Δp
	°C	°C	%	bar
Testo	25,9	-	53	0
Plugin thermometer*	26,0	19,1	52	0
Testo	23,8	-	58	-0,15
Puncture thermometer*	24,2	18,7	59	-0,15

Table 5-3: Verification of the psychrometric principle

Clearly, the results obtained from the testo humidity measurement device, and the psychrometric principle carried out with the plugin thermometer, fit to each other. Therefore, it can be assumed that the temperature and relative humidity measured with two plugin thermometers are appropriate for this application.

In Figure 5-11 the utilised measuring devices for verification and matching are shown.



Figure 5-11: Measuring devices for verification of measurements

### 5.3.2 Parameters to be investigated

The aim of this experimental was to investigate the influence of different parameters on the volumetric flow reduction of the moist air. The parameters are listed below and also how their influence on the volumetric flow reduction was evaluated is described. For reasons of time, effort and costs not all of them could be treated as preferred.

#### 1. Flow parameters

For comparison, exemplary flow parameters of industrial sized machines are shown in Figure 3-9.

- Vacuum levels

Two different vacuum adjustments were used for evaluation. The first  $\Delta p$  was approximately 0,15-0,17 bar relative with one vacuum pump in operation. By adding a second vacuum pump the vacuum reading  $\Delta p$  increased up to approximately 0,25-0,28bar relative pressure. As already described, the vacuum values at industrial machines are between 0,20 and 0,45bar relative, depending on the vacuum applied position. Unfortunately, it was not possible to increase the vacuum any higher as the available equipment at the pilot plant was not dimensioned for that big vacuum flows. The bottlenecks were the vacuum pumps and the water separators that cannot be changed and therefore, it was not possible to run higher vacuum levels.

- Volumetric flow & velocity of the moist air flow

The volumetric flow was adjusted by increasing or decreasing the vacuum values. Low vacuum levels of approximately 0,15-0,17bar relative (operating one vacuum pump) led to moist air flows of approximately 6m<sup>3</sup>/min. High vacuum levels of approximately 0,25-0,28bar relative (operating two vacuum pumps) led to moist air flows of approximately 9m<sup>3</sup>/min. These flows were by far below the flows of average industrial sized machines.

Depending on the temperature, vacuum level and volumetric flow a certain velocity was achieved accordingly. This speed was below the velocity of industrial sized machines as well.

- Temperature of the moist air

The temperature of the moist air was adjusted by increasing or decreasing the temperature of the hot water applied on the felt before the suction box. Two different temperatures of the hot water applied on the felt were investigated. The first hot water temperature was approximately 65°C, which resulted in a moist air temperature of approximately 49-52°C. By increasing hot water temperature up to approximately 78°C, moist air temperatures of approximately 55-57°C were achieved.

- Humidity of the moist air

With the above described procedure the relative humidity  $\varphi$  was measured with 100% several times. Consequently, it was not possible to investigate the effect of this parameter on the volumetric flow reduction.

#### 2. Geometry parameters of the piping

- Length of the pipe

To simulate the different lengths of the pipes of the different machines, several measuring positions were implemented after the spray was injected. They are shown in Figure 5-2. The reason for this was to measure the temperature as a function of the dwell time of the droplets in the pipe. As the flow speed of the moist air was low

compared to industrial sized machines, the dwell time of the spray was higher as well.

- Shape of the pipe

It was not possible to try different shapes of the pipe, such as rectangular shaped pipes, as the effort and costs for a potential rebuild were too high.

### 3. Spray parameters

- Spray direction

Various spray modules were used to measure the influence of different spray directions. Also, different mounting directions were tested for the skewed and the module that sprays in or against the moist air flow direction. The modules are shown in Figure 5-5.

- Size of the droplets

Three different nozzles with different nominal flows were tested to measure the influence of the different size of droplets on the volumetric flow reduction.

- Pressure, volumetric flow and velocity of the sprayed droplets

Pressure and velocity of the injected droplets depend on each other. Raising the pressure increased the velocity, and therefore, also the volumetric flow of the droplets. To investigate the influence on volumetric flow reduction of the moist air, for each of the three nozzles three different volumetric cooling flows were tested. The cooling flows used for the experiments are shown in Table 5-4. The nominal volumetric flow at a pressure of 2bar is shown for each nozzle as well.

Type	Q <sub>nom</sub>	Flows at experiments		
	@ 2bar	Q <sub>1</sub>	Q <sub>2</sub>	Q <sub>3</sub>
	l/min	l/min	l/min	l/min
<b>490.686</b>	5,0	3,0	5,0	8,0
<b>490.766</b>	8,0	5,0	8,0	12,0
<b>490.846</b>	12,0	8,0	12,0	15,0

Table 5-4: Variation of the flows for the different sizes of nozzles

- Temperature of the cooling water

The influence of the temperature of the sprayed water droplets was not investigated as the cooling water was taken from the available fresh water line. The temperature of the water was measured several times during the experiment and was constant with a temperature of 15°C.

### 5.3.3 Execution of the experiment

The experiment was carried out adjusting one parameter after another. After adjusting one of the prior described parameters all measured values were recorded to calculate the volumetric reduction for each set point.

The recorded values for each set point were:

- Initial conditions from Debimo differential pressure sensor
  - Absolute pressure
  - Vacuum level
  - Temperature
  - Volumetric flow
  - Velocity
- End conditions at measuring pipe (after spray water was injected)
  - Temperature  
Measured with plugin thermometer
- Spray water parameters
  - Temperature  
Measured several times with plugin thermometer
  - Volumetric water flow and pressure  
Measured with induction flow measurement device
  - Used nozzle

Due to the time restrictions, not the entire matrix of parameters was varied. Nevertheless, more than 100 different conditions with different parameters were tested. Detailed results of the experiment are provided in the appendices.

## 5.4 Results and explanation

After explaining the experimental setup and the methodology in the prior section of the thesis, the following chapter provides the results and other findings of the experiment.

### 5.4.1 Reduction of used nozzles per system

It was planned to use up to four nozzles in each spray module to allow higher amounts of water to be injected into the system. After starting the procedure with water amounts  $> 20\text{l/min}$  it soon became obvious that the high amount of water injected into the system was not capable for the available vacuum system. Water and moist air were divided badly in the separator and therefore, high amounts of water were sucked into the vacuum pump. This resulted in fluctuating vacuum values, volumetric flows and velocities of the moist air. It was necessary to reduce the amount of water injected into the system to ensure constant vacuum flows and levels. Therefore, only one nozzle was used at a time in a module.

### 5.4.2 Process water in the system

As specified by Andritz at the beginning of this thesis, it was assumed that the water sucked out of the pulp sheet or the felt is only a low amount and should not be considered. According to this assumption only moist air exists in the system but no process water. As there was a glass cylinder installed in the experimental setup to make atomization of the injected spray visible, it was discovered that a high amount of process water existed in the system. This is shown in the picture in Figure 5-12. In this picture no spray was injected, only the process water from the felt is shown. Neglecting the high amount of process water is not allowed thus resulting that the heat transfer from the process water to the droplets is high.



Figure 5-12: Flow of process water in the system;  $\Delta p \approx 0,16\text{bar}$ ;  $T \approx 55^\circ\text{C}$ ;  $\dot{V} \approx 5,7\text{m}^3/\text{min}$

With a felt measuring device, that gives the water load of a felt, it was discovered that, depending on the amount of water applied on the felt and the relative vacuum value, between 19 and 25 l/min of hot water, were sucked out of the felt and were forwarded into the vacuum system. By keeping the amount of hot water applied on the felt and the speed of the felt constant, the water amounts sucked out of the felt only depend on the vacuum level:

- Low vacuum level (approx. 0,15 - 0,17 bar relative) → approximately 20 l/min
- High vacuum level (approx. 0,25 - 0,28 bar relative) → approximately 24 l/min

For calculating the reduction of volumetric flow of the moist air the high amount of process water was considered to be cooled as well. For low vacuum levels a process water flow of 20l/min and for high vacuum levels a process water flow of 24l/min was considered.

A reduction of the hot water applied was not allowed as it would decrease the temperature of the moist air flow in the test system.

#### 5.4.3 Redirection of the spray

As already described prior, it was expected that droplets that are sprayed normal or skewed into the system will be redirected from the moist air flow. To make this redirection visible the installed glass cylinder had implemented a lab screw at the wall to insert a spray nozzle. This was done for each of the three nozzles with a flow of 8 l/min to find out if there was a difference in the redirection behaviour. The results are shown in the pictures in Figure 5-13. For this experiment, no hot water was applied to the felt and the vacuum level was low and therefore, also the speed in the pipe was low.



nozzle: 490.686,  $Q_{\text{nom}} = 5 \text{ l/min}$



nozzle: 490.766,  $Q_{\text{nom}} = 8 \text{ l/min}$



nozzle: 490.846,  $Q_{\text{nom}} = 12 \text{ l/min}$

Figure 5-13: Redirection of spray as a function of the droplet diameter;  
 $Q=8\text{l/min}$ ;  $\Delta p \approx 0,16\text{bar}$ ;  $T_{\text{moist\_air\_in}} \approx 28^\circ\text{C}$ ;  $\dot{V} \approx 6,1\text{m}^3/\text{min}$ ;  $v \approx 3,2\text{m/s}$

Evidently there is no redirection of the injected spray, neither for the nozzles with low nor with high nominal flow  $Q_{nom}$ . Instead of being redirected from the air flow, the spray splashes directly onto the wall of the glass cylinder. This means that the water flows down at the wall of the pipe. Therefore, the heat transfer decreases rapidly as the high surface to volume ratio of the droplets does not exist anymore. A possible reason for the poor redirection might be due to the low speed of the moist air flow of approximately 3,2m/s, and the narrow diameter of the pipe.

As there is nearly no redirection visible it is questionable if the redirection would work after increasing the flow speed and the diameter of the piping. From this perspective, it would be reasonable to continue experimental with modules that spray in the flow direction.

#### 5.4.4 Detailed results of the experimental setup

Despite all the issues which occurred, the experiments were continued to figure out at least some coherences between the parameters described in chapter 5.3.2 and the reduction of the volumetric flow. In the following chapter charts are presented that show the findings. They can be understood as tendencies but the experiment needs to be repeated for verification.

As already mentioned above, in the evaluation, the heat transfer from the large amount of process water to the droplets was considered and therefore, the cooling effect of the injected droplets was less than expected. It was assumed that the temperature measured with the plugin thermometer after injecting the cooling spray is the same for the moist air and the process water. The theoretical temperature of the injected spray water was calculated accordingly.

As the most important effect that should be reached is the reduction of the volumetric flow of the moist air, all charts have plotted this parameter on the y- axis. Additionally, a utilization factor of the injected water was defined, which is shown in some of the charts as second y- axis as well.

$$\eta = 1 - \frac{T_{moist\_air\_OUT} - T_{spray\_OUT}}{T_{moist\_air\_IN} - T_{spray\_IN}} \quad (5-5)$$

The utilization factor represents the quotient of the differences between the temperature of the moist air and the sprayed water at the outlet to the initial temperatures at the inlet. Both temperatures at the inlet and the temperature of the moist air at the outlet were measured. The theoretical spray temperature coming from the heat transfer at the outlet was calculated according to the measured data. In some charts the utilization factor exceeds 100% which can be explained by measuring errors.

The curves connecting the points in the charts with each other are polynomial curves of 2<sup>nd</sup> degree.

Detailed data of all measured points can be found in the appendices.

To better understand the charts, the following nomenclature is important:

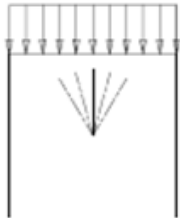
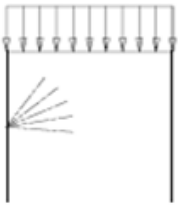
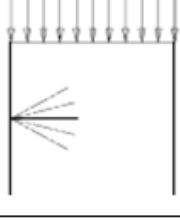
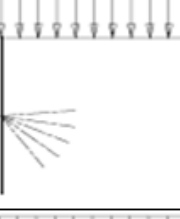
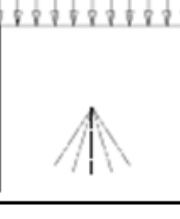
T	Temperature	low	~49 - 52 °C
		high	~55 - 57 °C
$\Delta p$	relative vacuum value	low	~0,15 - 0,17 bar
		high	~0,25 - 0,28 bar
spray direction: up			
spray direction: skewed up			
spray direction: normal			
spray direction: skewed down			
spray direction: down			

Table 5-5: Nomenclature for charts



### 5.4.4.1 Influence of vacuum value, volumetric flow and velocity on volumetric flow reduction

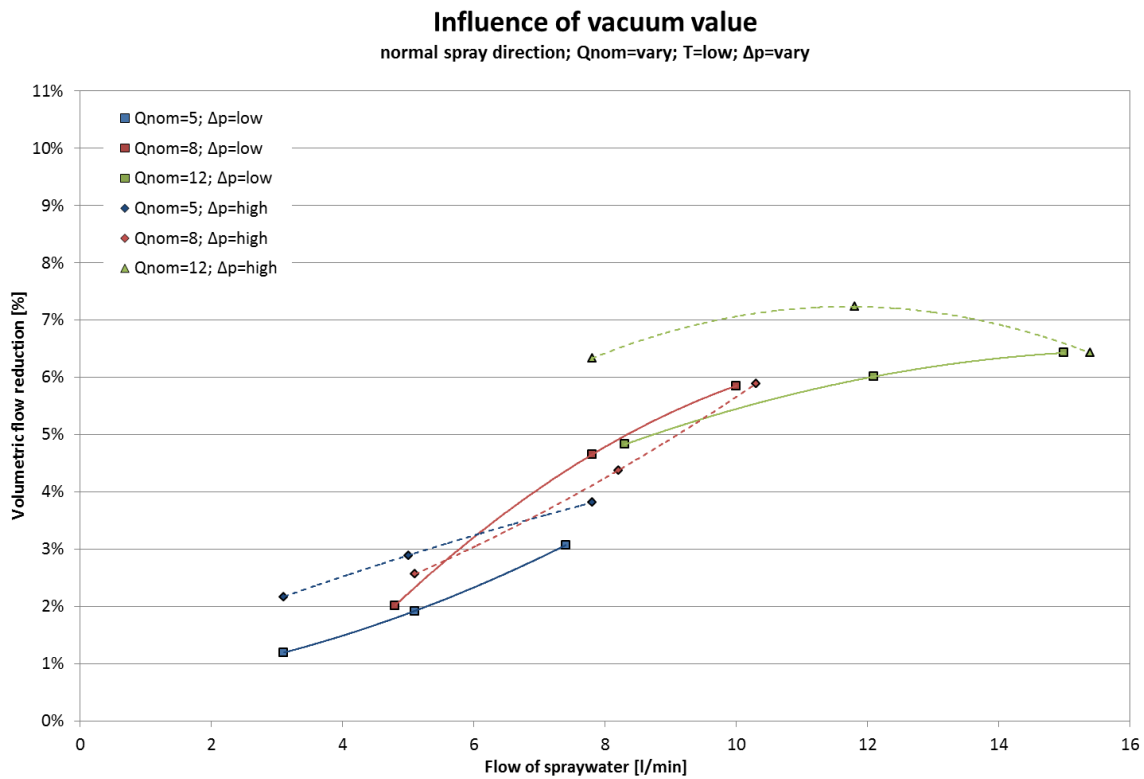


Figure 5-14: Influence of vacuum level and amount of spray water on volumetric flow reduction, normal spray direction

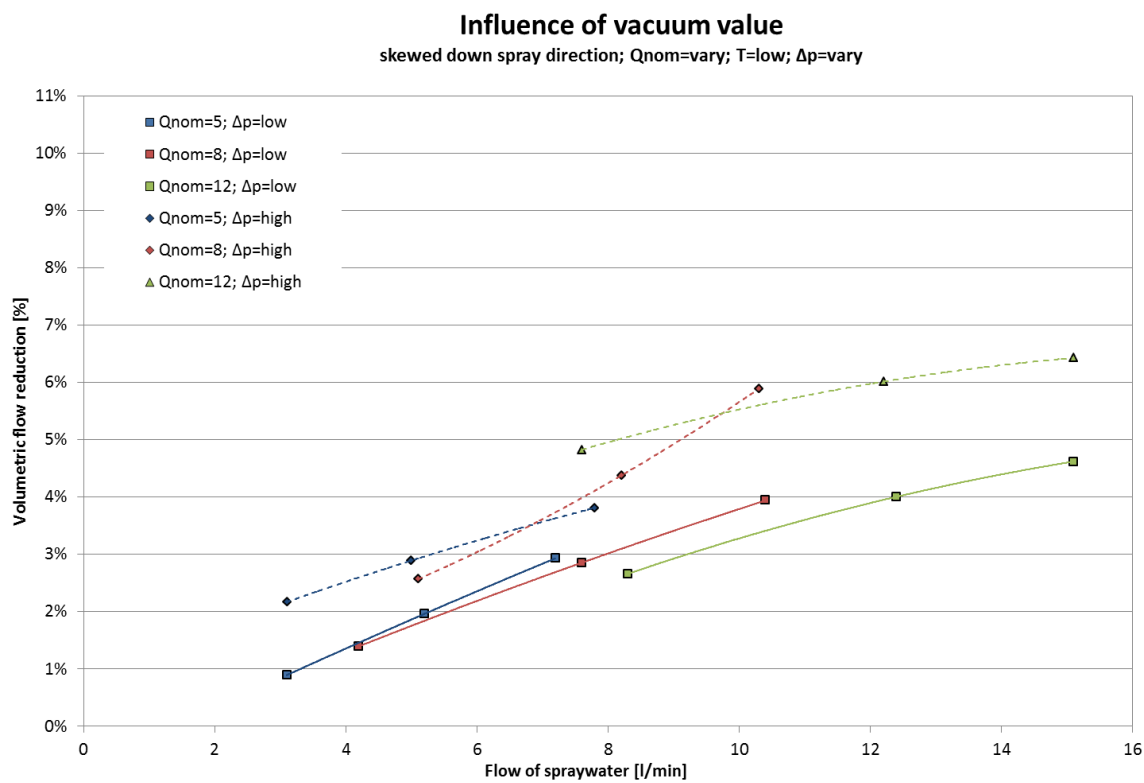


Figure 5-15: Influence of vacuum level and amount of spray water on volumetric flow reduction, skewed down spray direction

The presented charts show the influence of the vacuum values on the volumetric reduction of the moist air flow. Additionally, different nozzles and amounts of spray water were tested and their influence on the reduction on the volumetric flow was investigated. This is shown in Figure 5-14 for normal and in Figure 5-15 for skewed down spray direction.

- Increasing the injected water raises the volumetric flow reduction of the moist air.
- Injecting higher amounts of spray water (approx. > 12l/min) shows that the gradient of volumetric flow reduction of moist air decreases slightly.
- Higher  $\Delta p$  increases the reduction of volumetric flow of the moist air. This is a positive aspect as industrial machines run much higher vacuum levels compared to those in the experiments and therefore, higher volumetric flow reductions can be expected.

Although there was high water amount in the system (high energy transfer from process water to injected spray), this finding can be explained by thermodynamic theory. Increasing the vacuum level (=less absolute pressure) leads to higher degree of humidity  $x$ , which means that the volume- share of vapour in the moist air increases as well. Therefore, the volumetric flow reduction potential becomes higher, as the main share of the volumetric flow reduction can be repatriated on the vapour share in the moist air.

#### 5.4.4.2 Influence of moist air temperature on the volumetric flow reduction

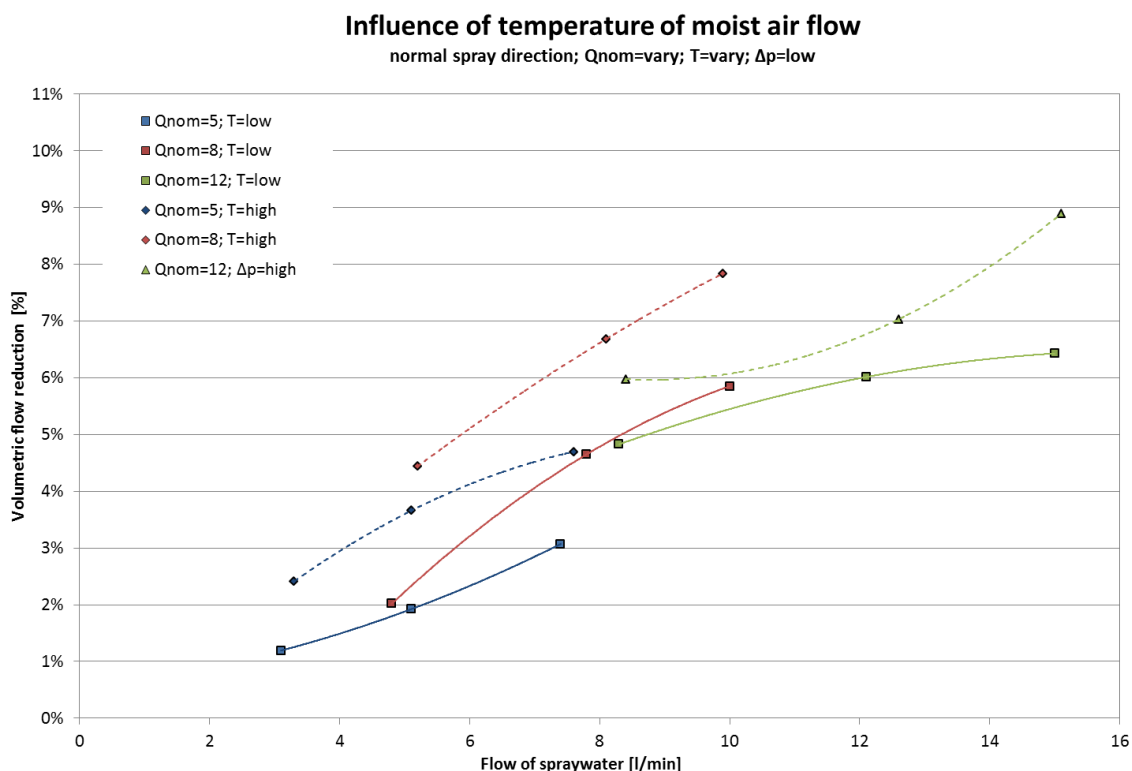


Figure 5-16: Influence of moist air temperature and amount of spray water on volumetric flow reduction, skewed down spray direction

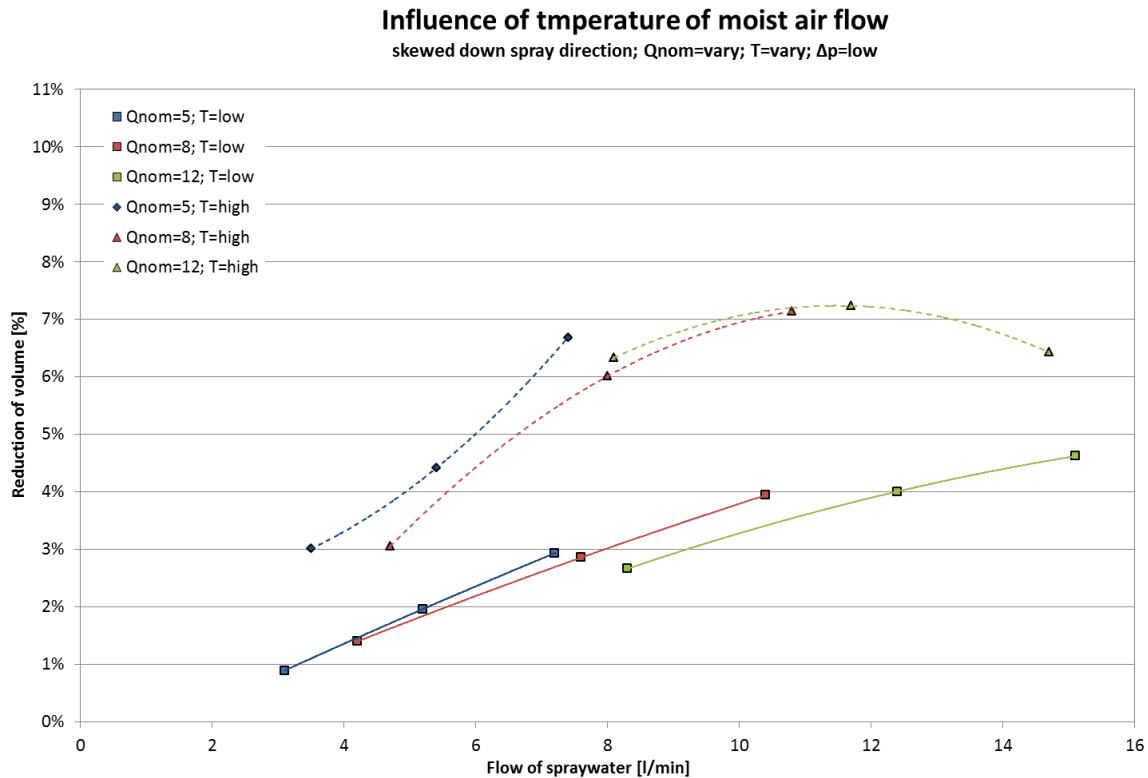


Figure 5-17: Influence of moist air temperature and amount of spray water on volumetric flow reduction, skewed down spray direction

Complementary to the prior described influence of the vacuum level, the same procedure was carried out for two temperature levels of the moist air flow. Different nozzles and amounts of spray water were tested and their influence on the volumetric reduction of the moist air flow was investigated, as shown in Figure 5-16 for normal and for skewed spray direction in Figure 5-17 as well.

- Comparable as described in 5.4.4.1, increasing the spray water flow leads to higher volumetric flow reduction.
- Furthermore, higher amounts of water show the tendency of decreasing volumetric reduction gradients. In Figure 5-16, trend “ $Q_{nom}=12; \Delta p=high$ ” shows a different trend compared to all other trends. This might be an outlier.
- Increasing the temperature of the moist air flow increases the volumetric reduction potential as well.

This effect can be explained thermodynamically as well. For both temperature levels, a relative humidity of 100% (saturated air) was measured several times. If the vacuum level stays constant, increasing the temperature leads to increased saturated partial pressure  $p_d'$  and higher degree of humidity  $x$ , which increases vapour content of the moist air as well. Therefore, volumetric reduction potential increases with higher temperatures.

### 5.4.4.3 Influence of the length of the pipe and dwell time on the volumetric flow reduction

Classification of the spray						Thermodynamic/downstream measurements				Utilization factor	
						position 1 at measuring pipe		position 4 at measuring pipe			
module	direction	$Q_{nom}$	$Q$	$T$	$\Delta p$	$T_{moist\ air\ out_1}$	$\Delta V_{moist\ air_1}$	$T_{moist\ air\ out_4}$	$\Delta V_{moist\ air_4}$	$\eta_1$	$\eta_4$
-	-	l/min	l/min	°C	bar	°C	%	°C	%	-	-
normal	-	5	3	l	l	47,4	1,13	47,3	1,19%	0,41	0,43
normal	-	5	5	l	l	46,6	1,97	46,6	1,92%	0,43	0,43
skewed	down	12	8	h	l	55,8	3,26	54,9	4,53%	0,38	0,47
skewed	down	12	15	h	l	54,1	5,62	52,8	7,17%	0,40	0,48
normal	-	5	3	l	h	48,6	2,21	48,6	2,17%	0,86	0,85
skewed	down	5	8	h	h	52,3	6,00	52,8	5,28%	0,83	0,77
skewed	down	8	5	h	h	55,5	0,91	55,1	1,54%	0,22	0,31

Table 5-6: Extract of the measured data showing the dwell time of the sprayed droplets

As given in Table 5-6, no major influence of the dwell time was measured. Dwell time is a function of the distance from the injected flow and can therefore be compared between measuring position 1 and 4 of the measuring pipe.

Analysing detailed data in the appendices shows that occasionally the temperatures were even higher with an increased dwell time. This can be explained by fluctuating properties in the system or by a measurement error.

Nonetheless, the results should not assign a too high value, as the spray was splashed directly onto the wall after injecting it into the system. Furthermore, the presence of a large amount of process water complicated the results. Therefore, it is necessary to verify the influence of the dwell time in an upcoming experiment after changing the setup.

### 5.4.4.4 Influence of spray direction on volumetric flow reduction of moist air flow

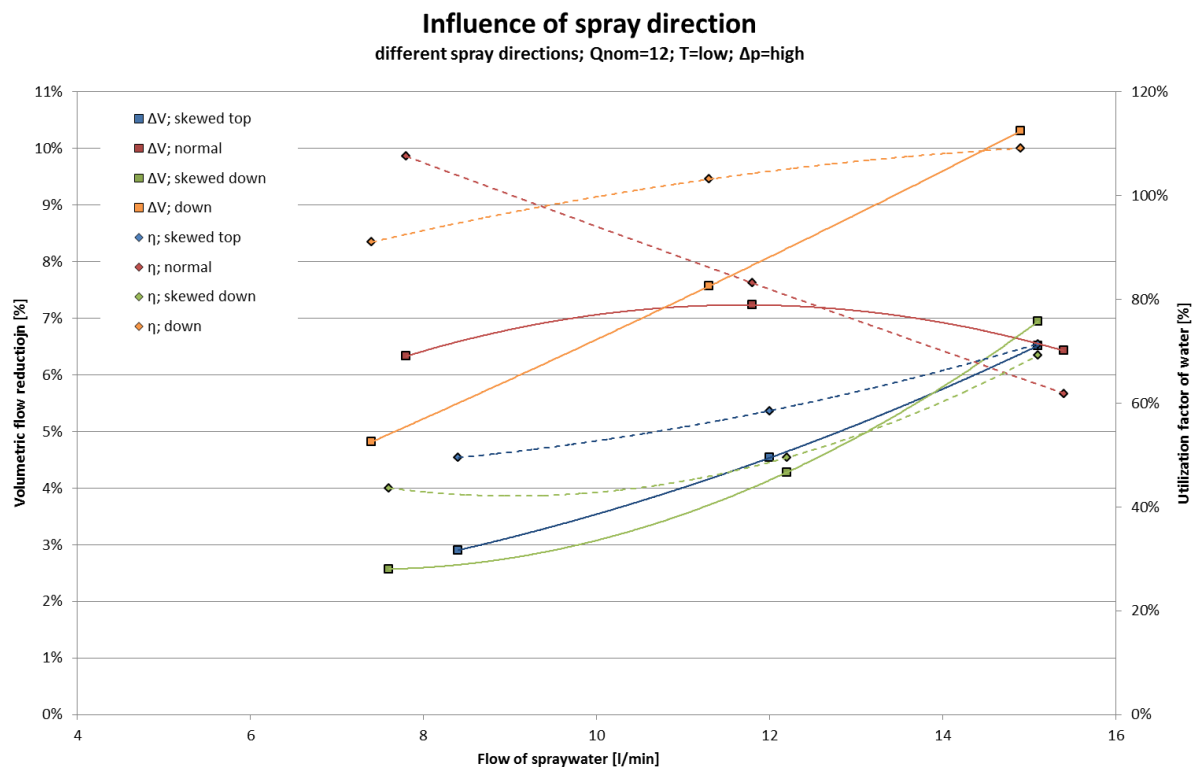


Figure 5-18: Influence of spray direction on volumetric flow reduction and utilization factor;  
 $Q_{nom} = 12$  l/min,  $\Delta p = high$

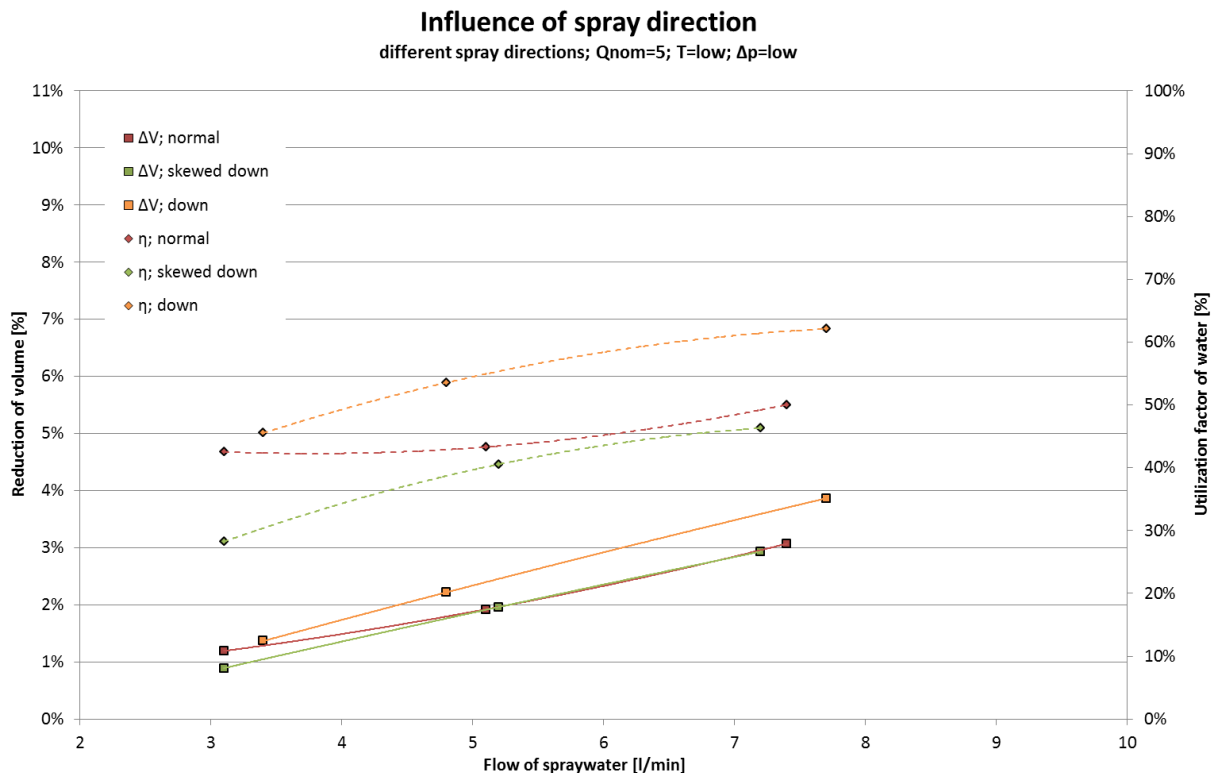


Figure 5-19: Influence of spray direction on volumetric flow reduction and utilization factor;  
 $Q_{nom} = 5$  l/min,  $\Delta p = low$

In both of the above presented charts two ordinates are used. Beside the volumetric flow reduction of the moist air, the utilization factor of water is shown. The utilization factor is defined in equation (5-5). Solid trends refer to the volumetric reduction of volume, while dashed trends refer to the utilization factor.

Both charts show the influence of the spray direction with different boundary conditions. In Figure 5-18, the nozzle used provided  $Q_{nom}=12$  l/min and the vacuum level  $\Delta p$  was low. In Figure 5-19, the nozzle used provided  $Q_{nom} = 5$  l/min and the pressure level was low.

- Once the cooling spray was injected directly in spray direction (down), the highest reduction of volumetric flow and highest utilization factors were reached. The second best results were reached by injecting the cooling spray normal to the moist air flow direction. The worst results were reached with skewed spray directions. Unfortunately, due to the time constraints toward the end of the experiments was not possible to test the spray direction directly against the moist air flow direction (top).
- It is not surprising that injecting the spray in the direction of the moist air flow gives the highest results for both ordinates, reduction of volumetric flow and utilization factor. As explained in chapter 5.4.3, a normal spray direction splashed directly onto the wall. A comparable behaviour is expectable for skewed spray directions. In comparison to this, injecting the spray in the moist air flow direction does not end up in splashing droplets directly onto the wall of the pipe. Therefore, the surface of the droplets stays available for condensation.
- A higher volumetric flow reduction leads to higher utilization factors.
- Nozzles with a higher nominal flow and high vacuum levels do not only have a higher volumetric flow reduction but show a tendency for higher utilization factors.

- The trend described in the prior evaluation, that with increasing the flow rate the gradient of the volumetric flow reduction decreases, cannot be confirmed in this evaluation.
- In Figure 5-18, some results in the chart exceed 100%. As the utilization factor is the result of several measured parameters the exceedance of 100% can be reduced by a measuring error or fluctuating boundary conditions.

#### 5.4.4.5 Influence of different nozzles on the volumetric flow reduction

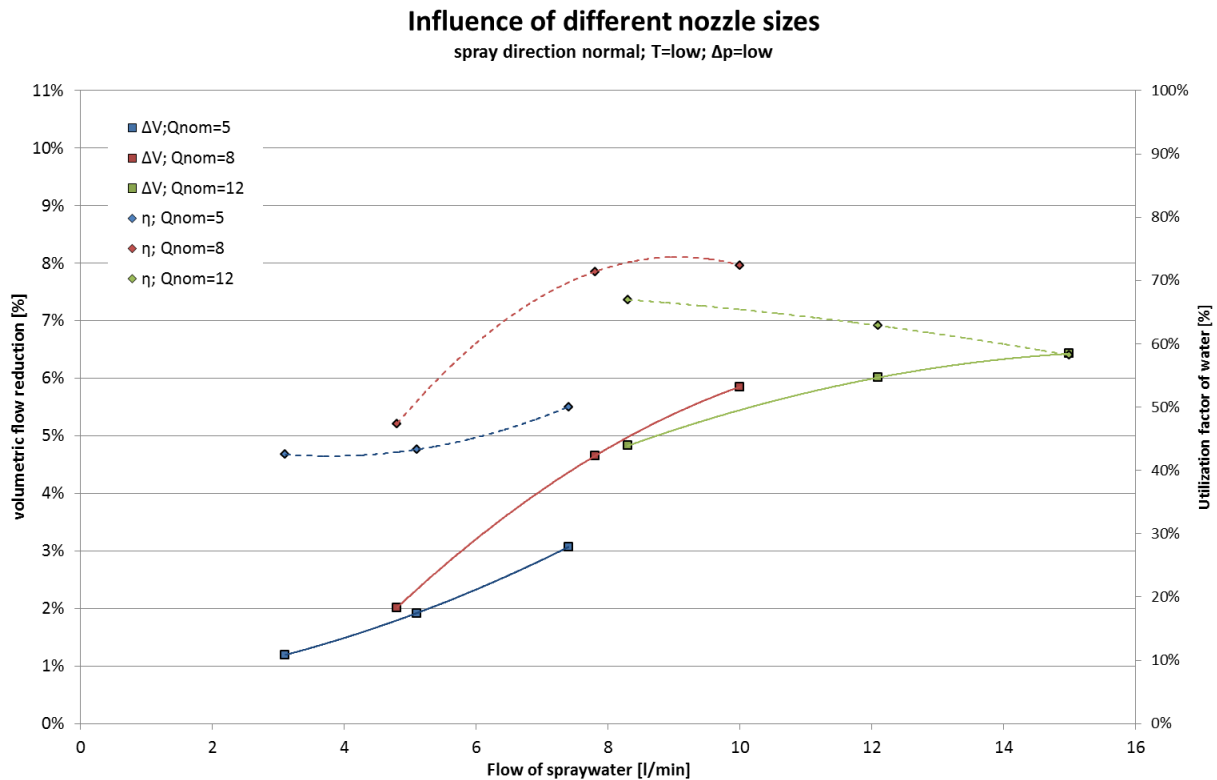


Figure 5-20: Influence of different nozzle types on volumetric flow reduction and utilization factor

In Figure 5-20, the influence of the injected spray flow on the volumetric flow reduction and the utilization factor is shown. For this evaluation all three different nozzle sizes were used. The spray direction was adjusted normal to the moist air flow. Temperature and vacuum level were low.

- The highest utilization factor was achieved with the nozzle  $Q_{nom} = 8$  l/min. Also, the volumetric flow reduction does not increase much further once the volumetric flow of the injected spray is raised to  $>10$  l/min.
- Therefore, injecting approximately 8 l/min with the nozzles  $Q_{nom} = 8$  l/min and  $Q_{nom} = 12$  l/min seems to be the optimal amount of water injected per nozzle.
- In this evaluation, it is evident once more that the decreasing gradient of volumetric flow reduction relates to increasing spray water flow.

## **5.5 Conclusion of the experimental investigation**

In this chapter an experimental investigation carried out on the Pilot Plant in Andritz AG is introduced. The schematic and the boundary conditions of the test stand are described, as well as all the used equipment and the measurement devices. With the experiment an investigation was executed to determine the effect of different parameters on the volumetric flow reduction.

It is shown that a high amount of process water exists in the system, which is not allowed to be neglected, against the specification from Andritz AG given at the beginning of the thesis. The high amount of process water disrupted the results of the experiment. Therefore, the experiment needs to be repeated for verification of the results. Despite all the issues, the effects of some parameters on the volumetric flow reduction could be presented in this chapter.

## 6 Conclusion

In this master thesis, the thermodynamic saving potential for the vacuum systems of pulp drying machines was researched. Owing to the big size and the enormous production of pulp drying machines the vacuum system is cost intensive in installation, as well as in operation, and the cost saving potential is shown as significant.

From thermodynamic considerations it was found out that there is a high volumetric flow reduction potential for the highly saturated moist air flow. It was shown that the volumetric flow reduction can be achieved by cooling down the moist air flow that is coming from the dewatering process. The reduction can be divided in two shares. The first share is the increase of density due to temperature reduction. The second share is the condensation of the vapour in the highly saturated moist air. The condensation of the vapour occupies the weigh bigger share. Depending on the temperature, vacuum level and relative humidity, which can be assumed to be close to 100%, volumetric flow reductions of up to 40% are possible thermodynamically. The reduction of the volumetric flow was carried out by injecting cold water droplets into the hot vacuum flow by the use of nozzles. The droplets provided a large surface to volume ratio and therefore, high condensation rates can be anticipated. Condensation takes place directly on the surface of the droplets.

In order to determine different flow parameters from the moist air and the injected spray, a CFD calculation with ANSYS Fluent 15.0 is carried out. For this purpose the DPM model was used together with the enabled energy equation. To simulate condensation of moist air on the surface of the sprayed droplets a UDF was implemented into ANSYS Fluent. Applying the correct settings it was shown that direct contact condensation can be simulated. Increasing the injected spray showed that the DPM model was limited with a maximum injection rate occupying 10-12% of the volume of a cell but by far the limit had to be exceeded in this project. To solve this issue, it was decided to manipulate the substance properties to reduce the volumetric share of the DPM, however the results achieved were not satisfactory. Neither the mass share of vapour nor the temperature of the moist air were fitting to the non-manipulated trends. Adding linear factors to the mass and energy transfer equation showed that this might be a solution but needs additional research effort. Other possible models, such as the DDPM or the multiphase model or further continued research with the DPM model were described but not followed up in this master thesis.

As for the dissatisfactory results obtained from the CFD calculation, an experiment at the pilot plant at Andritz AG in Graz was carried out. It was necessary to rebuild and modify some of the existing available vacuum system. It was not possible to rebuild the existing system in a way that it represented the vacuum system of industrial sized machines. A compromise between big sized equipment and convenient operation properties (vacuum level and flow) was taken.

The results from the experiments are as follows:

- Injecting the spray normal to the moist air flow ended up in droplets splashing directly onto the wall instead of being redirected in the moist air flow direction, which is most likely a result of the low vacuum level reached in the experiment. As a direct result of that the condensation cannot appear at the surface of the droplets anymore, which led to lower condensation rates.
- In contraction the assumption of low amount of process water in the system (given by Andritz), a high amount was evident. Therefore, not only the moist air flow had to be cooled but also the process water. This claimed high energy sources from the injected cooling spray which led to much lower volumetric flow reduction than expected.



As for the high amount of process water in the system, the experiment needs to be repeat with a rebuilt test stand to verify results. Nevertheless, the influence of some parameters can be presented:

- The spray direction seems to be best in the same direction as the moist air flow. All other spray directions splashed directly onto the wall of the pipe and condensation rates decreased.
- Higher temperatures and higher vacuum levels resulted in higher volumetric flow reductions.
- Increasing the amount of injected spray water led to increased volumetric flow reduction. From a certain level on a decreased gradient of volumetric flow reduction occurred. Therefore, the maximum amount of water injected per nozzle would be around 8-10l/min per nozzle. From the results, it can be assumed that the best nozzle would be  $Q_{nom}=8\text{l/min}$ .
- From the experiment, it cannot be forecasted how the behaviour of the volumetric flow reduction will develop if more than only one nozzle is used, as this would have exceeded the capability of the vacuum system at the pilot plant.

## 7 Next steps

As the thermodynamic saving potential is very high this project shall be continued based on the findings of this master thesis. The results obtained show that it is possible to reduce volumetric flow although a high amount of process water was in the vacuum system. The justification for putting further effort into this project is that after succeeding, the advantages for both, the customer, and Andritz as well, are expected. Andritz can reduce the size of the vacuum system which reduces the costs and provides a selling argument as well and lastly, the customers need less energy for operating the vacuum system of the pulp drying machine.

The research will be continued by adapting the test stand. Based on the results of this master thesis the next step will be to rebuild the actual test stand. The main modification will be that a second water separator will be installed to separate the process water from the moist air before the spray is injected, in order not to cool the process water but only the moist air flow. This separator will be larger sized to ensure optimal separation between the water and moist vacuum flow. A systematic drawing of the adaptation and the rebuild of the test stand is shown in Figure 7-1. The rebuild and modifications have already commenced while completing this master thesis. Finally, a comparable test programme with the same goals of investigating the influencing factors will be carried out. The results obtained in this master thesis will be verified and lastly, a basis for a decision to implement the system on an industrial sized machine will be taken.

A CFD calculation will not be continued in the foreseeable future, as the effort would be too high, and regardless, all results achieved from a CFD need to be verified by an experiment.

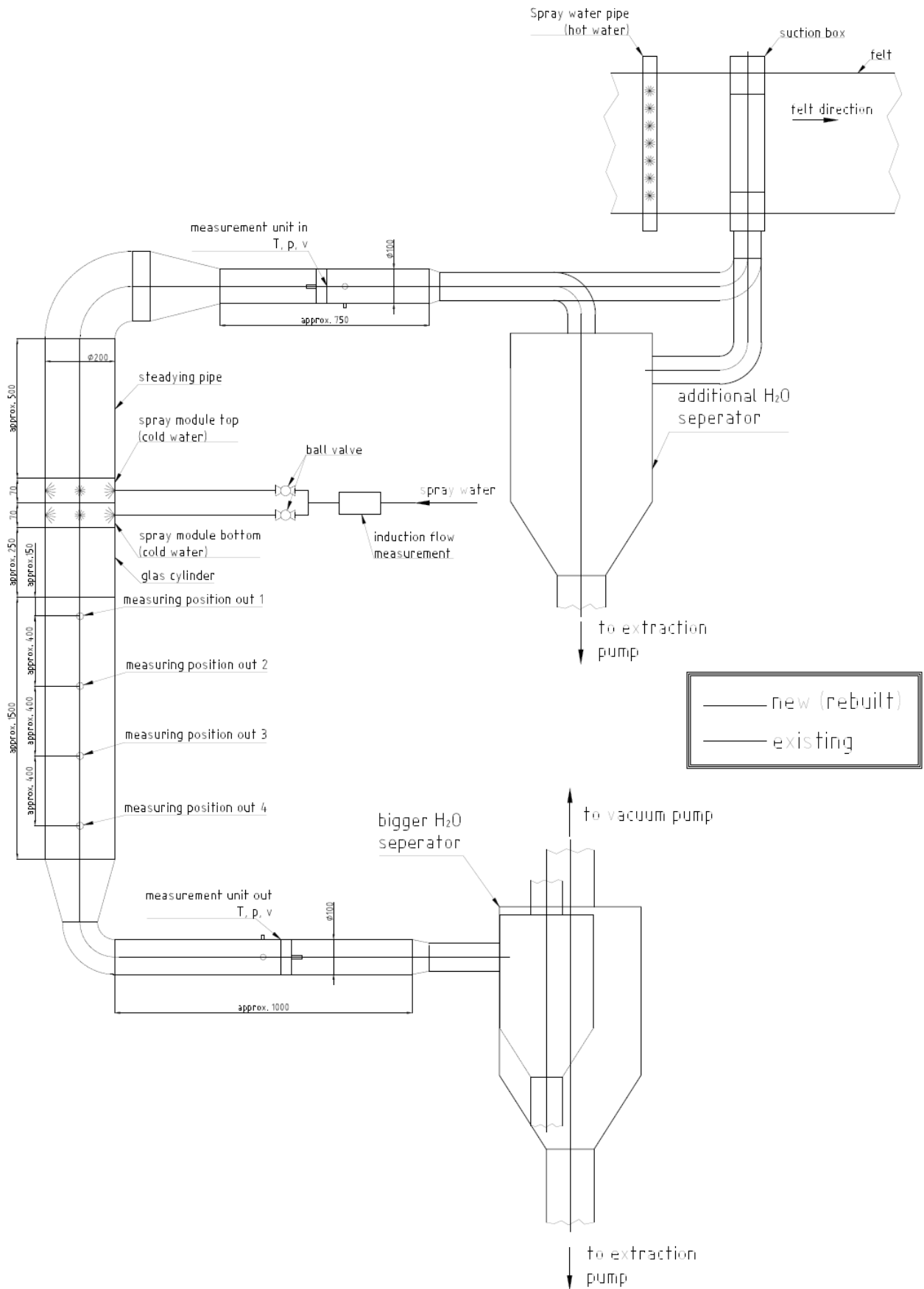


Figure 7-1: Rebuild of the existing experiment setup for further research

## Literature

- [1] Eichlseder, H.: Thermodynamik. Vorlesungsskriptum, Technische Universität Graz, 2014
- [2] Klell, M.: Höhere Thermodynamik. Vorlesungsskript, Technische Universität Graz, 2012
- [3] Brenn G.: Strömungslehre und Wärmeübertragung I. Vorlesungsskriptum, Technische Universität Graz, 2011
- [4] Steiner, H.: Höhere Strömungslehre und Wärmeübertragung. Vorlesungsskript, Technische Universität Graz, 2014
- [5] Numrich, R. et al., Verein Deutscher Ingenieure: VDI Wärmeatlas. Teil J1. Filmkondensation reiner Dämpfe, Springer-Verlag Berlin Heidelberg, 2013
- [6] Numrich, R., Verein Deutscher Ingenieure: VDI Wärmeatlas. Teil J2. Kondensation von mehrstoffgemischen, Springer-Verlag Berlin Heidelberg, 2013
- [7] Hochberg U., Verein Deutscher Ingenieure: VDI Wärmeatlas. Teil J4. Misch- und Sprühkondensation, Springer-Verlag Berlin Heidelberg, 2013
- [8] Spireax Sarco, Grundlagen Dampfkühlung. 2.2 Verfahren der Dampfkühlung, Spirax Sarco GmbH Konstanz, 2012
- [9] Institut für Verbrennungskraftmaschinen und Thermodynamik, Thermodynamik Studienblätter, Technische Universität Graz, September 2016
- [10] [http://www.chemgapedia.de/vsengine/vlu/vsc/de/ch/10/heterogene\\_reaktoren/reaktoren/reaktoren.vlu/Page/vsc/de/ch/10/heterogene\\_reaktoren/reaktoren/festbett\\_reaktoren/rohrbuendelreaktor/rohrbuendelreaktor.vscml/Supplement/3.html](http://www.chemgapedia.de/vsengine/vlu/vsc/de/ch/10/heterogene_reaktoren/reaktoren/reaktoren.vlu/Page/vsc/de/ch/10/heterogene_reaktoren/reaktoren/festbett_reaktoren/rohrbuendelreaktor/rohrbuendelreaktor.vscml/Supplement/3.html)
- [11] KIMO Instruments; DEBIMO Luftrömungsmessungs-Messblende; Electro-Mation GmbH; 22529 Hamburg, Germany
- [12] Lechler, Vollkegeldüsen Seite 3.6
- [13] Mennerich I, Das einfache „Psychrometer“, Schulbiologiezentrum Hannover, Juli 2015
- [14] Aktas, K. M. et al., Department of mechanical engineering, TOBB Economics and Technology Turkey, 2015
- [15] ANSYS, Inc, ANSYS FLUENT User's Guide, Release 14.0, November 2011
- [16] ANSYS, Inc, ANSYS FLUENT Customization Manual, Release 16.2, July 2015
- [17] ANDRITZ Pulp&Paper internal source
- [18] ANSYS, Inc, ANSYS FLUENT 12.0 Theory Guide, April 2009

## List of figures

Figure 1-1: Vacuum applied positions of a standard Twin Wire Former [17].....	1
Figure 2-1: T-s – diagram of a pure substance [1] .....	5
Figure 2-2: Spray condensation [4] .....	11
Figure 2-3: Trajectory of droplets in dependence of the radius [7] .....	13
Figure 2-4: End temperature $\theta_m$ , dwell time $t$ and volume share $dv/dx$ of the droplets [7].....	13
Figure 2-5: Influence of the inert gas share on the heat transfer [6] .....	14
Figure 2-6: Influence of air on the condensation of vapour (gaseous water) [6].....	14
Figure 3-1: Schematic overview of the process for cooling the moist air flow .....	15
Figure 3-2: Typical linings of the suction box of a dewatering machine [17].....	16
Figure 3-3: Typical water separators of a dewatering machine [17].....	17
Figure 3-4: Typical vacuum pumps (incl. drive) for a standard dewatering machine [17].....	17
Figure 3-5: Model and boundaries of the thermodynamic system.....	18
Figure 3-6: Ts diagram for water .....	19
Figure 3-7: Equal direction heat exchanger [4].....	22
Figure 3-8: Temperature development of an equal direction heat exchanger [10] .....	22
Figure 3-9: Thermodynamic saving potential at vacuum system for a standard TWF .....	24
Figure 4-1: Schematic for the spray dryer [14] .....	26
Figure 4-2: Lagrangian vs. Eulerian approach .....	27
Figure 4-3: Boundary conditions of the 2D model .....	30
Figure 4-4: Origin cell of the DPM spray .....	31
Figure 4-5: Position and 2D- geometry of the spray .....	34
Figure 4-6: Mass fraction profile of vapour in the moist air .....	35
Figure 4-7: Temperature profile of the moist air.....	36
Figure 4-8: Mass fraction of vapour in the moist air after manipulating the mass & energy equation .....	38
Figure 4-9: Temperature of the moist air after manipulating the mass & energy equation .....	38
Figure 4-10: Relative humidity, basis (non- manipulated) .....	39
Figure 4-11: Properties of the sprayed droplet and the condensing particle at state 0.....	40
Figure 4-12: Properties of the droplet and the condensed particle at state 1, is as follows: ....	41
Figure 4-13: Properties of the droplet and the particle at state 2 .....	42
Figure 5-1: Problem with too narrow pipe diameters .....	45
Figure 5-2: Schematic of the experimental setup.....	46
Figure 5-3: Photo of the experimental setup .....	47
Figure 5-4: Debimo air flow measurement [11].....	48
Figure 5-5: Used spray modules in experiment .....	49

Figure 5-6: Full cone nozzle from “Lechler” [12] .....	50
Figure 5-7: Glass cylinder with laboratory screw joint installed in the experimental setup ....	50
Figure 5-8: Principle of a psychrometer [1] .....	51
Figure 5-9: Relative humidity as a function of measured temperatures $t_{dry}$ and $t_{moist}$ [13] .....	52
Figure 5-10: Measurement of the temperature and relative humidity .....	52
Figure 5-11: Measuring devices for verification of measurements.....	55
Figure 5-12: Flow of process water in the system; $\Delta p \approx 0,16 \text{ bar}$ ; $T \approx 55^\circ \text{C}$ ; $\dot{V} \approx 5,7 \text{ m}^3/\text{min}$ .....	59
Figure 5-13: Redirection of spray as a function of the droplet diameter; .....	60
Figure 5-14: Influence of vacuum level and amount of spray water on volumetric flow reduction, normal spray direction.....	63
Figure 5-15: Influence of vacuum level and amount of spray water on volumetric flow reduction, skewed down spray direction .....	63
Figure 5-16: Influence of moist air temperature and amount of spray water on volumetric flow reduction, skewed down spray direction .....	64
Figure 5-17: Influence of moist air temperature and amount of spray water on volumetric flow reduction, skewed down spray direction .....	65
Figure 5-18: Influence of spray direction on volumetric flow reduction and utilization factor; $Q_{nom} = 12 \text{ l/min}$ , $\Delta p = \text{high}$ .....	66
Figure 5-19: Influence of spray direction on volumetric flow reduction and utilization factor; $Q_{nom} = 5 \text{ l/min}$ , $\Delta p = \text{low}$ .....	67
Figure 5-20: Influence of different nozzle types on volumetric flow reduction and utilization factor.....	68
Figure 7-1: Rebuild of the existing experiment setup for further research .....	73

## List of tables

Table 4-1: Properties of the discrete phase and the used model .....	31
Table 4-2: Settings and properties of the simulation.....	33
Table 4-3: Factors to adjust the mass and energy equation.....	37
Table 5-1: Used spray nozzle sizes [12].....	49
Table 5-2: Verification of the top Debimo differential pressure sensor .....	54
Table 5-3: Verification of the psychrometric principle.....	55
Table 5-4: Variation of the flows for the different sizes of nozzles.....	57
Table 5-5: Nomenclature for charts .....	62
Table 5-6: Extract of the measured data showing the dwell time of the sprayed droplets.....	66

## Appendices

### Appendix 1: Description of diameter D10, D20, D30, D32

www.duesen-schlick.de



#### Beschreibung der Durchmessermomentenverteilung

Ausgabemoment	Beschreibung
D10	Mittlerer Tropfendurchmesser
D20	Quadratisch mittlerer Tropfendurchmesser
D30	Volumetrisch mittlerer Tropfendurchmesser
D32	Sauter-Durchmesser
Dv0.1	Kumulativer 10%-Anteil: 10% der Gesamttropfen sind kleiner als dieser Durchmesser
Dv0.5	Kumulativer 50%-Anteil
Dv0.9	Kumulativer 90%-Anteil
Uflux	Volumenstrom des Sprays in Richtung der U-Geschwindigkeitskomponente (waagrecht) pro Flächen- und Zeiteinheit.

#### D10:

Der **mittlere Tropfendurchmesser** ist das arithmetische Mittel aus den gemessenen Tropfendurchmessern:

$$D_{10} = \frac{1}{N} \sum_{i=1}^N D_i$$

#### D20:

Der „**flächig**“ mittlere Tropfendurchmesser berechnet sich aus den Quadraten der gemessenen Tropfendurchmesser:

$$D_{20} = \left\{ \frac{1}{N} \sum_{i=1}^N D_i^2 \right\}^{1/2}$$

#### D30:

Der **volumetrisch mittlere Tropfendurchmesser** berechnet sich aus der 3. Potenz der gemessenen Tropfendurchmesser:

$$D_{30} = \left\{ \frac{1}{N} \sum_{i=1}^N D_i^3 \right\}^{1/3}$$

#### D32:

Der **Sauter-Durchmesser** berechnet sich wie folgt:

$$D_{32} = \frac{\sum_{i=1}^N D_i^3}{\sum_{i=1}^N D_i^2}$$

#### Dv0.1: Dv0.5: Dv0.9:

Die kummulative Tropfenverteilung stellt die Tropfendurchmesser, welche, bezogen auf die Gesamttropfenanzahl, kleiner als 10%, 50% oder 90% dieses Tropfendurchmessers sind, bzw. wo die kummulative Funktion der Volumenverteilung (Q3) den Wert 0.1, 0.5 oder 0.9 hat dar:

$$Q_3(Dv0.1)=0.1; \quad Q_3(Dv0.5)=0.5; \quad Q_3(Dv0.9)=0.9$$

*Important diameters for nozzles; Source: Schlick*

## Appendix 2: Data sheet of the used spray nozzles

### Droplet Size Analysis Tropfengrößensmessung

**460.686.17.CC.00.0**

Date of measurement: Tue Dec 08 2009

Datum der Messung

Liquid pressure: 2 bar

Druck Flüssigkeit

Liquid flow rate: 5 l/min

Volumenstrom Flüssigkeit

Air pressure: 0 bar

Druck Luft

Air flow rate: 0 m<sup>3</sup>/h i.N.

Volumenstrom Luft

Air/Liquid ratio: 0 (m<sup>3</sup>/h i.N.)/(l/min)

Luft-Wasser-Verhältnis

Meas. Location (x): - [mm]

Messort (x)

Meas. Location (y): - [mm]

Messort (y)

Meas. Location (z): 250 [mm]

Messort (z)

Measurement Type: Merged positions

Medium

Water



Lechler GmbH  
Präzisionsdüsen, Tropfenabscheider  
Ulmer Straße 128  
D-72555 Metzingen / Germany  
Telefon +49 (0)7123 962-0  
Telefax +49 (0)7123 962-444  
E-Mail info@lechler.de  
Internet http://www.lechler.de

Surface mean diameter = 117,0 µm

Flächen-Mittelwert (D20)

Volume mean diameter = 160,6 µm

Volumen-Mittelwert (D30)

D(VOL)10% = 164,3 µm

D(VOL)50% = 410,3 µm

D(VOL)90% = 723,2 µm

D(VOL)98% = 785,0 µm

D(VOL)99% = 786,0 µm

Dmax = 795,5 µm

Sauter mean diameter = 303,0 µm

Sauterdurchmesser (D32)

Mean velocity (vertical) = 4,9 m/s

Mittlere Geschwindigkeit (vertikal)

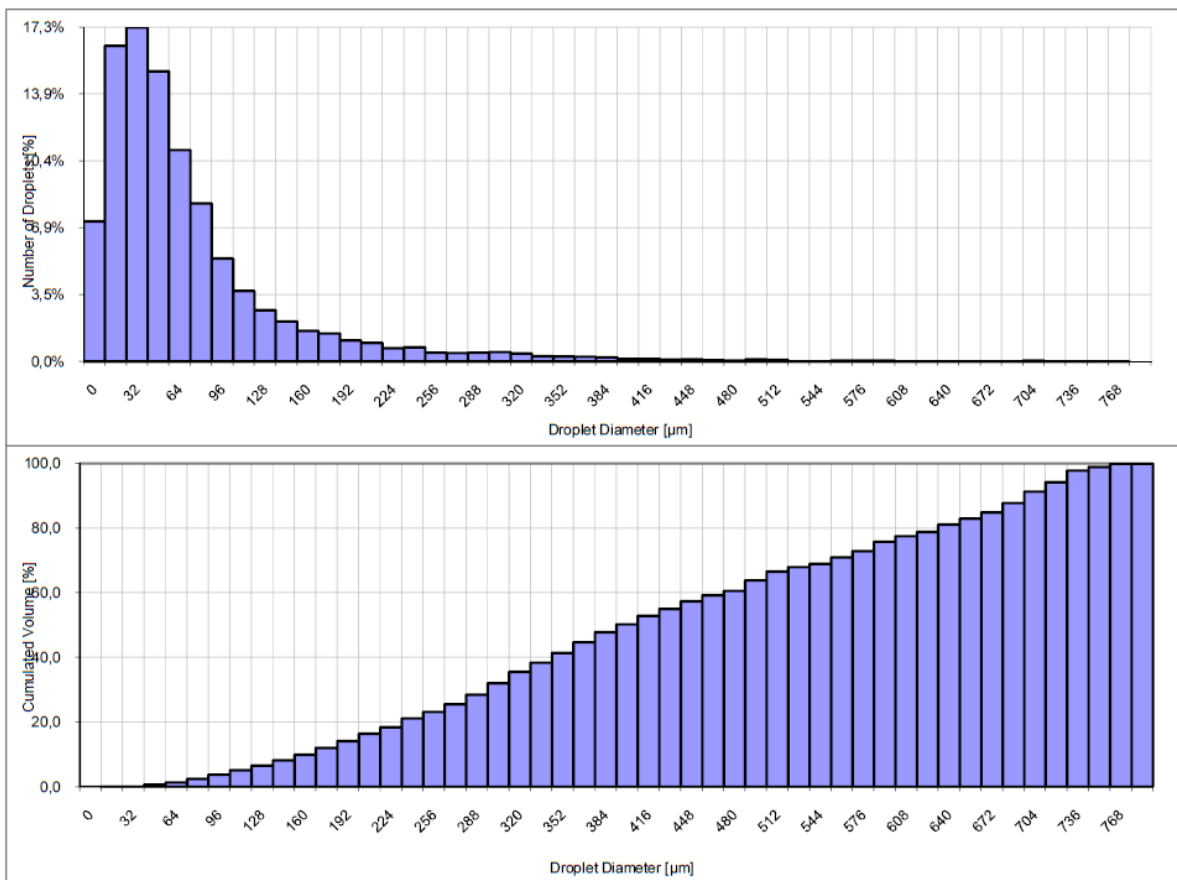
Distribution type: temporal

Messverfahren

Remark: -

Bemerkung

### Numerical Diameter | Cumulative Volume



Creator: DL - P. Würdinger

$Q_{nom}=5l/min$ ; source: Lechler



# Droplet Size Analysis

## Tropfengrößensmessung



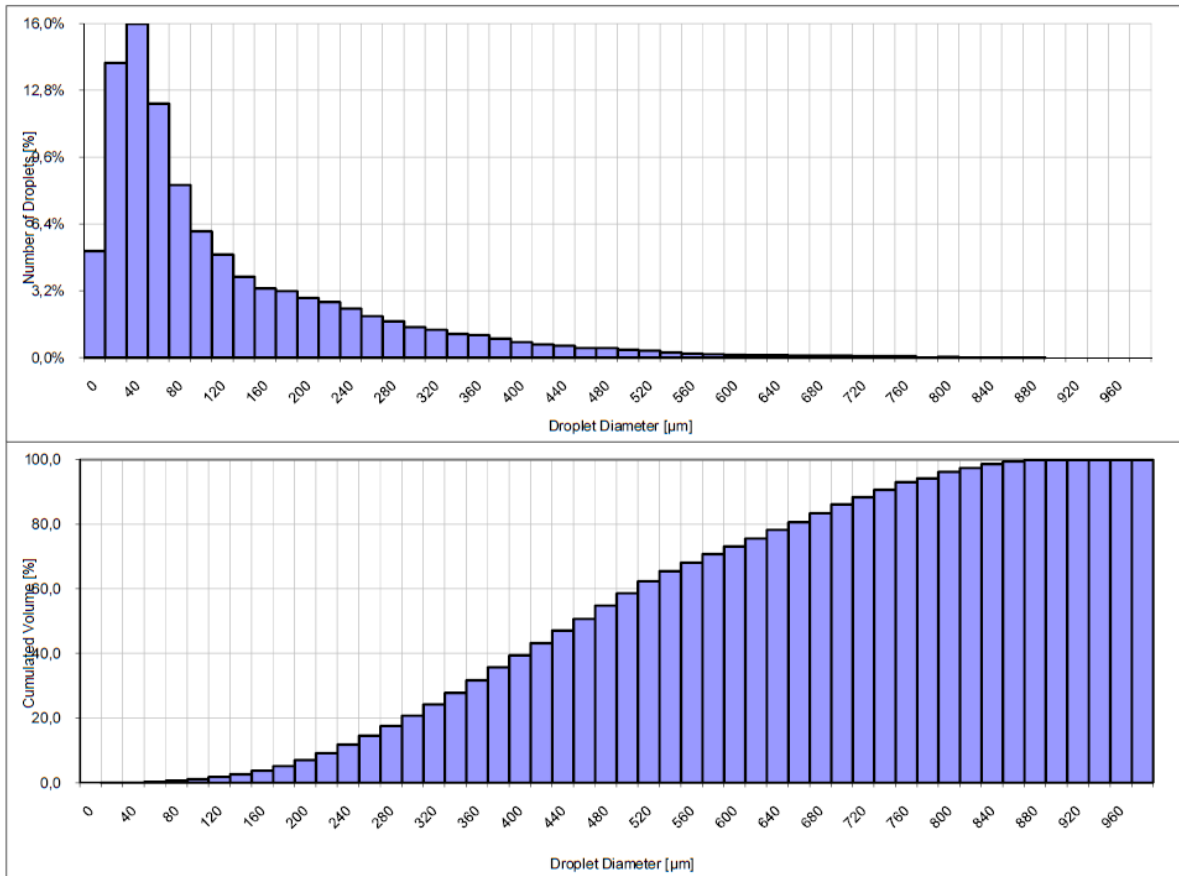
Lechler GmbH  
 Präzisionsdüsen, Tropfenabscheider  
 Ulmer Straße 128  
 D-72555 Metzingen / Germany  
 Telefon +49 (0)7123 962-0  
 Telefax +49 (0)7123 962-444  
 E-Mail info@lechler.de  
 Internet http://www.lechler.de

### 490.766.1Y.CE.00.0

Date of measurement: 16.08.2012  
 Datum der Messung  
 Liquid pressure: 2 bar  
 Druck Flüssigkeit  
 Liquid flow rate: 7,8 l/min  
 Volumenstrom Flüssigkeit  
 Air pressure: 0 bar  
 Druck Luft  
 Air flow rate: 0 m³/h i.N.  
 Volumenstrom Luft  
 Air/Liquid ratio: 0 (m³/h i.N.)/(l/min)  
 Luft-/Wasser-Verhältnis  
 Meas. Location (x): - [mm]  
 Messort (x)  
 Meas. Location (y): - [mm]  
 Messort (y)  
 Meas. Location (z): 250 [mm]  
 Messort (z)  
 Measurement Type: Merged positions  
 Medium: Water

Surface mean diameter = 188,1 µm  
 Flächen-Mittelwert (D20)  
 Volume mean diameter = 238,6 µm  
 Volumen-Mittelwert (D30)  
 D(VOL)10% = 237,2 µm  
 D(VOL)50% = 465,4 µm  
 D(VOL)90% = 752,4 µm  
 D(VOL)98% = 846,3 µm  
 D(VOL)99% = 863,0 µm  
 Dmax = 898,4 µm  
 Sauter mean diameter = 383,9 µm  
 Sauterdurchmesser (D32)  
 Mean velocity (vertical) = 6,2 m/s  
 Mittlere Geschwindigkeit (vertikal)  
 Distribution type: temporal  
 Messverfahren  
 Remark: LPV-001925  
 Bemerkung

### Numerical Diameter | Cumulative Volume



Creator: DL - P. Würdinger

$Q_{nom} = 8 \text{ l/min}; \text{ source: Lechler}$

## Droplet Size Analysis

### Tropfengrößenmessung

**490.848.1Y.CE.00.0**

Date of measurement: 06.06.2014  
Datum der Messung

Liquid pressure: 3 bar  
Druck Flüssigkeit

Liquid flow rate: 15,1 l/min  
Volumenstrom Flüssigkeit

Air pressure: 0 bar  
Druck Luft

Air flow rate: 0 m<sup>3</sup>/h i.N.  
Volumenstrom Luft

Air/Liquid ratio: 0 (m<sup>3</sup>/h i.N.)/(l/min)  
Luft-/Wasser-Verhältnis

Meas. Location (x): - [mm]  
Messort (x)

Meas. Location (y): - [mm]  
Messort (y)

Meas. Location (z): 250 [mm]  
Messort (z)

Measurement Type: Merged positions  
Medium: Water



Lechler GmbH  
Präzisionsdüsen, Tropfenabscheider  
Ulmer Straße 128  
D-72555 Metzingen / Germany  
Telefon +49 (0)7123 962-0  
Telefax +49 (0)7123 962-444  
E-Mail info@lechler.de  
Internet http://www.lechler.de

Surface mean diameter = 181,3 µm  
Flächen-Mittelwert (D20)

Volume mean diameter = 237,4 µm  
Volumen-Mittelwert (D30)

D(VOL)10% = 241,9 µm  
D(VOL)50% = 501,5 µm  
D(VOL)90% = 881,3 µm  
D(VOL)98% = 1120,3 µm  
D(VOL)99% = 1148,8 µm  
Dmax = 1195,7 µm

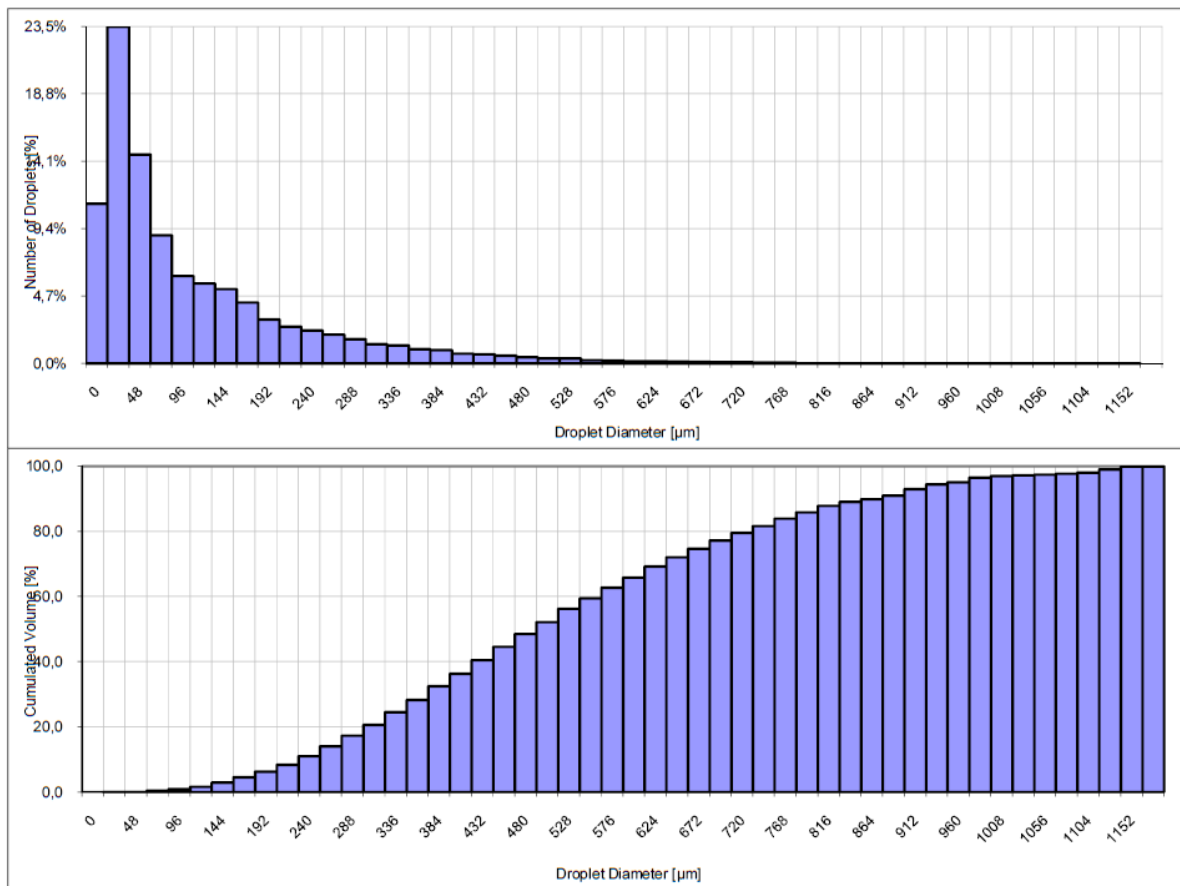
Sauter mean diameter = 406,9 µm  
Sauterdurchmesser (D32)

Mean velocity (vertical) = 5,9 m/s  
Mittlere Geschwindigkeit (vertikal)

Distribution type: temporal  
Messverfahren

Remark: LPV-002274  
Bemerkung

### Numerical Diameter | Cumulative Volume



Creator: DL - P. Würdinger

$Q_{nom}=12l/min$ ; source: Lechler





Experiment Nr.	Classification of the spray						1. Debimo differential pressure sensor					measuring pipe	Thermodynamically/downally measurements										Injected spray water					Utilization factor		Process H2O from felt		
	module	direction	Q <sub>nom</sub>	Q	T	Δp	ABS P	T	$\dot{V}$	ΔP	v		v	position 1 at measuring pipe					position 4 at measuring pipe					p <sub>w</sub>	T <sub>win</sub>	$\dot{V}_{water}$	T <sub>wout_1</sub>	T <sub>wout_4</sub>	η <sub>1</sub>		η <sub>4</sub>	m <sub>H2O_process</sub>
			l/min	l/min	°C	bar	Pa	°C	m <sup>3</sup> /min	bar	m/s	m/s	T <sub>moist air_out_1</sub>	Φ <sub>out_1</sub>	Δm <sub>vapour_1</sub>	Δm <sub>vapour_1</sub>	ΔV <sub>moist air_1</sub>	T <sub>moist air_out_4</sub>	Φ <sub>out_4</sub>	Δm <sub>vapour_4</sub>	Δm <sub>vapour_4</sub>	ΔV <sub>moist air_4</sub>	°C							-		
99	skewed	up	8	10	h	h	0,75	56,4	8,7	0,25	18,9	4,73	51,2	1,00	0,27	27,02	7,61%	51	1,00	0,28	27,91	7,83%	4,5	15	10,1	44,73	45,28	0,84	0,86	24		
100	skewed	up	12	8	h	h	0,74	56,2	8,8	0,26	19,4	4,85	53,8	1,00	0,14	13,70	3,84%	53,7	1,00	0,15	14,15	3,93%	4,5	15	8,6	32,23	32,57	0,48	0,49	24		
101	skewed	up	12	12	h	h	0,74	56	8,9	0,26	20	5,00	52,3	1,00	0,20	19,95	5,58%	52,5	1,00	0,19	18,94	5,26%	4,5	15	12,3	32,15	31,63	0,51	0,49	24		
102	skewed	up	12	15	h	h	0,75	55,8	9,4	0,25	20,1	5,03	50,3	1,00	0,30	28,39	7,82%	50,7	1,00	0,28	26,48	7,25%	4,5	15	15,1	35,48	34,64	0,64	0,61	24		
103	up/down	down	12	8	h	h	0,74	56,3	9	0,26	19,3	4,83	52,6	1,00	0,21	20,06	5,67%	52,5	1,00	0,22	20,50	5,76%	4,5	15	8,3	42,15	42,51	0,75	0,76	24		
104	up/down	down	12	12	h	h	0,75	56,4	9,2	0,25	18,9	4,73	50,5	1,00	0,29	30,21	8,52%	51,2	1,00	0,26	26,99	7,57%	4,5	15	12	40,86	39,21	0,77	0,71	24		
105	up/down	down	12	15	h	h	0,72	56,5	9	0,28	19,8	4,95	48,3	1,00	0,43	39,18	11,55%	48,9	1,00	0,41	37,05	10,85%	4,5	15	15,3	44,59	43,62	0,91	0,87	24		
106	up/down	down	12	8	l	h	0,75	50	8,3	0,25	19,6	4,90	45,3	1,00	0,18	24,19	5,41%	45,8	1,00	0,16	21,68	4,82%	4,5	15	7,4	44,29	42,67	0,97	0,91	24		
107	up/down	down	12	12	l	h	0,74	50,8	0,2	0,26	19,2	4,80	44,2	1,00	0,29	32,46	7,61%	44,2	1,00	0,29	32,42	7,57%	4,5	15	11,3	45,35	45,33	1,03	1,03	24		
108	up/down	down	12	15	l	h	0,75	51,6	9	0,25	19,1	4,78	42	1,00	0,36	43,31	10,52%	42,2	1,00	0,36	42,60	10,31%	4,5	15	14,9	45,80	45,54	1,10	1,09	24		